

ISSN 1854-6250

**APEM**  
*journal*

# Advances in Production Engineering & Management

Volume 11 | Number 2 | June 2016





University of Maribor

Published by PEI  
[apem-journal.org](http://apem-journal.org)

# Advances in Production Engineering & Management

## Identification Statement

	ISSN 1854-6250   Abbreviated key title: <b>Adv produc engineer manag</b>   Start year: 2006 ISSN 1855-6531 (on-line)
	Published quarterly by <b>Production Engineering Institute (PEI), University of Maribor</b> Smetanova ulica 17, SI – 2000 Maribor, Slovenia, European Union (EU) Phone: 00386 2 2207522, Fax: 00386 2 2207990 Language of text: English APEM homepage: <a href="http://apem-journal.org">apem-journal.org</a> University homepage: <a href="http://www.um.si">www.um.si</a>

## APEM Editorial

### Editor-in-Chief

#### Miran Brezocnik

editor@apem-journal.org, info@apem-journal.org  
University of Maribor, Faculty of Mechanical Engineering  
Smetanova ulica 17, SI – 2000 Maribor, Slovenia, EU

### Desk Editor

#### Tomaz Irgolic

desk1@apem-journal.org

### Website Master

#### Lucija Brezocnik

lucija.brezocnik@um.si

### Editorial Board Members

Eberhard Abele, Technical University of Darmstadt, Germany  
Bojan Acko, University of Maribor, Slovenia  
Joze Balic, University of Maribor, Slovenia  
Agostino Bruzzone, University of Genoa, Italy  
Borut Buchmeister, University of Maribor, Slovenia  
Ludwig Cardon, Ghent University, Belgium  
Edward Chlebus, Wroclaw University of Technology, Poland  
Franci Cus, University of Maribor, Slovenia  
Igor Drstvensek, University of Maribor, Slovenia  
Illes Dudas, University of Miskolc, Hungary  
Mirko Ficko, University of Maribor, Slovenia  
Vlatka Hlupic, University of Westminster, UK  
David Hui, University of New Orleans, USA  
Pramod K. Jain, Indian Institute of Technology Roorkee, India

Isak Karabegović, University of Bihać, Bosnia and Herzegovina  
Janez Kopac, University of Ljubljana, Slovenia  
Iztok Palcic, University of Maribor, Slovenia  
Krsto Pandza, University of Leeds, UK  
Andrej Polajnar, University of Maribor, Slovenia  
Antonio Pouzada, University of Minho, Portugal  
Rajiv Kumar Sharma, National Institute of Technology, India  
Katica Simunovic, J.J. Strossmayer University of Osijek, Croatia  
Daizhong Su, Nottingham Trent University, UK  
Soemon Takakuwa, Nagoya University, Japan  
Nikos Tsourveloudis, Technical University of Crete, Greece  
Tomo Udiljak, University of Zagreb, Croatia  
Ivica Veza, University of Split, Croatia

**Limited Permission to Photocopy:** Permission is granted to photocopy portions of this publication for personal use and for the use of clients and students as allowed by national copyright laws. This permission does not extend to other types of reproduction nor to copying for incorporation into commercial advertising or any other profit-making purpose.

**Subscription Rate:** 120 EUR for 4 issues (worldwide postage included); 30 EUR for single copies (plus 10 EUR for postage); for details about payment please contact: [info@apem-journal.org](mailto:info@apem-journal.org)

**Cover and interior design:** Miran Brezocnik

**Printed:** Tiskarna Koštomaj, Celje, Slovenia

**Subsidizer:** The journal is subsidized by Slovenian Research Agency

Statements and opinions expressed in the articles and communications are those of the individual contributors and not necessarily those of the editors or the publisher. No responsibility is accepted for the accuracy of information contained in the text, illustrations or advertisements. Production Engineering Institute assumes no responsibility or liability for any damage or injury to persons or property arising from the use of any materials, instructions, methods or ideas contained herein.

Copyright © 2016 PEI, University of Maribor. All rights reserved.

*Advances in Production Engineering & Management* is indexed and abstracted in the **WEB OF SCIENCE** (maintained by **THOMSON REUTERS**): **Science Citation Index Expanded**, **Journal Citation Reports** – Science Edition, **Current Contents** – Engineering, Computing and Technology • **Scopus** (maintained by **Elsevier**) • **Inspec** • **EBSCO**: Academic Search Alumni Edition, Academic Search Complete, Academic Search Elite, Academic Search Premier, Engineering Source, Sales & Marketing Source, TOC Premier • **ProQuest**: CSA Engineering Research Database – Cambridge Scientific Abstracts, Materials Business File, Materials Research Database, Mechanical & Transportation Engineering Abstracts, ProQuest SciTech Collection • **TEMA (DOMA)** • The journal is listed in **Ulrich's** Periodicals Directory and **Cabell's** Directory



University of Maribor  
Production Engineering Institute (PEI)

# Advances in Production Engineering & Management

Volume 11 | Number 2 | June 2016 | pp 73–154

## Contents

---

<b>Scope and topics</b>	<b>76</b>
<b>A simulation approach to the process planning problem using a modified particle swarm optimization</b>	<b>77</b>
Wang, J.F.; Kang, W.L.; Zhao, J.L.; Chu, K.Y.	
<b>Surface roughness assessing based on digital image features</b>	<b>93</b>
Simunovic, G.; Svalina, I.; Simunovic, K.; Saric, T.; Havrlisan, S.; Vukelic, D.	
<b>Visual measurement of layer thickness in multi-layered functionally graded metal materials</b>	<b>105</b>
Zuperl, U.; Radic, A.; Cus, F.; Irgolic, T.	
<b>Modelling supply risks in interdependent manufacturing systems: A case study</b>	<b>115</b>
Omega, R.S.; Noel, V.M.; Masbad, J.G.; Ocampo, L.A.	
<b>Analysis for prevalence of carpal tunnel syndrome in shocker manufacturing workers</b>	<b>126</b>
Kumar, S.; Muralidhar, M.	
<b>Simultaneous determination of production and shipment decisions for a multi-product inventory system with a rework process</b>	<b>141</b>
Chiu, Y.P.; Chiang, K.-W.; Chiu, S.W.; Song, M.-S.	
<b>Calendar of events</b>	<b>152</b>
<b>Notes for contributors</b>	<b>153</b>

---

Journal homepage: [apem-journal.org](http://apem-journal.org)

ISSN 1854-6250 (print)

ISSN 1855-6531 (on-line)

©2016 PEI, University of Maribor. All rights reserved.

## Scope and topics

*Advances in Production Engineering & Management (APEM journal)* is an interdisciplinary refereed international academic journal published quarterly by the *Production Engineering Institute* at the *University of Maribor*. The main goal of the *APEM journal* is to present original, high quality, theoretical and application-oriented research developments in all areas of production engineering and production management to a broad audience of academics and practitioners. In order to bridge the gap between theory and practice, applications based on advanced theory and case studies are particularly welcome. For theoretical papers, their originality and research contributions are the main factors in the evaluation process. General approaches, formalisms, algorithms or techniques should be illustrated with significant applications that demonstrate their applicability to real-world problems. Although the *APEM journal* main goal is to publish original research papers, review articles and professional papers are occasionally published.

Fields of interest include, but are not limited to:

Additive Manufacturing Processes	Machine Learning in Production
Advanced Production Technologies	Machine Tools
Artificial Intelligence in Production	Machining Systems
Assembly Systems	Manufacturing Systems
Automation	Materials Science, Multidisciplinary
Computer-Integrated Manufacturing	Mechanical Engineering
Cutting and Forming Processes	Mechatronics
Decision Support Systems	Metrology
Discrete Systems and Methodology	Modelling and Simulation
e-Manufacturing	Numerical Techniques
Evolutionary Computation in Production	Operations Research
Fuzzy Systems	Operations Planning, Scheduling and Control
Human Factor Engineering, Ergonomics	Optimisation Techniques
Industrial Engineering	Project Management
Industrial Processes	Quality Management
Industrial Robotics	Risk and Uncertainty
Intelligent Manufacturing Systems	Self-Organizing Systems
Joining Processes	Statistical Methods
Knowledge Management	Supply Chain Management
Logistics	Virtual Reality in Production



# A simulation approach to the process planning problem using a modified particle swarm optimization

Wang, J.F.<sup>a,\*</sup>, Kang, W.L.<sup>a</sup>, Zhao, J.L.<sup>a</sup>, Chu, K.Y.<sup>a</sup>

<sup>a</sup>Department of Mechanical Engineering, North China Electric Power University, Baoding, China

## ABSTRACT

Due to the complexity and variety of practical manufacturing conditions, computer-aided process planning (CAPP) systems have become increasingly important in the modern production system. In CAPP, the process planning (PP) problem involves two tasks: operation determining and operation sequencing. To optimize the process plans generated from complex parts, the traditional particle swarm optimization (PSO) algorithm is modified. Efficient encoding and decoding population initialization methods have been developed to adapt the PP problem for the PSO approach. In addition, to avoid the proposed approach becoming trapped in local convergences and achieving local optimal solutions, parameters are set to control the iterations. Several extended operators for the different parts of the particles have been incorporated into the traditional PSO. Simulation experiments have been run to evaluate and verify the effectiveness of the modified PSO approach. The simulation results indicate that the PP problem can be more effectively solved by the proposed PSO approach than other approaches.

© 2016 PEI, University of Maribor. All rights reserved.

## ARTICLE INFO

### Keywords:

Process planning  
Operation determining  
Operation sequencing  
Particle swarm optimization  
Extended operator

### \*Corresponding author:

wjf266@163.com  
(Wang, J.F.)

### Article history:

Received 29 January 2016  
Revised 27 March 2016  
Accepted 10 May 2016

## 1. Introduction

In the modern computer-integrated manufacturing system (CIMS), the CAPP system plays an important role [1]. Generally, process planning involves two activities: operation determining and operation sequencing. In CAPP systems, these two activities must be executed simultaneously to achieve a good solution. Thus far, some effort has been made to address this problem, for instance, by designing a more feasible mathematical model or developing a more efficient approach. The application of some artificial intelligence approaches in the PP problem has especially promoted the development of CAPP technology. These approaches can be categorized as the genetic algorithm (GA) [1, 2], simulated annealing (SA) [2, 3], tabu search (TS) [4, 5], ant colony optimization (ACO) [6-8], particle swarm optimization (PSO) [9-13], honey bees mating optimization [14], and hybrid approaches [2, 15].

In 1995, Kennedy and Eberhart proposed the PSO algorithm [16]. The PSO is a new swarm optimization approach that can optimize engineering problems in aspects such as turning process modelling [17], assembly sequence planning [18], and process parameter optimization (TSP) [19].

The search for applications of PSO in the PP problem was first introduced by Guo et al. [9]. The process plan particle encoded/decoded strategy and some modified operators were designed. Kafashi et al. [10] optimized the setup planning using cost indices based on constraints such as the TAD (tool approach direction), the tolerance relation between features, and the feature precedence relations. Wang et al. [11] proposed an innovative process plan representation in

which operation selection and operation sequencing were introduced simultaneously in a particle. Two local search operators are incorporated into the traditional PSO to achieve the optimal solution. Li et al. [12] modified the traditional PSO for the process planning problem. Miljković et al. [13] adopted the AND/OR network representation to describe the flexibility of the machine, tool, TAD, process and sequence and a performed multi-objective optimization procedure for the minimization of the production time and production cost using a modified PSO algorithm on this representation.

Zhang et al. [1] proposed a GA for a novel CAPP model. Li et al. [2] incorporated an SA into a GA to improve its searching efficiency. Ma et al. [3] modeled the PP problem as a combinational optimization problem with constraints. An entire solution space is constructed in reference to precedence constraints among operations. An SA algorithm is then proposed to address the PP problem. Li et al. [4] applied a TS-based approach to address the PP problem. In this approach, a mapping relationship is established between process constraints among features and precedence constraints among operations. Lian et al. [5] proposed a multi-dimensional tabu search (MDTS) approach to address the PP problem. Some local search strategies for different parts have been integrated into this TS approach. Liu et al. [6] constructed a mathematical model for the PP problem by considering the process constraints and optimization objectives. The ACO approach has been developed to optimize the PP problem based on this mathematical model. Wang et al. [7] represented the PP problem by an improved directed/undirected graph. A two-stage approach based on ACO was developed to optimize the process plans on the directed/undirected graph. Wen et al. [14] proposed a new method based on the honey bees mating optimization (HBMO) approach to optimize the PP problem. The solution encoding, crossover operator, and local search strategies were developed according to the characteristics of the PP problem. Huang et al. [15] designed a hybrid algorithm combining a graph and the GA to optimize process plans. The precedence constraints are mapped to an operation precedence graph on which an improved GA was applied to solve the PP problem.

Although there have been some significant improvements in solving the PP problem, there still remains the potential for further improvement [20]. Up to now, some heuristics or evolutionary approaches have been applied to optimize the PP problem, but the major difficulty is that the search space is too large for parts with complex features to find optimal solutions efficiently. To address this problem, a traditional PSO approach is modified to solve the PP problem in this paper. The main work includes the following two aspects:

- The representation of a process plan mapped to a particle is modified to facilitate the discrete PP problem. A new particle encoding/decoding strategy is adapted to make the search more efficient.
- A diverse searching mechanism has been adopted to improve the performance of the PSO approach. To avoid local convergence, some modifications to the traditional PSO approach have been adopted to better explore the solution space. Several operators for the different parts of the particles have been incorporated into the traditional PSO.

Section 2 describes the process planning model. Section 3 introduces the particle swarm optimization approach. Section 4 introduces an application of the modified PSO approach to the PP problem. Section 5 presents the simulation results of the proposed PSO algorithm. Finally, some conclusions and outlook are given in Section 6.

## 2. Problem modelling

### 2.1 Problem description

In the PP problem, two tasks have to be performed, namely, operation determining and operation sequencing. For operation determining, the method of mapping from features to operations is widely used in the PP problem. The attributes of each feature determines the corresponding machining methods, which can be expressed by the alternative operations. The combination of machines, cutting tools, and tool approach directions (TAD) comprise all of the different opera-

tion types (OPTs) for a feature of a part, which will be selected to determine the final process plans [1, 11].

For an operation, there are a set of OPTs under which the operation can be executed. Accordingly, an integrated process plan can be represented as follows.

$$PP = \{OP_1, OP_2, \dots, OP_i, \dots, OP_n\} \tag{1}$$

$$OP_i = \{OPT_{i1}, OPT_{i2}, \dots, OPT_{ij}, \dots, OPT_{im}\} \tag{2}$$

$$OPT_{ij} = \{M_{ij}, T_{ij}, TAD_{ij}\} \tag{3}$$

$OP_i$  is the  $i$ -th operation, and  $OPT_{ij}$  is the  $j$ -th alternative selection of the operation  $OP_i$ .  $M_{ij}$ ,  $T_{ij}$  and  $TAD_{ij}$  are the ID of the selected machine, tool and  $TAD$  for operation  $OPT_{ij}$ , respectively.

An example part in Fig. 1 is used to demonstrate the representation of a process plan [7]. The candidate operations are listed in Table 1.

In addition to operation determining, operation sequencing is another task in the PP problem. The operations should be sequenced under the conditions of satisfying the precedence constraints among operations [4, 6, 12, 15]. The constraints of Part 1 are shown in Table 2.

According to the precedence constraints in Table 2, an available process plan for Part 1 is shown in Table 3.

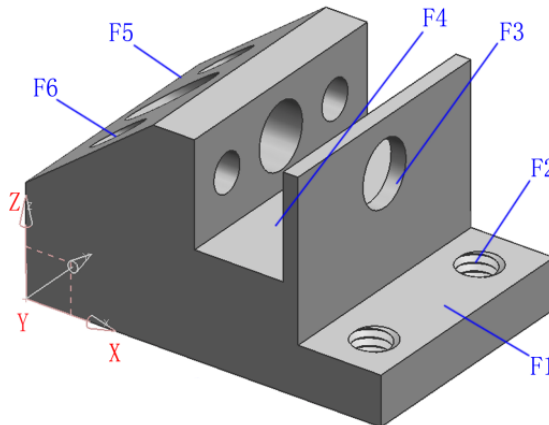


Fig. 1 An example part – Part 1

Table 1 Candidate operations for Part 1

Features	Operations	Operation types	Machines	Tools	TADs	Description
F1	Milling (OP <sub>1</sub> )	OPT <sub>11</sub> , OPT <sub>12</sub>	M2	T1	+X, +Z	M1: Drilling press M2: Vertical milling machine
F2	Drilling (OP <sub>2</sub> )	OPT <sub>21</sub> , OPT <sub>22</sub>	M1, M2	T2	-Z	T1: Milling cutter T2: Drill1
	Tapping (OP <sub>3</sub> )	OPT <sub>31</sub> , OPT <sub>32</sub>		T3		T3: Tapping tool
F3	Drilling (OP <sub>4</sub> )	OPT <sub>41</sub> , OPT <sub>42</sub>	M1, M2	T4	-X	T4: Drill2
	Reaming (OP <sub>5</sub> )	OPT <sub>51</sub> , OPT <sub>52</sub>		T5		T5: Reamer1
F4	Milling (OP <sub>6</sub> )	OPT <sub>61</sub>	M2	T6	+Z	T6: Slot cutter
F5	Milling (OP <sub>7</sub> )	OPT <sub>71</sub> , OPT <sub>72</sub>	M2	T7	+Y, -Z	T7: Chamfer cutter
F6	Drilling (OP <sub>8</sub> )	OPT <sub>81</sub> , OPT <sub>82</sub>	M1, M2	T8	+X	T8: Drill3
	Reaming (OP <sub>9</sub> )	OPT <sub>91</sub> , OPT <sub>92</sub>		T9		T9: Reamer2

**Table 2** Constraints for Part 1 [7]

Operations	Precedence constraint description	Constraint types
OP <sub>1</sub>	OP <sub>1</sub> is prior to OP <sub>2</sub> and OP <sub>3</sub> .	Hard
	OP <sub>1</sub> is prior to OP <sub>4</sub> and OP <sub>5</sub> .	Soft
OP <sub>2</sub>	OP <sub>2</sub> is prior to OP <sub>3</sub> .	Hard
OP <sub>4</sub>	OP <sub>4</sub> is prior to OP <sub>5</sub> .	Hard
OP <sub>4</sub> , OP <sub>5</sub>	OP <sub>4</sub> and OP <sub>5</sub> are prior to OP <sub>6</sub> .	Hard
OP <sub>6</sub>	OP <sub>6</sub> is prior to OP <sub>2</sub> and OP <sub>3</sub> .	Hard
OP <sub>8</sub>	OP <sub>8</sub> is prior to OP <sub>9</sub> .	Hard
OP <sub>8</sub> , OP <sub>9</sub>	OP <sub>8</sub> and OP <sub>9</sub> are prior to OP <sub>7</sub> .	Hard

**Table 3** Available process plan for Part 1

Operation	Machine	Tool	TAD
OP <sub>1</sub>	M2	T1	+X
OP <sub>8</sub>	M1	T8	+X
OP <sub>9</sub>	M1	T9	+X
OP <sub>4</sub>	M1	T4	-X
OP <sub>5</sub>	M1	T5	-X
OP <sub>6</sub>	M2	T6	+Z
OP <sub>7</sub>	M2	T7	-Z
OP <sub>2</sub>	M1	T2	-Z
OP <sub>3</sub>	M1	T3	-Z

## 2.2 Mathematical model

The criterion of minimizing production costs (CP) is usually used to evaluate the process plan. The CP includes the machine cost (CM), cutting tool cost (CT), machine-changing cost (CMC), cutting tool changing cost (CTC), and set-up cost (CSC) [2, 3, 6, 8, 11, 14, 15].

The machine cost is

$$CM = \{cm_1, cm_2, \dots, cm_i, \dots, cm_{N_M}\} \quad (4)$$

where  $N_M$  is the number of machines.

The cutting tool cost is

$$CT = \{ct_1, ct_2, \dots, ct_i, \dots, ct_{N_T}\} \quad (5)$$

where  $N_T$  is the number of cutting tools.

As shown in Eq. 2 and Eq. 3, an operation is selected from several alternative OPTs. The machine cost for an operation varies according to the alternative OPTs, so the machine cost  $CM_{ij}$  for an OPT  $OPT_{ij}$  can be given as

$$CM_{ij} = cm_{M_{ij}} \quad (6)$$

where  $M_j$  is explained in Eq. 3.

The cutting tool cost  $TC_{ij}$  for an OPT  $OPT_{ij}$  can be given as

$$CT_{ij} = ct_{T_{ij}} \quad (7)$$

where  $T_{ij}$  is explained in Eq. 3.

The machine changing cost  $CMC_{iji'j'}$  between OPT  $OPT_{ij}$  and OPT  $OPT_{i'j'}$  can be given as

$$CMC_{iji'j'} = \Phi(M_{ij}, M_{i'j'}) \times C^{cm} \quad (8)$$

where  $C^{cm}$  is the cost of machine changing, which is considered to be the same for each machine change.  $\Phi(X, Y)$  can be calculated as follows:

$$\Phi(X, Y) = \begin{cases} 1 & X \neq Y \\ 0 & X = Y \end{cases} \quad (9)$$

The cutting tool changing cost  $CTC_{ijij'}$ , between  $OPT_{ij}$  and  $OPT_{i'j'}$  can be given as

$$CTC_{ijij'} = \Omega(\Phi(M_{ij}, M_{i'j'}), \Phi(T_{ij}, T_{i'j'})) \times C^{ct} \quad (10)$$

where  $C^{ct}$  is the cutting tool changing cost, which is considered to be the same for each cutting tool change.  $\Omega(X, Y)$  can be calculated as follows.

$$\Omega(X, Y) = \begin{cases} 0 & X = Y = 0 \\ 1 & otherwise \end{cases} \quad (11)$$

The set-up cost  $CS_{ijij'}$ , between  $OPT_{ij}$  and  $OPT_{i'j'}$  can be given as

$$CS_{ijij'} = \Omega(\Phi(M_{ij}, M_{i'j'}), \Phi(TAD_{ij}, TAD_{i'j'})) \times C^{cs} \quad (12)$$

where  $TAD_{ij}$  is explained in Eq. 3, and  $C^{cs}$  is the cost for a set-up, which is considered to be the same for each set-up.

The definitions of machine changing, tool changing, and set-up changing have been explained in reference [2]. Based on the above analysis, the mathematical model of the PP problem is formulated as follows [6]:

*Objectives:*

(i) A combination of  $CM$ ,  $CT$ ,  $CMC$ ,  $CTC$ , and  $CS$  will be considered as  $CP$ , and minimizing  $CP$  is the objective of PP.

$$\text{Min } CP = \sum_{i=1}^n \sum_{j=1}^m u_{ij} (\omega_1 \cdot CM_{ij} + \omega_2 \cdot CT_{ij}) + \sum_{i=1}^n \sum_{j=1}^m \sum_{i' \neq i}^n \sum_{j' \neq j}^m v_{ijij'} (\omega_3 \cdot CMC_{ijij'} + \omega_4 \cdot CS_{ijij'} + \omega_5 \cdot CTC_{ijij'}) + C^{sc} \quad (13)$$

*Subject to:*

(ii)  $n$  operations have to be selected while machining a part.

$$\sum_{i=1}^n \sum_{j=1}^m u_{ij} = n \quad (14)$$

(iii) For an operation, one and only one OPT can be selected from its  $m$  alternative OPTs.

$$\sum_{j=1}^m u_{ij} = 1 \quad (i = 1, 2, \dots, n) \quad (15)$$

(iv) For a process plan consisting of  $n$  operations, the numbers of operation changes is  $n - 1$ , and the changes of combinations of machines, cutting tools, and set-ups are accompanied by operation changes.

$$\sum_{i=1}^n \sum_{j=1}^m \sum_{i' \neq i}^n \sum_{j' \neq j}^m v_{ijij'} = n - 1 \quad (16)$$

(v) For each OPT, only one adjacent operation is lined up before it.

$$\sum_{i=1}^n \sum_{j=1}^m v_{ijij'} \leq 1 \quad (17)$$

(vi) For each OPT, only one adjacent operation is lined up after it.

$$\sum_{i'=1}^n \sum_{j'=1}^m v_{ij'i'j'} \leq 1 \tag{18}$$

(vii)  $u_{ij}$  is an integer enumeration variable.

$$u_{ij} = \begin{cases} 1 & \text{if OPT}_{ij} \text{ is selected for operation } OP_i \\ 0 & \text{otherwise} \end{cases} \tag{19}$$

(viii)  $v_{ij'i'j'}$  is an integer enumeration variable.

$$v_{ij'i'j'} = \begin{cases} 1 & \text{if OPT}_{i'j'} \text{ is selected after OPT}_{ij} \text{ is executed} \\ 0 & \text{otherwise} \end{cases} \tag{20}$$

Eq. 13 means that the objective function of the PP is to minimize the total production cost. The constraints are in Eq. 14 to Eq. 20. Constraints in Eq. 14 and Eq. 15 ensure that all the operations are carried out. The constraint in Eq. 16 ensures that  $n - 1$  changing costs of machines, cutting tools, and set-ups are added into the PC among  $n$  operations. Constraints in Eq. 17 and Eq. 18 ensure that every operation except the first and the last have only one adjacent operation on each side.

### 3. Introduction of the particle swarm optimization approach

PSO is a swarm optimization approach [16]. Every particle in the population represents an  $N$ -dimensional solution that constructs a search space for every particle. The particles fly freely to search for the optimal position at a given velocity. Hence, for the particle  $i$ , the vectors  $X_i^t$  and  $V_i^t$  at the  $t$ -th iteration can be denoted as  $X_i^t = \{X_{i1}^t, X_{i2}^t, \dots, X_{ik}^t, \dots, X_{iN}^t\}$  and  $V_i^t = \{V_{i1}^t, V_{i2}^t, \dots, V_{ik}^t, \dots, V_{iN}^t\}$ , respectively. With the emergence of the optimal position at iteration  $t + 1$ , the vectors  $X_i^t$  and  $V_i^t$  can be updated as follows:

$$V_{ik}^{t+1} = w * V_{ik}^t + c_1 * Rand( ) * (P_{ik}^t - X_{ik}^t) + c_2 * Rand( ) * (P_{gk}^t - X_{ik}^t) \tag{21}$$

$$X_{ik}^{t+1} = X_{ik}^t + V_{ik}^{t+1} \tag{22}$$

In Eq.21 and Eq.22,  $V_{ik}^{t+1}$  is the velocity on dimension  $k$ , and  $X_{ik}^{t+1}$  is the position on dimension  $k$ .  $P_{ik}^t$  is the local optimal position on dimension  $k$ , and  $P_{gk}^t$  is the global optimal position on dimension  $k$ . The weight  $w$  is used to control the iteration. The constants  $c_1$  and  $c_2$  control the balance between a local optimal position and the global optimal position.  $Rand( )$  is limited in  $[0, 1]$ . The traditional PSO approach is carried out in four steps:

Step 1: Population initialization.

Step 2: Update the vectors  $X_i^t$  and  $V_i^t$  according to Eq. 21 and Eq. 22.

Step 3: Update  $P_{ik}^t$  and  $P_{gk}^t$  according to the performance of the population

Step 4: Loop to Step 2 until a termination condition is met.

## 4. The proposed PSO approach

### 4.1 Solution representation

It is necessary to modify the traditional PSO for the PP problem to include, for example, particle representation and the particle movement strategy. In applying the PSO approach to the PP problem, three tasks have to be performed, namely, particle encoding, particle validation and particle decoding. The first task is to encode a process plan to an appropriate particle. Because operation determining and operation sequencing have to be performed simultaneously in pro-

cess planning, the particle structure should be considered to comprise the information of determining and sequencing operations. The details of a particle are listed in Table 4.

According to the definition of a particle, we modified a particle  $i$  of a  $2 \times n$  matrix to represent a process plan at iteration  $t$  [11], i.e.

$$X_i^t = \begin{bmatrix} x_{i11}^t, x_{i12}^t, \dots, x_{i1n}^t \\ x_{i21}^t, x_{i22}^t, \dots, x_{i2n}^t \end{bmatrix} \tag{23}$$

The first row  $x_{i1n}^t$  is the Operation Determining (OD) part and represents the operation selection for each feature. The second row  $x_{i2n}^t$  is the Operation Sequencing (OS) part and represents the priority among operations.  $x_{i2n}^t$  is initialized randomly in the range of 0 and 1 according to the priority among operations, and  $x_{i1n}^t$  can be calculated by Eq. 24.

$$X_{i1n}^t = (a^2 * ix\_m + a * ix\_c + ix\_t) / a^3 \tag{24}$$

In Eq. 24,  $ix\_m$ ,  $ix\_c$ , and  $ix\_t$  are generated randomly from the candidate machine set, cutting tool set, and TAD set for executing the operation.  $a$  can be given by the equation

$$a = \text{Max}(N_M, N_T, N_S) + 1 \tag{25}$$

where  $N_S$  is the number of TADs.

To illustrate the particle encoding, the process plan in Table 3 is taken as an example and the corresponding encoding of  $x_{i1n}^t$  is shown in Fig. 2. For instance, the values of  $ix\_m$ ,  $ix\_c$ , and  $ix\_t$  are set to 1 if the OPTs of M2, T1 and +X, respectively, are selected to process operation  $OP_1$ . If the OPTs of M2, T1 and +Z are selected to process operation  $OP_1$ , the values of  $ix\_m$ ,  $ix\_c$ , and  $ix\_t$  will be 1, 1, and 3, respectively.

For the process plan in Table 3, a feasible particle is listed in Table 5. In Table 5, the first row means the operations. The second row represents the calculated value of its assigned OPT, and the third row represents the priority among the operations. The second task is to validate the particles to accord with the precedence constraints. A particle represents a process plan. Nevertheless, process plans generated by particles flying freely in solution space are usually invalid against the precedence constraints. To validate each particle, an  $n \times n$  constraint matrix  $P$  is proposed to incorporate the precedence constraints among the operations into the particles.

**Table 4** Detail of a particle

Data type	Variable	Description
Integer	$ix\_o$	Id of an operation, which corresponds to the index of the operation set.
Integer	$ix\_m$	Id of a machine, which corresponds to the index of the machine set.
Integer	$ix\_c$	Id of a cutting tool, which corresponds to the index of the cutting tool set.
Integer	$ix\_t$	Id of a TAD, which corresponds to the index of the TAD set.

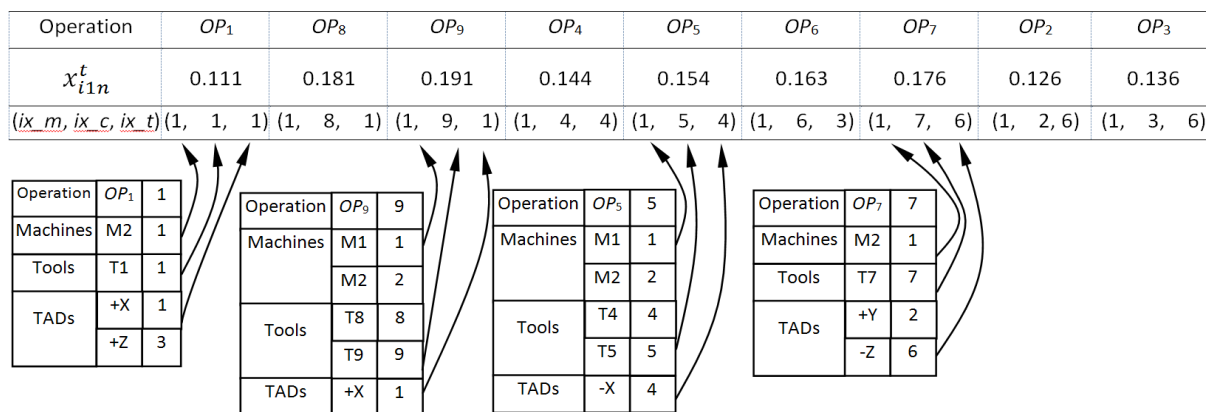


**Fig. 2** Encoding of  $x_{i1n}^t$  for the process plan in Table 3

**Table 5** A feasible particle for the process plan in Table 3

Operation	$OP_1$	$OP_2$	$OP_3$	$OP_4$	$OP_5$	$OP_6$	$OP_7$	$OP_8$	$OP_9$
$x_{i1n}^t$	0.111	0.126	0.136	0.144	0.154	0.164	0.176	0.181	0.191
$x_{i2n}^t$	1	0.50	0.40	0.85	0.75	0.70	0.60	0.95	0.90

The second task is to validate the particles to accord with the precedence constraints. A particle represents a process plan. Nevertheless, process plans generated by particles flying freely in solution space are usually invalid against the precedence constraints. To validate each particle, an  $n \times n$  constraint matrix  $P$  is proposed to incorporate the precedence constraints among the operations into the particles.

$$P = (p_{ij})_{n \times n} \tag{26}$$

$$P_{ij} = \begin{cases} 1 & OP_i \text{ is prior to } OP_j \text{ or } i = j \\ 0 & \text{otherwise} \end{cases} \tag{27}$$

The precedence constraint matrix for the precedence constraints in Table 2 is shown as follows:

$$\begin{bmatrix} 1 & 0 & 0 & 0 & 0 & 0 & 0 & 0 & 0 \\ 1 & 1 & 0 & 0 & 0 & 1 & 0 & 0 & 0 \\ 1 & 1 & 1 & 0 & 0 & 1 & 0 & 0 & 0 \\ 1 & 0 & 0 & 1 & 0 & 0 & 0 & 0 & 0 \\ 1 & 0 & 0 & 1 & 1 & 0 & 0 & 0 & 0 \\ 0 & 0 & 0 & 1 & 1 & 1 & 0 & 0 & 0 \\ 0 & 0 & 0 & 0 & 0 & 0 & 1 & 1 & 1 \\ 0 & 0 & 0 & 0 & 0 & 0 & 0 & 1 & 0 \\ 0 & 0 & 0 & 0 & 0 & 0 & 0 & 1 & 1 \end{bmatrix} \tag{28}$$

The third task is to decode a particle into a solution. According to the input of encoded position matrix, a particle can be decoded to obtain a process plan. The particle decoding includes the following two steps.

First, determine the machine, cutting tool and TAD according to the value  $x_{i1n}^t$ . The decoding approach for  $x_{i1n}^t$  is

$$y_{in} = x_{i1n}^t * a^3 \tag{29}$$

$$ix\_m_{in} = \lfloor y_{in}/a^2 \rfloor \tag{30}$$

$$ix\_c_{in} = \lfloor (y_{in} - ix\_m_{in} * a^2)/a \rfloor \tag{31}$$

$$ix\_t_{in} = y_{in} - ix\_m_{in} * a^2 - ix\_c_{in} * a \tag{32}$$

where  $y_{in}$  is an integer.

Second, sequence these determined operations according to the precedence value  $x_{i2n}^t$ . If the sequence of operations violates the precedence constraints, the operations should be sequenced again according to the precedence value  $x_{i2n}^t$  with the help of the precedence matrix  $P_m$ .

$$x_{i2n}^t = x_{i2n}^t \times P_m \tag{33}$$

Similarly, for particle  $i$ , a velocity matrix at iteration  $t$  can be represented as

$$V_i^t = [v_{i1}^t, v_{i2}^t, \dots, v_{ik}^t, \dots, v_{in}^t] \tag{34}$$

where  $v_{in}^t$  is initialized randomly in the range of  $-1$  to  $1$ .



## 4.2 Population initialization

The particle swarm is initialized in three steps:

- (i) Set the population size  $P_{max}$  and the maximum iteration number  $N_{max}$ .
- (ii) Initialize each particle. The initial position and velocity of each of the particles in the population are generated.
- (iii) Decode every particle to the process plan according to Eq. 29 to Eq. 33, and then calculate CP. Get the local optimal position  $P_i^0$  and the global optimal position  $P_g^0$ .

## 4.3 Iteration and control

For every selected particle, the position and velocity can be updated according to Eq. 21 and Eq. 22. To ensure the process plan validity, decoding every newly generated particle to the process plan is necessary. If the new process plans violate the precedence constraints, the corresponding particles will be normalized by using the constraint matrix  $P$ . For each valid particle, the CP of the corresponding process plan will be calculated. If a lower CP is achieved, the local optimal position  $P_i$  and the global optimal position  $P_g$  will be updated.

When the traditional PSO is applied in the PP problem, a quick local convergence at an early stage of the PSO usually has to be faced. The quick local convergence will make further exploration difficult and can generate an undesirable solution. To solve this problem, some modifications are suggested to enhance the performance of the traditional PSO algorithm [9, 10, 13]. Four operators are incorporated into the traditional PSO approach. Because the position of a particle is expressed as a  $2 \times n$  matrix, in which the first row is the OD part and the second row is the OS part, the operators for the different rows vary independently.

For the OD part, two types of mutation operator are designed to generate a new solution.

### *Mutation operator 1*

One particle in the swarm is chosen for a mutation operation with a predefined probability ( $p_{ms}$ ). First, for the OD part of this particle, one position point  $L$  is randomly selected. Second, decode the particle to a process plan, and obtain the machine, cutting tool, and TAD (M, T, TAD) of the  $L$ th operation in this process plan. Third, from the machine set, cutting tool set, and TAD set of the  $L$ th operation, an alternative selection of machine, cutting tool, and TAD is determined to replace the current machine, cutting tool, and TAD.

### *Mutation operator 2*

One particle is chosen for a mutation operation with a predefined probability ( $p_{ss}$ ). For the OD part of this particle, two adjacent position points  $L_1$  and  $L_2$  are randomly selected. Decode the particle to a process plan, and obtain the machines, cutting tools, and TADs (Ms, Ts, TADs) of the  $L_1$ -th and  $L_2$ -th operations in this process plan. If  $M_{L_2} = M_{L_1}$ , let  $T_{L_1} = T_{L_2}$  or  $TAD_{L_1} = TAD_{L_2}$ , or otherwise the position points  $L_1, L_2$  will be reselected.

With respect to the OS part, two operators are employed, crossover and shift.

### *Crossover operator*

Two particles,  $A$  and  $B$ , are selected to execute a crossover operation with a predefined probability ( $p_{cq}$ ). For the OS part of those two particles, one position point  $L$  is randomly determined. The OS part is divided into two parts. Subsequently, the value of the front part of  $OS_A$  is taken out and inserted before the cutting point of  $OS_B$ , and the value of the left part of  $OS_B$  is taken out and inserted before the cutting point of  $OS_A$ .

### *Shift operator*

One particle is chosen for a shift operation with a predefined probability ( $p_{sq}$ ). For the OS part of this particle, two position points  $L_1, L_2$  are randomly selected, and their values  $x_{i1L_1}^t, x_{i1L_2}^t$  exchanged.

#### 4.4 Termination

If the max number of iterations  $N_{max}$  is reached, the iteration will be terminated. Decode the obtained particle position  $P_g^t$  to achieve the final process plan.

The flowchart is described in Fig. 3.

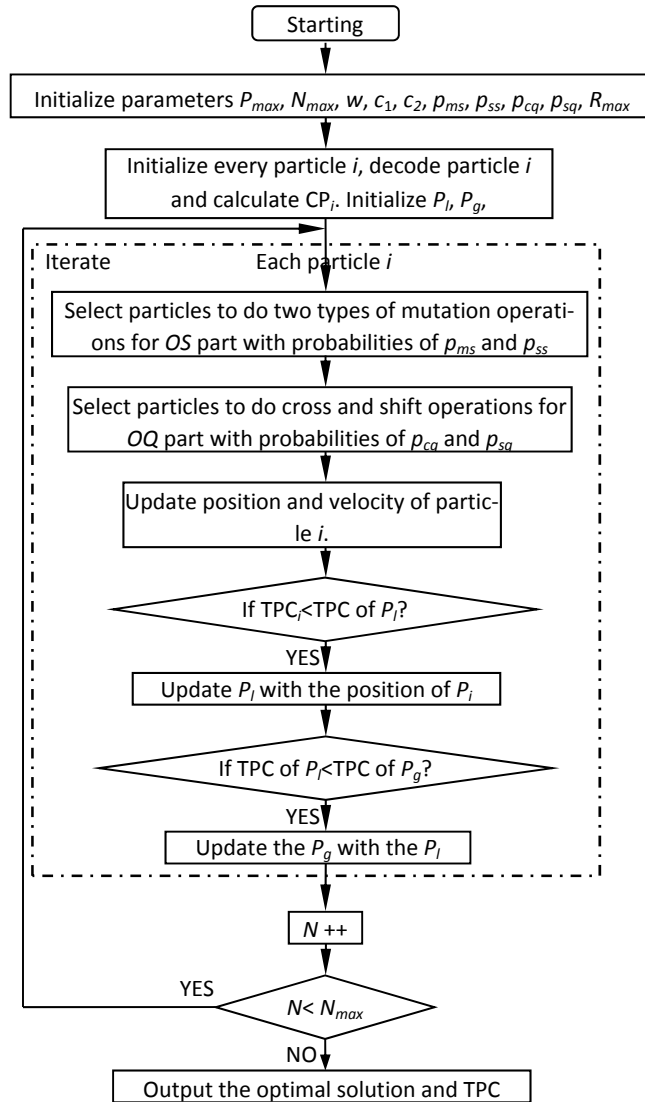


Fig. 3 Flowchart of the modified PSO approach

### 5. Experiments and results

Two characteristic parts are used for the simulation experiments. The first part is shown in Fig. 4 [1] (Part 2), and the second part is shown in Fig. 5 [2] (Part 3). The detailed information on Part 2 and Part 3 is introduced in the research of Li et al. [4]. All of the simulation experiments will be performed on a PC with 2.8 GHz and the Windows 7 operating system.

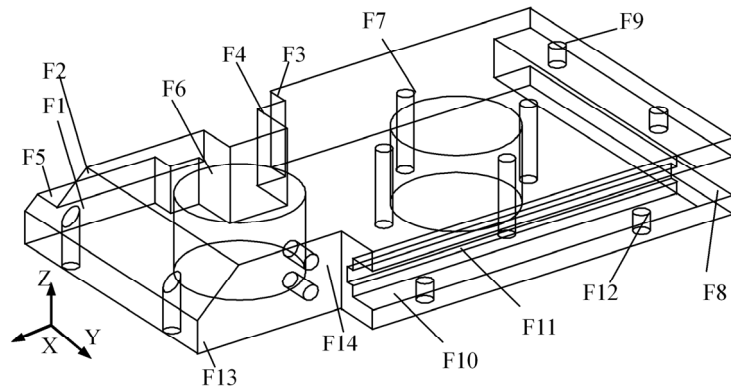


Fig. 4 An example part - Part 2

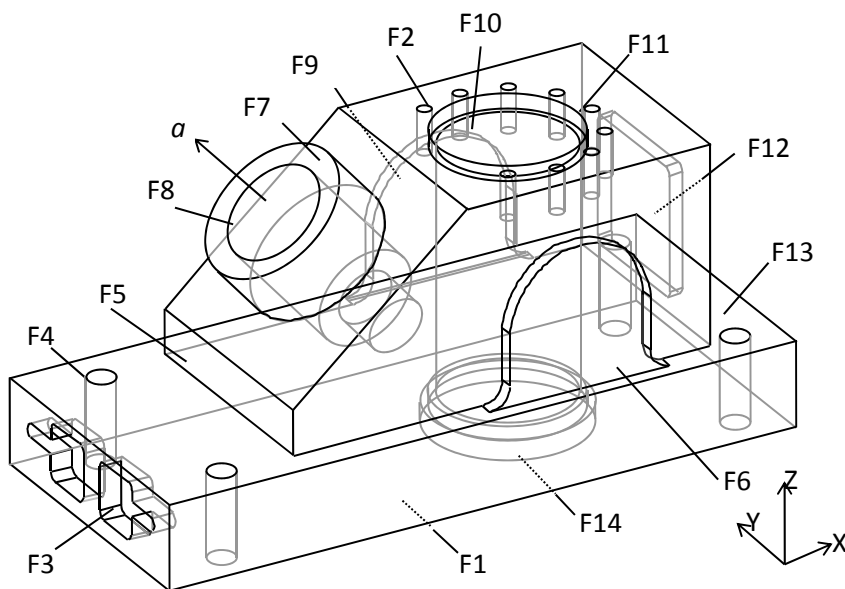


Fig. 5 An example part - Part 3

### 5.1 Simulation experiments

While applying PSO to solve the process planning problem, the key parameters have to be determined to facilitate the performance of the modified PSO. Accordingly, many preliminary simulation experiments have to be carried out to determine those parameters. The process planning problem for Part 2 is used to illustrate how the key parameters are determined. It is assumed that  $\omega_1$  to  $\omega_5$  in Eq. 13 are set as 1.

The key parameters may be analysed from two aspects, namely, the swarm characteristic parameters of PSO ( $P_{max}$ ,  $N_{max}$ ,  $w$ ,  $c_1$ ,  $c_2$ ) and the problem data ( $p_{ms}$ ,  $p_{ss}$ ,  $p_{cq}$ ,  $p_{sq}$ ). The swarm size  $P_{max}$  and iteration number  $N_{max}$  will be increased with the increased complexity of the part. For Part 2, after many trials,  $P_{max}$  and  $N_{max}$  are fixed at 2000 and 300, respectively.

The constants  $c_1$  and  $c_2$  are used to balance the velocity tendency to the local optimal position  $P_l$  and the global optimal position  $P_g$ . If  $c_1$  and  $c_2$  are too large, the search space of the particles will be expanded, which may even lead to no convergence of the PSO. If  $c_1$  and  $c_2$  are too small, slow convergence may cause the computation time to be very long. In the case of problems with  $P_{max} = 2000$ ,  $N_{max} = 300$ ,  $w = 0.75$ ,  $p_{ms} = 0.6$ ,  $p_{ss} = 0.6$ ,  $p_{cq} = 0.2$ ,  $p_{sq} = 0.2$ , 50 trials were separately conducted by varying the values of  $c_1 = c_2 \in \{1, 1.5, 2\}$ . The average results are summarized in Fig. 6.

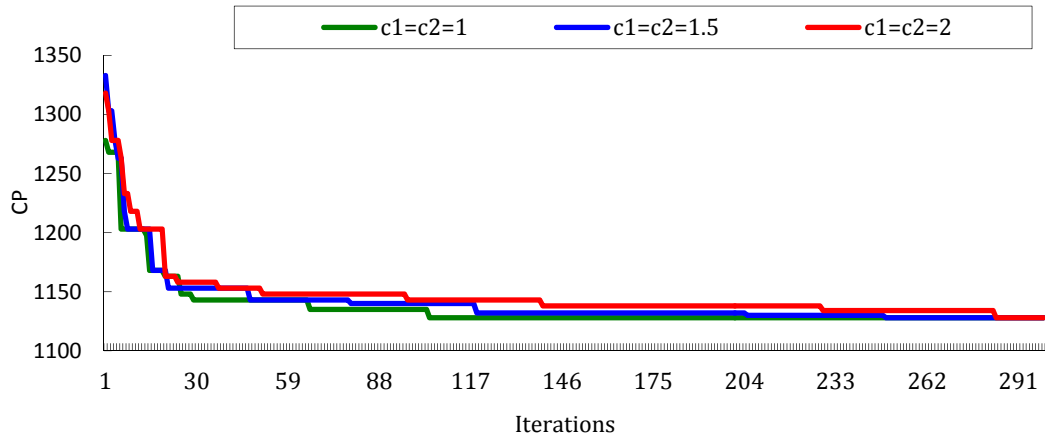


Fig. 6 CP of the proposed PSO with different constants  $c_1$  and  $c_2$

From Fig. 6, when  $c_1$  and  $c_2$  are both set to be 1, the PSO algorithm shows fast convergence and good computational efficiency.

The inertia weight  $w$  is set to coordinate the local exploration and the global exploration. If  $w$  is too large, there may be a quick local convergence at an early stage of the PSO. If  $w$  is too small, the computation time for each iteration will be long, and the optimization rate will become very slow. In the case of problems with  $P_{max} = 2000$ ,  $N_{max} = 300$ ,  $c_1 = c_2 = 1$ ,  $p_{ms} = 0.6$ ,  $p_{ss} = 0.6$ ,  $p_{cq} = 0.2$ ,  $p_{sq} = 0.2$ , 50 trials were separately conducted by varying the values of  $w \in \{0.75, 1, 1.25\}$ . The average results are summarized in Fig. 7.

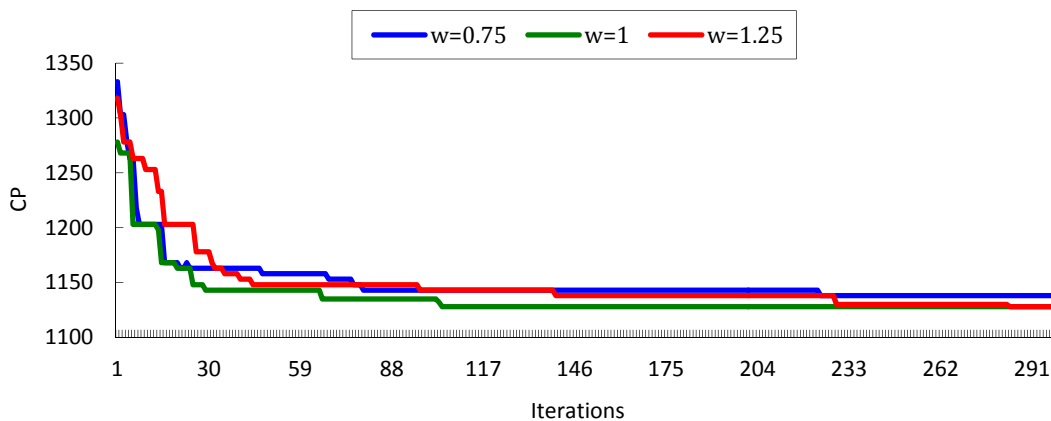


Fig. 7 CP of the proposed PSO with different inertia weights  $w$

From Fig. 7, the optimal efficiency and stability are achieved under the condition of  $w = 1$ . The problem data ( $p_{ms}$ ,  $p_{ss}$ ,  $p_{cq}$ ,  $p_{sq}$ ) are determined to help the approach escape from local convergences. Fifty trials are conducted in 8 group combinations of the four parameters  $p_{ms}$ ,  $p_{ss}$ ,  $p_{cq}$ ,  $p_{sq}$  to illustrate the selection of these parameters. The average CPs for the 50 trials are listed in Table 6. It is shown that the combination of  $p_{ms} = 0.6$ ,  $p_{ss} = 0.6$ ,  $p_{cq} = 0.2$  and  $p_{sq} = 0.2$  can yield the best performance. In conclusion, the performance of the modified PSO for Part 2 is good, and  $P_{max} = 2000$ ,  $N_{max} = 300$ ,  $w = 1$ ,  $c_1 = c_2 = 1$ ,  $p_{ms} = 0.6$ ,  $p_{ss} = 0.6$ ,  $p_{cq} = 0.2$ ,  $p_{sq} = 0.2$ . The best simulation result and average simulation result are shown in Table 7 and Table 8, respectively.

Table 6 Determination of four probabilities of the modified PSO

	(Mutation1: $p_{ms}$ , Mutation2: $p_{ss}$ , Crossover: $p_{cq}$ , Shift: $p_{sq}$ )							
	(0.6, 0.4, 0.2, 0.4)	(0.4, 0.6, 0.4, 0.2)	(0.6, 0.6, 0.4, 0.4)	(0.6, 0.6, 0.2, 0.2)	(0.4, 0.4, 0.2, 0.2)	(0.4, 0.4, 0.4, 0.4)	(0.4, 0.6, 0.2, 0.4)	(0.6, 0.4, 0.4, 0.2)
Mean	1198.5	1198.8	1308.4	1131.8	1136.6	1541.3	1206.1	1186.7
Maximum	1263	1318	1713	1163	1188	1998	1318	1263
Minimum	1143	1143	1148	1128	1128	1158	1143	1143

**Table 7** Best simulation result for Part 2

Operation	Machine	Tool	TAD	Result
6	2	2	-Z	<i>CM</i> = 490
1	2	1	-Z	<i>CT</i> = 98
7	2	1	-Z	<i>CTC</i> = 60
9	2	1	-Z	<i>CS</i> = 480
12	2	1	-Z	<i>CP</i> = 1128
5	2	5	-Z	
3	2	5	+Y	
4	2	5	+Y	
8	2	5	+X	
10	2	5	-Y	
11	2	5	-Y	
13	2	5	-Y	
14	2	1	-Y	
2	2	8	-Y	

**Table 8** Average simulation result of 50 trials for Part 2

Type	Mean	Maximum	Minimum	Standard deviation
<i>CM</i>	490	490	490	0
<i>CT</i>	98.2	103	98	0.98
<i>CMC</i>	0	0	0	0
<i>CTC</i>	60.9	75	60	3.56
<i>CS</i>	480	480	480	0
<i>CP</i>	1128.9	1143.0	1128	3.56

The above method of determining the key parameters is based on Part 2. The method of choosing parameters for Part 3 is same as for Part 2. In the case of problems with  $P_{max} = 2000$ ,  $N_{max} = 500$ ,  $w = 1.25$ ,  $c_1 = c_2 = 1$ ,  $p_{ms} = 0.6$ ,  $p_{ss} = 0.6$ ,  $p_{cq} = 0.3$ ,  $p_{sq} = 0.3$ , 50 trials were separately conducted. The best process plans are listed in Table 9, and the average results are listed in Table 10.

**Table 9** Best simulation result for Part 3

Operation	Machine	Tool	TAD	Result
1	2	6	+Z	<i>CM</i> = 770
3	2	6	+X	<i>CT</i> = 235
5	2	6	+X	<i>CMC</i> = 320
6	2	6	-Z	<i>CTC</i> = 200
2	2	6	-Z	<i>CS</i> = 1000
18	2	6	-Z	<i>CP</i> = 2525
11	2	7	-Z	
12	2	2	-Z	
13	2	9	-Z	
17	2	7	-X	
7	2	7	-a	
8	2	2	-a	
9	2	9	-a	
19	2	9	+Z	
14	4	10	-Z	
20	4	10	+Z	
10	4	10	-a	
4	1	2	-Z	
15	1	1	-Z	
16	1	5	-Z	

**Table 10** Average simulation result of 50 trials for Part 3

Type	Mean	Maximum	Minimum	Standard deviation
<i>CM</i>	770	770	770	0
<i>CT</i>	240	267	235	10.13
<i>CMC</i>	320	320	320	0
<i>CTC</i>	197.2	180	200	6.94
<i>CS</i>	1000	1000	1000	0
<i>CP</i>	2527.2	2535.0	2525.0	3.28

## 5.2 Extensive comparative experiments

The following three conditions are used to verify the modified PSO approach for the example parts [2, 4, 6]:

- All machines and cutting tools are available, and  $\omega_1$  to  $\omega_5$  in Eq. 13 are set as 1.
- All machines and cutting tools are available, and  $\omega_1 = \omega_5 = 0$ ,  $\omega_2 = \omega_3 = \omega_4 = 1$ .
- $M_2$  and  $T_7$  are down,  $\omega_2 = \omega_5 = 0$ ,  $\omega_1 = \omega_3 = \omega_4 = 1$ .

For Part 2, 50 trials were performed under conditions (a) and (b). A penalty cost is included in the *CP* to facilitate the comparison with other approaches, which is 200 for Part 2 [4, 7]. A comparison with the results obtained using the GA and SA approaches [2], TS [4], and HBMO [14], as well as the two-stage ACO [7], is provided in Table 11.

Under condition (a), this approach is same as SA, TS, HBMO, and two-stage ACO and is better than GA using the minimum machine costs. Using the maximum machine costs, the *CP* (1328.0) is the same as that of HBMO, and it is better than the other four approaches. This approach has the best performance in the mean machine cost (1328). It is obvious that the same *CP* (1328.0) is achieved 50 times and is superior to all of the other approaches.

Under condition (b), the performance of this approach is the same as those of HBMO and the two-stage ACO. Using the minimum machine costs, this approach is better than GA, and it is the same as the other four approaches. Using the maximum and mean machine costs, this approach is better than GA, SA, and TS.

For Part 3, 50 trials were carried out under conditions (a), (b), and (c). A comparison of the results with those of TS [4], PSO [9], and HBMO [14], as well as the two-stage ACO [7] is provided in Table 12.

**Table 11** Results compared to other approaches

Condition	Proposed approach	GA	SA	TS	HBMO	Two-stage ACO
(a)						
Mean	1328	1611.0	1373.5	1342.6	1328	1329
Maximum	1328	1778	1518	1378	1328	1348
Minimum	1328	1478	1328	1328	1328	1328
(b)						
Mean	1170	1482	1217	1194	1170	1170
Maximum	1170	1650	1345	1290	1170	1170
Minimum	1170	1410	1170	1170	1170	1170

**Table 12** Results compared to other approaches

Condition	Proposed approach	TS	PSO	HBMO	Two-stage ACO
(a)					
Mean	2527.2	2609.6	2680.5	2543.5	2552.4
Maximum	2535	2690	-	2557	2557
Minimum	2525	2527	2535	2525	2525
(b)					
Mean	2093.0	2208.0	-	2098.0	2120.5
Maximum	2120	2390	-	2120	2380
Minimum	2090	2120	-	2090	2090
(c)					
Mean	2593.2	2630.0	-	2592.4	2600.8
Maximum	2600	2740	-	2600	2740
Minimum	2590	2580	-	2590	2590

Under condition (a), the minimum machine cost is the same as that of HBMO and the two-stage ACO, and it is better than TS and PSO. Among the 50 trial results, *CP* (2525) occurs 23 times, *CP* (2527) occurs 20 times, and *CP* (2535) occurs 7 times. Accordingly, this approach is superior to all of the other approaches on the mean machine cost. Under condition (b), the minimum machine cost (2090) is the same as that of HBMO and the two-stage ACO. *CP* (2090) occurs 45 times, and *CP* (2120) occurs 5 times in 50 trials; the mean machine cost is the best among all of the approaches. Under condition (c), *CP* (2590) occurs 34 times, and *CP* (2600) occurs 16 times in 50 trials. Generally, the performance of this approach is similar to that of HBMO under condition (c) and is superior to those of the two-stage ACO and TS.

## 6. Conclusions

A traditional PSO approach is modified to solve the PP problem. Efficient encoding and decoding, population initialization, and iteration and control methods have been designed. Meanwhile, to avoid local convergence, several new operators for the different parts of the particles have been designed and incorporated into the traditional PSO to improve the particles' movements. Simulation experiments show that the modified PSO algorithm can perform the process plan optimization competently and consistently and generate better solutions compared with other approaches.

In the simulation experiment, a small change in the parameters induces computational result saltation. Hence, a deep discussion of selecting the modified PSO approach parameters will be conducted. Additionally, integrated process planning and scheduling that considers the better performance of manufacturing systems may be a direction for further study [21, 22].

## References

- [1] Zhang, F., Zhang, Y.F., Nee, A.Y.C. (1997). Using genetic algorithms in process planning for job shop machining, *IEEE Transactions on Evolutionary Computation*, Vol. 1, No. 4, 278-289, doi: [10.1109/4235.687888](https://doi.org/10.1109/4235.687888).
- [2] Li, W.D., Ong, S.K., Nee, A.Y.C. (2002). Hybrid genetic algorithm and simulated annealing approach for the optimization of process plans for prismatic parts, *International Journal of Production Research*, Vol. 40, No. 8, 1899-1922, doi: [10.1080/00207540110119991](https://doi.org/10.1080/00207540110119991).
- [3] Ma, G.H., Zhang, Y.F., Nee, A.Y.C. (2000). A simulated annealing-based optimization algorithm for process planning, *International Journal of Production Research*, Vol. 38, No. 12, 2671-2687, doi: [10.1080/002075400411420](https://doi.org/10.1080/002075400411420).
- [4] Li, W.D., Ong, S.K., Nee, A.Y.C. (2004). Optimization of process plans using a constraint-based tabu search approach, *International Journal of Production Research*, Vol. 42, No. 10, 1955-1985, doi: [10.1080/00207540310001652897](https://doi.org/10.1080/00207540310001652897).
- [5] Lian, K.L., Zhang, C.Y., Shao, X.Y., Zeng, Y.H. (2011). A multi-dimensional tabu search algorithm for the optimization of process planning, *Science China Technological Sciences*, Vol. 54, No. 12, 3211-3219, doi: [10.1007/s11431-011-4594-7](https://doi.org/10.1007/s11431-011-4594-7).
- [6] Liu, X.-J., Yi, H., Ni, Z.-H. (2013). Application of ant colony optimization algorithm in process planning optimization, *Journal of Intelligent Manufacturing*, Vol. 24, No. 1, 1-13, doi: [10.1007/s10845-010-0407-2](https://doi.org/10.1007/s10845-010-0407-2).
- [7] Wang, J.F., Wu, X., Fan, X. (2015). A two-stage ant colony optimization approach based on a directed graph for process planning, *The International Journal of Advanced Manufacturing Technology*, Vol. 80, No. 5, 839-850, doi: [10.1007/s00170-015-7065-7](https://doi.org/10.1007/s00170-015-7065-7).
- [8] Hu, Q., Qiao, L., Peng, G. (2015). An ant colony approach to operation sequencing optimization in process planning, (In press), *Proceedings of the Institution of Mechanical Engineers, Part B: Journal of Engineering Manufacture*, doi: [10.1177/0954405415616786](https://doi.org/10.1177/0954405415616786).
- [9] Guo, Y.W., Mileham, A.R., Owen, G.W., Li, W.D. (2006). Operation sequencing optimization using a particle swarm optimization approach, *Proceedings of the Institution of Mechanical Engineers, Part B: Journal of Engineering Manufacture*, Vol. 220, No. 12, 1945-1958.
- [10] Kafashi, S., Shakeri, M., Abedini, V. (2012). Automated setup planning in CAPP: a modified particle swarm optimisation-based approach, *International Journal of Production Research*, Vol. 50, No. 15, 4127-4140, doi: [10.1080/00207543.2011.592157](https://doi.org/10.1080/00207543.2011.592157).
- [11] Wang, Y.F., Zhang, Y.F., Fuh, J.Y.H. (2012). A hybrid particle swarm based method for process planning optimisation, *International Journal of Production Research*, Vol. 50, No. 1, 277-292, doi: [10.1080/00207543.2011.571459](https://doi.org/10.1080/00207543.2011.571459).
- [12] Li, X., Gao, L., Wen, X. (2013). Application of an efficient modified particle swarm optimization algorithm for process planning, *The International Journal of Advanced Manufacturing Technology*, Vol. 67, No. 5, 1355-1369, doi: [10.1007/s00170-012-4572-7](https://doi.org/10.1007/s00170-012-4572-7).

- [13] Miljković, Z., Petrović, M. (2016). Application of modified multi-objective particle swarm optimisation algorithm for flexible process planning problem, (In press), *International Journal of Computer Integrated Manufacturing*, doi: [10.1080/0951192X.2016.1145804](https://doi.org/10.1080/0951192X.2016.1145804).
- [14] Wen, X.-Y., Li, X.-Y., Gao, L., Sang, H.-Y. (2014). Honey bees mating optimization algorithm for process planning problem, *Journal of Intelligent Manufacturing*, Vol. 25, No. 3, 459-472, doi: [10.1007/s10845-012-0696-8](https://doi.org/10.1007/s10845-012-0696-8).
- [15] Huang, W., Hu, Y., Cai, L. (2012). An effective hybrid graph and genetic algorithm approach to process planning optimization for prismatic parts, *The International Journal of Advanced Manufacturing Technology*, Vol. 62, No. 9, 1219-1232, doi: [10.1007/s00170-011-3870-9](https://doi.org/10.1007/s00170-011-3870-9).
- [16] Kennedy, J., Eberhart, R. (1995). Particle swarm optimization, In: *Proceedings of the 1995 IEEE International Conference on Neural Networks*, Perth, WA, IEEE Press, Vol. 4, 1942-1948, doi: [10.1109/icnn.1995.488968](https://doi.org/10.1109/icnn.1995.488968).
- [17] Hrelja, M., Klančnik, S., Irgolic, T., Paulic, M., Jurkovic, Z., Balic, J., Brezocnik, M. (2014). Particle swarm optimization approach for modelling a turning process, *Advances in Production Engineering & Management*, Vol. 9, No. 1, 21-30, doi: [10.14743/apem2014.1.173](https://doi.org/10.14743/apem2014.1.173).
- [18] Wang, Y., Liu, J.H. (2010). Chaotic particle swarm optimization for assembly sequence planning, *Robotics and Computer-Integrated Manufacturing*, Vol. 26, No. 2, 212-222, doi: [10.1016/j.rcim.2009.05.003](https://doi.org/10.1016/j.rcim.2009.05.003).
- [19] Malik, J., Mishra, R., Singh, I. (2011). PSO-ANN approach for estimating drilling induced damage in CFRP laminates, *Advances in Production Engineering & Management*, Vol. 6, No. 2, 95-104.
- [20] Xu, X., Wang, L., Newman, S.T. (2011). Computer-aided process planning – A critical review of recent developments and future trends, *International Journal of Computer Integrated Manufacturing*, Vol. 24, No. 1, 1-31, doi: [10.1080/0951192X.2010.518632](https://doi.org/10.1080/0951192X.2010.518632).
- [21] Dai, M., Tang, D., Xu, Y., Li, W. (2015). Energy-aware integrated process planning and scheduling for job shops, *Proceedings of the Institution of Mechanical Engineers, Part B: Journal of Engineering Manufacture*, Vol. 229, No. 1, 13-26, doi: [10.1177/0954405414553069](https://doi.org/10.1177/0954405414553069).
- [22] Wang, J., Fan, X., Zhang, C., Wan, S. (2014). A graph-based ant colony optimization approach for integrated process planning and scheduling, *Chinese Journal of Chemical Engineering*, Vol. 22, No. 7, 748-753, doi: [10.1016/j.cjche.2014.05.011](https://doi.org/10.1016/j.cjche.2014.05.011).



# Surface roughness assessing based on digital image features

Simunovic, G.<sup>a,\*</sup>, Svalina, I.<sup>a</sup>, Simunovic, K.<sup>a</sup>, Saric, T.<sup>a</sup>, Havrlisan, S.<sup>a</sup>, Vukelic, D.<sup>b</sup>

<sup>a</sup>Mechanical Engineering Faculty in Slavonski Brod, University of Osijek, Croatia

<sup>b</sup>Faculty of Technical Sciences, University of Novi Sad, Serbia

## ABSTRACT

The paper gives an account of the machined surface roughness investigation based on the features of a digital image taken subsequent to the technological operation of milling of aluminium alloy Al6060. The data used for investigation were obtained by mixed-level factorial design with two replicates. Input variables (factors) are represented by the face milling basic machining parameters: spindle speed (at five levels: 2000; 3500; 5000; 6500; 8000 rev/min, respectively), feed per tooth (at six levels: 0.025; 0.1; 0.175; 0.25; 0.325; 0.4 mm/tooth, respectively) and depth of cut (at two levels: 1; 2 mm, respectively). Output variable or response is the most frequently used surface roughness parameter – arithmetic average of the roughness profile, *Ra*. Digital image of the machined surface is provided for every test sample. Based on experimental design and obtained results of roughness measuring, a base has been created of input data (features) extracted from digital images of the samples' machined surfaces. This base was later used for generating the fuzzy inference system for prediction of the surface roughness using the adaptive neuro-fuzzy inference system (ANFIS). Assessing error, i.e. comparison of the assessed value *Ra* provided by the system with real *Ra* values, is expressed with the normalized root mean square error (NRMSE) and it is 0.0698 (6.98 %).

© 2016 PEI, University of Maribor. All rights reserved.

## ARTICLE INFO

### Keywords:

Surface roughness  
Face milling  
Digital image  
Adaptive neuro-fuzzy inference system

### \*Corresponding author:

goran.simunovic@sfsb.hr  
(Simunovic, G.)

### Article history:

Received 7 March 2016  
Revised 15 May 2016  
Accepted 16 May 2016

## 1. Introduction

Surface roughness is an important technological parameter and indicator of the machined surface quality. Requirements for lower values of surface roughness simultaneously affect the prolongation of machining time and increase of production costs. Surface roughness is conditioned by a larger number of controlled and uncontrolled process parameters (including cutting speed, depth of cut and feed rate, raw material properties, cutting conditions, tool properties, tool machine vibrations, tool wear etc.). By regular monitoring the results of a machining process and expanding the knowledge base about the monitored parameters of observed processes, it is possible to continuously improve a product characteristic and production results.

There is a great number of scientific investigations aimed at prediction and control of surface roughness [1-4]. The models defined in these investigations can be divided into regression (statistic), analytic (mathematic) and those based on the application of artificial intelligence (AI) [5-8].

It is often the case that the digital image features of the machined surfaces are used in controlling or assessing the machined surface roughness. The image features are used as input variables for the assessing model [9-13], and they are mostly represented by statistic values such as arithmetic mean and standard deviation [14], different kinds of standards such as the Euclidean and the Hamming norm [15], wave transformations such as the Haar wavelet transform [16] and

the two-dimensional Fourier transform [17] etc. Adaptive neuro-fuzzy inference system (ANFIS), artificial neural networks (ANN), regression analysis and others are the methods mostly used for assessing.

Lee et al. [14] propose a method using an adaptive neuro-fuzzy inference system (ANFIS) to establish the relationship between actual surface roughness and texture features of the surface image. The input parameters of a training model are spatial frequency, arithmetic mean value, and standard deviation of grey levels from the surface image. In paper [18] the ANFIS is also used in assessing the surface roughness using cutting parameters (cutting speed, feed rate, and depth of cut) and grey level of the surface image. The assessing model error is less than 4.6 %. In papers [19] and [20] machine vision system is also used integrated with ANFIS. Paper [19] assesses  $R_a$ , tool wear ratio and metal removal rate in micro-turning process. The assessing error is less than 3.5 %. Investigation in paper [20] is directed to assessment of surface roughness of end milled parts. Using a two dimensional Fourier transform (2D FT) features of image texture are extracted, such as peak frequency, principal component magnitude squared value and the average grey level. The ANFIS and the neural networks methods used in assessing roughness are compared and the assessing errors are very close and less than 2.5 %.

In paper [21] the Euclidean and Hamming distances of the surface images are used for surface recognition. Machined surface images with different values of surface roughness were collected. The base is formed of referent images with known values of surface roughness. The Euclidean and Hamming distances between the tested surface and the referent surface image were used in the base to predict the surface roughness of the unknown surface. Excellent concluding results were obtained and the system is suitable for online surface characterization of machined surfaces. The paper [16] presents methodology based on the extraction of texture features from part surface images in the frequency domain using wavelet transform. One-level Haar wavelet transform is applied to the original surface images. Surface evaluation was accomplished by means of the analysis of grey levels in the vertical detail sub-image of surface images. Experimental results show that the proposed approach achieves error rates between 2.59% and 4.17%. Paper [22] is also based on the application of the wavelet transform. Authors apply vision system for acquiring digital images of machined surfaces, analyse the image parameters and connect them with the roughness of the surface machined by turning. The machined surface digital images are described using the one-dimensional digital wavelet transform. The neural networks based system is used for assessing roughness. The testing phase error is a bit more than 5 %. Papers [23, 24] also apply Machine Vision and ANN. In paper [23] they are used to assess  $R_a$  values using the input obtained from the digital images of inclined surfaces which include optical roughness parameters (major peak frequency, principal component magnitude squared, average power spectrum, central power spectrum percentage, ratio of major axis to minor axis). To improve the quality of the images shadow removal algorithm is used. The high value of the ANN model correlation coefficient (87 %) confirms its applicability. Through computer vision system authors in paper [24] collect features of image texture of machined surface (major peak frequency, principal component magnitude squared value and the standard deviation of grey level and by the application of abductive networks they assess surface roughness of turned parts. The assessment error is around 15 %. Authors in papers [25-27] analyse interconnection between the machined surface texture and the machining time, in other words condition and wear of tools. Authors [25] have investigated the relationship between texture features of the grey-level co-occurrence matrix and the machining time in turning operations. Results of investigation have shown that the error between the actual and the calculated machining time ranges from -4.65 % to 7.79 %. Authors in paper [26] used machine vision technique to detect the condition of tools on the basis of turned surface images using an accurate grey level co-occurrence matrix. In paper [27] authors investigated cutting tool nose wear area and surface roughness of turned parts using machine vision system. They developed an algorithm that uses Wiener filtering and simple thresholding on backlit images in order to reduce the impact of ambient factors (ambient lighting) and vibrations. The developed system roughness assessing error was 10 %. In paper [28] authors investigated connection between surface roughness of AA 6061 alloy end milling and image texture features of milled surface. They used grey level co-occurrence matrix to ex-

tract the image texture features (contrast, homogeneity, correlation and energy). For establishing the relation between surface roughness and image texture the regression analysis is applied. The paper [29] demonstrates that some roughness parameters ( $Ra$ ,  $Rq$ ,  $Rv$ ,  $Rt$  and  $Rz$ ) can be estimated using only image-extracted features and models, without the knowledge of machining parameters. Authors observe three image texture features of turned surface: gradient factor of surface, average cycle of texture and average grey level. There is a very high correlation between surface roughness and the given features of digital image. Authors in [9] investigated surface lay in the surface roughness evaluation using machine vision. Numerous parameters of digital image are considered such as grey level average, grey level co-occurrence matrix based image quantification parameters (contrast, correlation, energy or uniformity, maximum probability and differential box courting based fractal dimension) of machined surface while changing the angle of taking images. Therefore, it can be concluded that investigations were directed towards building a system (machine vision system) for a quicker and cheaper control, i.e. assessment of the roughness of machined surfaces in real time. The actual paper investigations are an additional contribution for assessing roughness of machined surface based on the features of digital image using the adaptive neuro-fuzzy inference system (ANFIS).

## 2. Experimental and methodology

### 2.1 Experimental

Investigation is conducted on the material of samples Al6060 T66 (in accordance with the European norms EN AW-6060 T66 [AlMgSi]). Chemical composition of the alloy Al6060 or EN AW-6060 according to EN 573-3 is given in Table 1.

Mass fraction of other elements can be to the maximum of 0.15 %, and individually 0.05 %. Mechanical and physical properties (at 20 °C) of alloy Al6060 or EN AW-6060 according to EN 755-2 are given in Table 2.

Dimensions of samples are 100 × 60 × 10 mm. Samples (Fig. 1) are machined from flat bars of transverse section 60 × 10 mm.

For face milling of 100 × 60 mm surface vertical CNC milling machine was used produced by HASS type VF-2 and face milling cutter of diameter 40 mm produced by Walter with four cutting inserts (holder mark: F 4042.B.040.Z04.15 and inserts mark: ADMT160608R-F56 WKP35S). The machining was carried out based on CNC programme that repeated the same path of the tool. The following machining parameters were being changed: spindle speed, feed per tooth, and depth of cut in an order defined by the selected mixed-level factorial design. For clamping of samples a hydraulic machine vice Alfa NCO-A was used.

As the applied fuzzy inference system will have three inputs, the suggested factorial design has three factors. By a detailed analysis, considering the total number of input/output experimental data for the training phase and the checking phase of inference system, a mixed-level factorial design was selected. Five spindle speeds (2000; 3500; 5000; 6500; 8000 rev/min, respectively), six feeds per tooth (0.025; 0.1; 0.175; 0.25; 0.325; 0.4 mm/tooth, respectively) and two depths of cut (1; 2 mm, respectively) are used, and two replicates of a mixed-level factorial design are run.

**Table 1** Chemical composition of Al6060 according to EN 573-3 (wt%)

Si	Fe	Cu	Mn	Mg	Cr	Zn	Ti
0.3-0.6	0.1-0.3	max 0.1	max 0.1	0.35-0.6	max 0.1	max 0.1	max 0.1

**Table 2** Mechanical and physical properties (at 20 °C) of material Al6060 according to EN 755-2

Yield tensile strength, MPa	150	Density, kg/m <sup>3</sup>	2700
Ultimate tensile strength, MPa	195	Melting point, °C	585-650
Elongation at break, %	8	Electrical conductivity, mS/m	28-34
Hardness, HB	65	Thermal conductivity, W/mK	200-220
Modulus of elasticity, GPa	70	Coefficient of thermal expansion, 10 <sup>-6</sup> /K	23.4

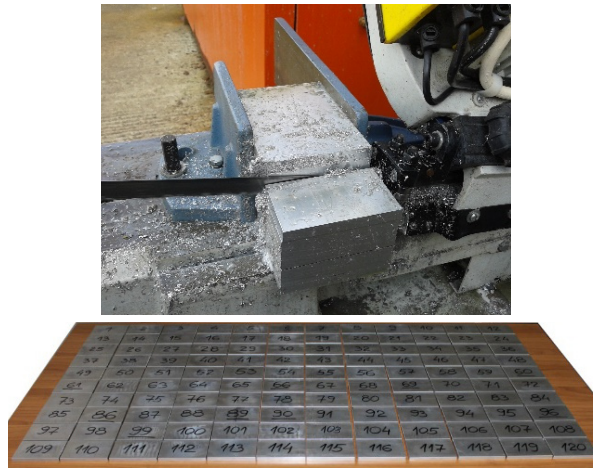


Fig. 1 Preparation of samples

All other features specific for end milling: tool stepover between neighbour paths, number of passes, total length of paths, are held-constant factors, the same as the Maxol cooling/lubricating fluid produced by Forol d.d., tool (milling cutter) and material of the sample.

### 2.2 Methodology

Adaptive neuro-fuzzy inference system (ANFIS) method for generating fuzzy inference system requires a set of input/output experimental data. The fuzzy inference system (FIS) has three input variables. In generating FIS the ANFIS method with three membership functions per each input was used. Therefore, 27 different fuzzy rules are used to form the base of fuzzy rules.

For the FIS first row the base of fuzzy rules can be written as:

Rule 1: If  $x$  is  $A_1$  and  $y$  is  $B_1$  and  $w$  is  $C_1$  then  $z$  is  $f_1(x, y, w)$

Rule 2: If  $x$  is  $A_2$  and  $y$  is  $B_2$  and  $w$  is  $C_2$  then  $z$  is  $f_2(x, y, w)$

...

Rule 27: If  $x$  is  $A_3$  and  $y$  is  $B_3$  and  $w$  is  $C_3$  then  $z$  is  $f_{27}(x, y, w)$

where  $x, y$  and  $w$  present ANFIS inputs,  $A_j, B_j$  and  $C_j$  fuzzy sets, and  $f_i(x, y, w)$  is the polynomial first row and represents the output of the first row of Sugeno FIS. The system has adaptive nodes (the sets' parameters that are changeable-adaptive) and fixed nodes (the sets' parameters that are fixed-unchangeable). By arrangement, the nodes outputs are marked as  $Q_{l,i}$  where  $l$  represents the layer and  $i$  the number of nodes.

Five layers are usually used to explain the ANFIS architecture.

Layer 1 contains adaptive nodes. Layer 1 node functions are described as:

$$\begin{aligned}
 Q_{1,i} = \mu_{A_j}(x) & \begin{cases} j = 1 \text{ for } i = 1, \dots, 9 \\ j = 2 \text{ for } i = 10, \dots, 18 \\ j = 3 \text{ for } i = 19, \dots, 27 \end{cases} \\
 Q_{1,i} = \mu_{B_j}(y) & \begin{cases} j = 1 \text{ for } i = 1, 2, 3, 10, 11, 12, 19, 20, 21 \\ j = 2 \text{ for } i = 4, 5, 6, 13, 14, 15, 22, 23, 24 \\ j = 3 \text{ for } i = 7, 8, 9, 16, 17, 18, 25, 26, 27 \end{cases} \\
 Q_{1,i} = \mu_{C_j}(w) & \begin{cases} j = 1 \text{ for } i = 1, 4, 7, \dots, 25 \\ j = 2 \text{ for } i = 2, 5, 8, \dots, 26 \\ j = 3 \text{ for } i = 3, 6, 9, \dots, 27 \end{cases}
 \end{aligned} \tag{1}$$

where  $x, y$  and  $w$  present node inputs,  $A_j, B_j$  and  $C_j$  linguistic labels and  $\mu_{A_j}, \mu_{B_j}$  and  $\mu_{C_j}$  membership functions. Membership functions determine the degree in which some variable satisfies a specific rule premise. There are various membership functions. In this paper a bell-shape membership function is applied whose general form can be written as:

$$\mu(x) = \frac{1}{1 + \left(\frac{x - c_i}{a_i}\right)^{b_i}} ; \mu(y) = \frac{1}{1 + \left(\frac{y - c_i}{a_i}\right)^{b_i}} ; \mu(w) = \frac{1}{1 + \left(\frac{w - c_i}{a_i}\right)^{b_i}} \quad (2)$$

where  $a_i, b_i$  and  $c_i$  are parameters of fuzzy sets.

Layer 2 contains fixed nodes  $\Pi$ . This layer fixed nodes represent multiplication of input signals whose product is the output for each node.

$$Q_{2,i} = \omega_i = \mu_{A_j} \cdot \mu_{B_j} \cdot \mu_{C_j}, \quad \text{for } i = 1, \dots, 27 \quad (3)$$

Output  $\omega_i$  is called the firing strength of a fuzzy rule.

Layer 3 contains fixed nodes  $N$ . This layer node functions calculate the ratio of the  $i$ -th firing strength of a rule and the firing strength of all rules.

$$Q_{3,i} = \bar{\omega}_i = \frac{\omega_i}{\sum \omega_i}, \quad \text{for } i = 1, \dots, 27 \quad (4)$$

Output  $\bar{\omega}_i$  is called normalized firing strength of a fuzzy rule.

Layer 4 contains adaptive nodes. This layer node functions are expressed as:

$$Q_{4,i} = \bar{\omega}_i \cdot f_i, \quad \text{for } i = 1, \dots, 27 \quad (5)$$

where  $f_i$  represents conclusions of fuzzy rules for which is valid:

$$f_i = p_i x + q_i y + r_i w + s_i, \quad \text{for } i = 1, \dots, 27 \quad (6)$$

where  $p_i, q_i, r_i$  and  $s_i$  are called consequent parameters.

Layer 5 contains only one fixed node. Function of this node is to calculate the overall output using:

$$Q_5 = f_{out} = \sum_{i=1}^{27} \bar{\omega}_i \cdot f_i = (\bar{\omega}_i x) p_i + (\bar{\omega}_i y) q_i + (\bar{\omega}_i w) r_i + (\bar{\omega}_i) s_i \quad (7)$$

The arithmetic average of the roughness profile  $Ra$  can be expressed as:

$$Ra = \sum_{i=1}^n \bar{\omega}_i \cdot f_i = \sum_{i=1}^n \bar{\omega}_i (k_{i0} + k_{i1} \cdot n + k_{i2} \cdot f_z + k_{i3} \cdot a_p) \quad (8)$$

where  $k = [k_{10}, k_{11}, k_{12}, k_{13}, k_{20}, k_{21}, k_{22}, k_{23}, \dots, k_{n0}, k_{n1}, k_{n2}, k_{n3}]$  represents the consequent parameters vector,  $n$  spindle speed,  $f_z$  feed per tooth,  $a_p$  depth of cut,  $\bar{\omega}_i$  normalized firing strength and as output the arithmetic average of the roughness profile  $Ra$ .

Output of every fuzzy rule is connected with the output function defined by three different consequent parameters. It can be concluded from the foregoing that in training of the system 81 parameters are being adapted which then requires minimally 81 sets of input/output experimental data for the training of the FIS for assessing surface roughness. In addition to the training phase, the input/output experimental data are necessary for the checking phase too. For the checking phase 10 % of input/output experimental data are to be provided.

### 3. Results and discussion

Fig. 2 shows a machined sample. The arithmetic average of the roughness profile  $Ra$  is measured according to the standard ISO 4288 by means of a portable surface roughness tester produced by Taylor & Hobson model Surtronic S128.

The arithmetic average of the roughness profile  $Ra$  is measured on mid part of samples (between two white horizontal lines) as shown in Fig. 2 for each run separately. The upper and lower lines are 40 mm apart from the ends of the samples so that the central part width is 20 mm. The arithmetic average of the roughness profile  $Ra$  is measured vertically to the tangents of tool traces on the line where the tool traces are most apart, this line being at 10 mm distance from the left and the right edge of the sample and is parallel with them. For the measuring data processing the Talyprofile software produced by Taylor & Hobson is applied, designed to be used with the Surtronic series S-100 instruments.

After the experiment the acquisition of machined surfaces digital images of all samples was carried out using table scanner Scanjet 3100. The scanner optical resolution of 1200 points per inch was used to obtain greyscale image, i.e. image of the grey colour shades. For the greyscale image 8 bits per pixel were used while the grey colour shades values were represented in 256 levels.

After the acquisition all digital images are registered in matrix form from which input variables are quantified: greyscale mean value of all digital image matrix members, greyscale standard deviation of all digital image matrix members and the digital image matrix greyscale entropy that are, along with the measured arithmetic average of the roughness profile  $Ra$ , used as an input/output data base in creating the FIS for surface roughness assessing.

The greyscale mean value of digital image matrix is:

$$Mean = \frac{1}{N \times N} \sum_{x=1}^N \sum_{y=1}^N f(x,y) \tag{9}$$

where  $N$  presents the number of columns and number of rows of digital image, and  $f(x,y)$  is a greyscale intensity value of the digital image matrix member defined by  $x$  and  $y$ .

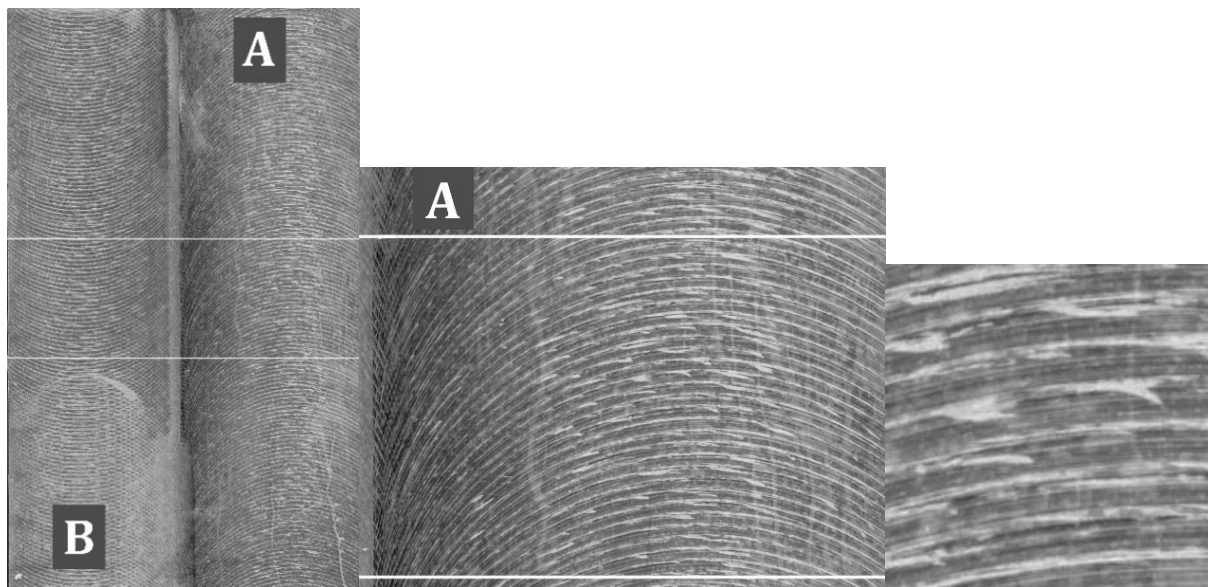


Fig. 2 Machined sample and roughness measuring points

The greyscale standard deviation of all digital image matrix members ( $N = 250$ ) can be described as:

$$Std = \frac{1}{N} \sqrt{\sum_{x=1}^N \sum_{y=1}^N (f(x, y) - \bar{f})^2} \quad (10)$$

where  $N$  presents the number of columns and number of rows of the digital image matrix,  $f(x, y)$  is a greyscale intensity value of the digital image matrix defined by  $x$  and  $y$  while  $\bar{f}$  is the digital image matrix mean greyscale value.

Entropy is a statistical measure of randomness that can be used to characterize the texture of the input image. The digital image matrix greyscale entropy is described as:

$$E = \sum_{i=1}^{256} (p_i \times \log_2 p_i) \quad (11)$$

where  $E$  is a scalar value representing the entropy of greyscale image  $I$ , and  $p$  is a vector which contains the histogram counts.

Resolution of all digital images used in this investigation was  $250 \times 250$  pixels. The used resolution represents the size of the machined surface digital images denoting the place where the arithmetic average of the roughness profile  $Ra$  was measured along with the surrounding surface. The surface shown in the used digital images is between the white horizontal lines of the samples displayed in Fig. 2 for each run separately. To serve the needs of the current paper the digital images are used of those runs in which a higher value of the arithmetic average of the roughness profile  $Ra$  was measured. The digital image matrix consists of 250 rows and 250 columns.

Table 3 displays the extracted values of roughness (higher values  $Ra_{max}$  are displayed of two repeated measurements), and the earlier described input variables for creating the fuzzy inference system (mean greyscale value of all digital image matrix members, greyscale standard deviation of all digital image matrix members and the digital image greyscale matrix entropy). The given data were used for generating FIS for assessing surface roughness using ANFIS. This system assesses the  $Ra$  values on the basis of the machined surfaces digital images and their features. The error of assessing i.e. of comparisons provided by the system with real values  $Ra$ , is expressed by the average normalized root mean square error (NRMSE). The assessing error of the fuzzy inference system created in this investigation is 0.0698 or 6.98 %.

The figures that follow demonstrate the arithmetic average of the roughness profile  $Ra$  dependence on greyscale standard deviation of all digital image matrix members and greyscale mean value of all digital image matrix members (Fig. 3), on entropy of digital image greyscale matrix and greyscale standard deviation of all digital image matrix members (Fig. 4), on entropy of digital image greyscale matrix and on the greyscale mean value of all digital image matrix members (Fig. 5).

The arithmetic average of the roughness profile  $Ra$  ranging from  $0.194 \mu\text{m}$  to  $1.68 \mu\text{m}$  has been measured in the experimental investigations. The measured outputs are ranged in four classes of surface roughness: N3 (from  $0.1 \mu\text{m}$  to  $0.2 \mu\text{m}$ ), N4 (from  $0.2 \mu\text{m}$  to  $0.4 \mu\text{m}$ ), N5 (from  $0.4 \mu\text{m}$  to  $0.8 \mu\text{m}$ ), N6 (from  $0.8 \mu\text{m}$  to  $1.6 \mu\text{m}$ ) and N7 (from  $1.6 \mu\text{m}$  to  $3.2 \mu\text{m}$ ). The applicable parts of response surface in this particular case are given separately in Fig. 6.

It can be seen from Fig. 6 that slight changes in input variables have a considerable effect on output variable, the arithmetic average of the roughness profile  $Ra$ .

**Table 3** Extracted values of roughness depending on technological parameters of machining, and the digital image values of variables for creating the fuzzy inference system

STD	RUN	Feed per tooth, mm/tooth	Bench feed, mm/min	Spindle speed, rev/min	Depth of cut, mm	$Ra_{max}$ , $\mu\text{m}$	Greyscale mean value	Greyscale standard deviation	Greyscale matrix entropy
1	99	0.175	2450	3500	2	0.236	201.3327	12.9087	5.7077
2	32	0.1	800	2000	2	0.194	215.8912	14.4114	5.8688
3	40	0.25	3500	3500	2	0.340	216.4442	10.9891	5.4273
4	22	0.25	6500	6500	1	0.325	211.9918	14.9249	5.8883
5	34	0.25	2000	2000	2	0.291	211.6711	18.7212	6.2131
6	92	0.1	800	2000	2	0.259	207.0648	11.9313	5.6197
7	91	0.025	200	2000	2	0.295	205.5052	14.2197	5.8618
8	119	0.325	10400	8000	2	0.284	202.4441	21.4677	6.3535
9	112	0.25	6500	6500	2	0.892	172.1966	23.6160	6.5007
10	35	0.325	2600	2000	2	1.270	203.2657	26.0274	6.6797
11	6	0.4	3200	2000	1	1.050	181.5731	33.5879	7.0212
12	55	0.025	800	8000	2	0.549	200.8293	9.9470	5.3400
13	3	0.175	1400	2000	1	0.510	138.9439	30.9279	6.8194
14	96	0.4	3200	2000	2	1.300	192.3719	27.7303	6.7241
15	68	0.1	1400	3500	1	0.405	138.9501	18.3823	6.2209
16	16	0.25	5000	5000	1	0.845	146.9739	29.7534	6.8952
17	69	0.175	2450	3500	1	0.504	134.2705	27.7919	6.7490
18	115	0.025	800	8000	2	0.333	197.0068	8.3465	5.0556
19	11	0.325	4550	3500	1	0.755	124.9713	27.7997	6.6697
20	101	0.325	4550	3500	2	1.340	169.0206	24.9581	6.6209
21	54	0.4	10400	6500	2	1.560	175.4106	26.5330	6.5932
22	105	0.175	3500	5000	2	0.631	141.6713	18.3205	6.0764
23	30	0.4	12800	8000	1	1.030	149.9594	29.6730	6.8415
24	45	0.175	3500	5000	2	0.462	139.8943	19.5561	6.1107
25	77	0.325	6500	5000	1	0.684	142.7332	23.7919	6.5355
26	60	0.4	12800	8000	2	1.680	171.5458	25.1323	6.5677
27	113	0.325	8450	6500	2	1.660	150.6172	23.1638	6.5385
28	74	0.1	2000	5000	1	0.413	142.7963	19.5778	6.2314
29	78	0.4	8000	5000	1	1.040	149.5937	21.4949	6.4195
30	72	0.4	5600	3500	1	1.310	149.2047	21.1949	6.4186
31	62	0.1	800	2000	1	0.408	146.4589	17.7637	6.0372
32	70	0.25	3500	3500	1	0.742	159.4245	25.2728	6.5954
33	107	0.325	6500	5000	2	1.570	157.0338	26.5375	6.7189
34	51	0.175	4550	6500	2	0.359	142.6573	22.1164	6.4169
35	33	0.175	1400	2000	2	0.417	155.2297	20.8527	6.3764
36	7	0.025	350	3500	1	0.459	197.1356	8.5898	5.0740
37	86	0.1	3200	8000	1	0.376	150.2156	20.6194	6.3526
38	103	0.025	500	5000	2	0.342	216.3073	10.3385	5.3718
39	38	0.1	1400	3500	2	0.526	166.4716	21.4820	6.4444
40	100	0.25	3500	3500	2	1.140	164.7204	33.5821	7.0123
41	58	0.25	8000	8000	2	1.270	177.2273	29.6023	6.8859
42	76	0.25	5000	5000	1	0.802	157.8756	26.7976	6.6881
43	81	0.175	4550	6500	1	0.521	134.4788	22.0851	6.3085
44	89	0.325	10400	8000	1	0.761	152.5526	20.9315	6.3611
45	42	0.4	5600	3500	2	1.210	167.3245	21.3705	6.4070
46	28	0.25	8000	8000	1	0.855	145.4409	25.8796	6.5799
47	17	0.325	6500	5000	1	0.812	147.7410	20.9663	6.4149
48	41	0.325	4550	3500	2	1.540	171.2488	20.8178	6.3214
49	120	0.4	12800	8000	2	1.470	156.4950	21.1037	6.4185
50	47	0.325	6500	5000	2	1.090	176.9611	27.9537	6.8013
51	111	0.175	4550	6500	2	0.470	140.2953	20.8329	6.3067
52	98	0.1	1400	3500	2	0.374	145.4403	24.1626	6.4329
53	80	0.1	2600	6500	1	0.399	162.8991	21.2284	6.3343
54	14	0.1	2000	5000	1	0.366	154.3155	19.6337	6.2506
55	46	0.25	5000	5000	2	1.040	176.2519	32.7465	6.9622
56	56	0.1	3200	8000	2	0.364	155.8688	17.3140	6.0190
57	63	0.175	1400	2000	1	0.597	153.3269	29.7856	6.8004
58	104	0.1	2000	5000	2	0.386	159.6362	20.5342	6.2324
59	93	0.175	1400	2000	2	0.422	165.1706	23.2286	6.4068
60	117	0.175	5600	8000	2	0.508	149.4792	19.4560	6.0821



**Table 3** Extracted values of roughness depending on technological parameters of machining, and the digital image values of variables for creating the fuzzy inference system (continuation)

STD	RUN	Feed per tooth, mm/tooth	Bench feed, mm/min	Spindle speed, rev/min	Depth of cut, mm	$Ra_{max}$ , $\mu\text{m}$	Greyscale mean value	Greyscale standard deviation	Greyscale matrix entropy
61	8	0.1	1400	3500	1	0.402	156.5143	28.9983	6.7787
62	67	0.025	350	3500	1	0.463	224.1073	11.3163	5.4469
63	84	0.4	10400	6500	1	0.977	151.3250	27.0345	6.6960
64	90	0.4	12800	8000	1	0.945	155.1779	25.9010	6.6127
65	97	0.025	350	3500	2	0.202	218.8573	11.8558	5.5605
66	83	0.325	8450	6500	1	0.666	154.6065	27.3491	6.7255
67	59	0.325	10400	8000	2	1.300	152.1983	24.2644	6.5952
68	106	0.25	5000	5000	2	1.150	157.4970	30.3303	6.7487
69	79	0.025	650	6500	1	0.336	174.5179	16.0944	5.9967
70	5	0.325	2600	2000	1	0.778	152.4728	23.3246	6.5248
71	48	0.4	8000	5000	2	1.600	163.3946	25.3079	6.6660
72	108	0.4	8000	5000	2	1.560	158.2985	19.6642	6.2761
73	53	0.325	8450	6500	2	1.460	176.6186	27.1825	6.7422
74	29	0.325	10400	8000	1	0.715	173.9498	23.3387	6.5550
75	21	0.175	4550	6500	1	0.513	157.2126	25.0313	6.5654
76	25	0.025	800	8000	1	0.257	194.3272	17.8550	6.0991
77	52	0.25	6500	6500	2	1.500	176.9590	34.1330	7.0064
78	109	0.025	650	6500	2	0.510	215.7320	7.6283	4.9336
79	37	0.025	350	3500	2	0.264	184.7601	12.6105	5.6820
80	64	0.25	2000	2000	1	0.932	164.4880	23.3275	6.4361
81	31	0.025	200	2000	2	0.326	196.8387	9.8417	5.3327
82	49	0.025	650	6500	2	0.277	196.4967	18.2400	6.1901
83	27	0.175	5600	8000	1	0.418	180.7377	30.4711	6.7616
84	110	0.1	2600	6500	2	0.319	194.5997	16.2075	6.0494
85	61	0.025	200	2000	1	0.449	202.4482	12.0212	5.6169
86	88	0.25	8000	8000	1	0.345	208.5057	18.1894	6.2054
87	50	0.1	2600	6500	2	0.362	216.7653	12.7031	5.6936
88	87	0.175	5600	8000	1	0.315	203.7227	16.5828	6.0807
89	26	0.1	3200	8000	1	0.377	204.2278	17.9229	6.1923
90	43	0.025	500	5000	2	0.322	225.7510	4.8023	4.3056
91	94	0.25	2000	2000	2	0.391	185.6580	17.7899	6.1080
92	19	0.025	650	6500	1	0.412	226.0397	4.4847	4.2012
93	102	0.4	5600	3500	2	0.657	193.8495	17.3608	6.1385
94	44	0.1	2000	5000	2	0.302	205.5300	15.0375	5.9108
95	15	0.175	3500	5000	1	0.317	198.4703	17.8107	6.1613
96	73	0.025	500	5000	1	0.361	217.4270	5.6124	4.5311
97	1	0.025	200	2000	1	0.404	210.2537	11.3657	5.5270
98	36	0.4	3200	2000	2	0.652	183.9130	18.6225	6.1525
99	116	0.1	3200	8000	2	0.371	210.2263	13.8650	5.8338
100	82	0.25	6500	6500	1	0.359	194.8133	13.8527	5.8269
101	71	0.325	4550	3500	1	0.454	179.7367	21.4364	6.3853
102	23	0.325	8450	6500	1	0.413	200.2917	16.8814	6.0965
103	65	0.325	2600	2000	1	0.550	183.4905	18.8896	6.2459
104	2	0.1	800	2000	1	0.371	220.3295	13.6538	5.8036
105	114	0.4	10400	6500	2	0.561	185.6083	18.8118	6.2636
106	4	0.25	2000	2000	1	0.369	201.7676	15.8028	6.0238
107	18	0.4	8000	5000	1	0.544	186.0058	22.0295	6.4740
108	85	0.025	800	8000	1	0.408	219.5023	5.5210	4.4854
109	75	0.175	3500	5000	1	0.347	187.1892	15.5448	5.9636
110	24	0.4	10400	6500	1	0.529	205.4299	15.7066	6.0073
111	95	0.325	2600	2000	2	0.557	176.9512	21.9477	6.4261
112	39	0.175	2450	3500	2	0.336	190.3445	19.2155	6.2940
113	13	0.025	500	5000	1	0.415	225.9157	5.7998	4.5690
114	9	0.175	2450	3500	1	0.323	188.4408	17.3426	6.1525
115	66	0.4	3200	2000	1	0.566	182.2851	19.7799	6.3321
116	20	0.1	2600	6500	1	0.378	218.3453	12.7629	5.6885
117	57	0.175	5600	8000	2	0.332	186.9872	18.1653	6.2152
118	10	0.25	3500	3500	1	0.356	189.2162	16.7248	6.1067
119	12	0.4	5600	3500	1	0.495	184.4284	19.5615	6.3077
120	118	0.25	8000	8000	2	0.321	192.7420	17.5391	6.1643

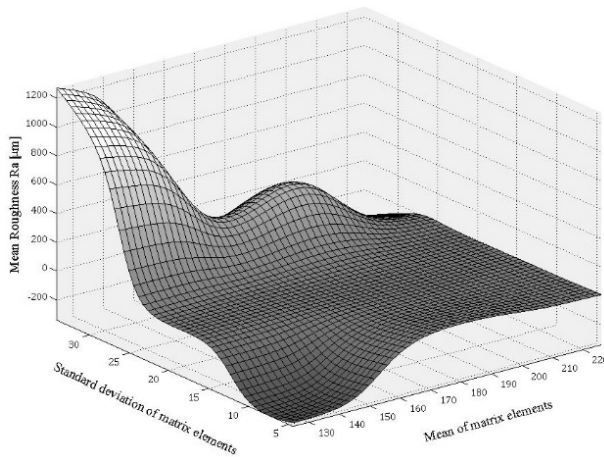


**Fig. 3** Dependence of  $Ra$  on standard deviation and mean value of digital image matrix members

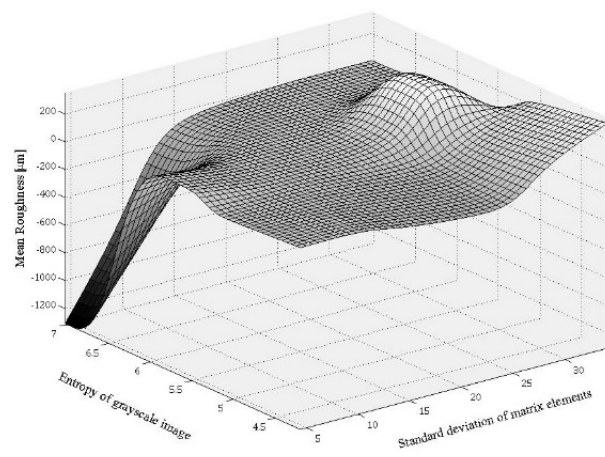


**Fig. 4** Dependence of  $Ra$  on entropy and standard deviation of digital image matrix members

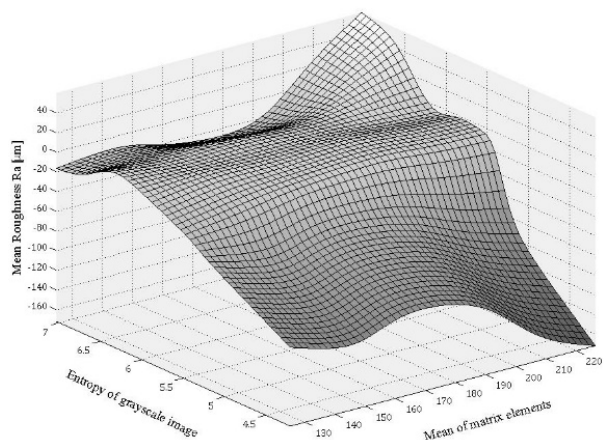


**Fig. 5** Dependence of  $Ra$  on entropy and mean value of digital image matrix members

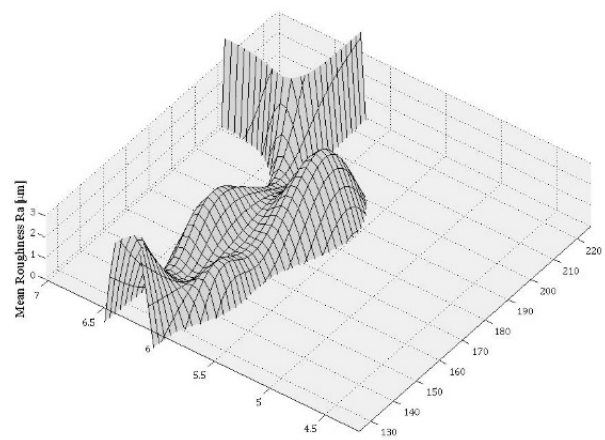


**Fig. 6** Applicable part of the response surface shown in Fig. 5

It can be seen from the papers that deal with assessing the roughness of machined surfaces on the basis of the features of digital image that the range of measured roughness has a great impact on the level of error assessing. The wider the range of measured roughness, with the uniform distribution by the roughness classes, the lower the error of assessment. The error of assessment in this study (6.98 %) was significantly influenced by outlier values. Specifically, almost 97 % of the measured values of roughness belong to the roughness classes N4, N5 and N6. The remaining values and part of roughness values in class N6 are outliers. Without outliers the error of assessment of the machined surface roughness is expected to be significantly lower.

#### 4. Conclusion

The conducted investigation is part of a project whose ultimate objective is to build an online system for machined surface roughness monitoring i.e. roughness monitoring in real time. The system should faster carry out the activities of required control of machined surfaces, testing would be cheaper, and monitoring during machining would help to timely react to possible deviations and to reduce subsequent costs. The investigations in this paper are focused on assessing the machined surface roughness based on the features of digital image with the use of adaptive neuro-fuzzy inference system (ANFIS). A controlled parameter of surface roughness is the arithmetic average of the roughness profile  $Ra$ . The following features of digital image are studied in the paper: mean greyscale values of all digital image matrix members, standard greyscale deviation of all digital image matrix members and entropy of digital image greyscale matrix. Comparison of real values  $Ra$  and the values provided by the built system is shown by the nor-

malized root mean square error (NRMSE), or assessing error. The conducted investigation enters the area of high speed machining. Therefore the machined surfaces are of high quality and the measured roughness is very small. Thus the features of digital images become quite similar and a higher assessing error is expected. The fuzzy inference system obtained in the present investigation has an assessing error of 6.98 %. However, even with such an error, the technical requirements set on the workpiece as regards quality of machining, should not be diminished.

The plan is to expand the research on existing material, but also conduct research on other materials. This would be a way to expand the base of digital photos and their features and to accumulate sufficient knowledge to influence the reduction of assessing errors.

## Acknowledgement

This research is accomplished within the projects Nos. IZIP-2014-95 and INGI-2015-28 financed by the Josip Juraj Strossmayer University of Osijek.

## References

- [1] Stankovic, I., Perinic, M., Jurkovic, Z., Mandic, V., Maricic, S. (2012). Usage of neural network for the prediction of surface roughness after the roller burnishing, *Metalurgija*, Vol. 51, No. 2, 207-210.
- [2] Simunovic, K., Simunovic, G., Saric, T. (2015). Single and multiple goal optimization of structural steel face milling process considering different methods of cooling/lubricating, *Journal of Cleaner Production*, Vol. 94, 321-329, doi: [10.1016/j.jclepro.2015.02.015](https://doi.org/10.1016/j.jclepro.2015.02.015).
- [3] Zuperl, U., Cus, F. (2015). Simulation and visual control of chip size for constant surface roughness, *International Journal of Simulation Modelling*, Vol. 14, No. 3, 392-403, doi: [10.2507/IJSIMM14\(3\)2.282](https://doi.org/10.2507/IJSIMM14(3)2.282).
- [4] Vukelic, D., Tadic, B., Miljanic, D., Budak, I., Todorovic, P.M., Randjelovic, S., Jeremic, B.M. (2012). Novel workpiece clamping method for increased machining performance, *Tehnički vjesnik – Technical Gazette*, Vol. 19, No. 4, 837-846.
- [5] Brezocnik, M., Kovacic, M., Ficko, M. (2004). Prediction of surface roughness with genetic programming, *Journal of Materials Processing Technology*, Vol. 157-158, 28-36, doi: [10.1016/j.jmatprotec.2004.09.004](https://doi.org/10.1016/j.jmatprotec.2004.09.004).
- [6] Pare, V., Agnihotri, G., Krishna, C. (2015). Selection of optimum process parameters in high speed CNC end-milling of composite materials using meta heuristic techniques – A comparative study, *Strojniški vestnik – Journal of Mechanical Engineering*, Vol. 61, No. 2, 176-186, doi: [10.5545/sv-jme.2014.1914](https://doi.org/10.5545/sv-jme.2014.1914).
- [7] Simunovic, G., Simunovic, K., Saric, T. (2013). Modelling and simulation of surface roughness in face milling, *International Journal of Simulation Modelling*, Vol. 12, No. 3, 141-153, doi: [10.2507/IJSIMM12\(3\)1.219](https://doi.org/10.2507/IJSIMM12(3)1.219).
- [8] Çolak, O. (2014). Optimization of machining performance in high-pressure assisted turning of Ti6Al4V alloy, *Strojniški vestnik – Journal of Mechanical Engineering*, Vol. 60, No. 10, 675-681, doi: [10.5545/sv-jme.2014.1914](https://doi.org/10.5545/sv-jme.2014.1914).
- [9] Nammi, S., Ramamoorthy, B. (2014). Effect of surface lay in the surface roughness evaluation using machine vision, *Optik – International Journal for Light and Electron Optics*, Vol. 125, No. 15, 3954-3960, doi: [10.1016/j.ijleo.2014.01.152](https://doi.org/10.1016/j.ijleo.2014.01.152).
- [10] Klancnik, S., Ficko, M., Balic J., Pahole, I. (2015). Computer vision-based approach to end mill tool monitoring, *International Journal of Simulation Modelling*, Vol. 14, No. 4, 571-583, doi: [10.2507/IJSIMM14\(4\)1.301](https://doi.org/10.2507/IJSIMM14(4)1.301).
- [11] Krolczyk, G., Raos, P., Legutko, S. (2014). Experimental analysis of surface roughness and surface texture of machined and fused deposition modelled parts, *Tehnički vjesnik – Technical Gazette*, Vol. 21, No. 1, 217-221.
- [12] Samtaş, G. (2014). Measurement and evaluation of surface roughness based on optic system using image processing and artificial neural network, *The International Journal of Advanced Manufacturing Technology*, Vol. 73, No. 1, 353-364, doi: [10.1007/s00170-014-5828-1](https://doi.org/10.1007/s00170-014-5828-1).
- [13] Stępień, K., Makiela, W., Stoić, A., Samardžić, I. (2015). Defining the criteria to select the wavelet type for the assessment of surface quality, *Tehnički vjesnik – Technical Gazette*, Vol. 22, No. 3, 781-784, doi: [10.17559/TV-20140124110406](https://doi.org/10.17559/TV-20140124110406).
- [14] Lee, K.C., Ho, S.J., Ho, S.Y. (2005). Accurate estimation of surface roughness from texture features of the surface image using an adaptive neuro-fuzzy inference system, *Precision Engineering*, Vol. 29, No. 1, 95-100, doi: [10.1016/j.precisioneng.2004.05.002](https://doi.org/10.1016/j.precisioneng.2004.05.002).
- [15] Jeyapooan, T., Murugan, M. (2013). Surface roughness classification using image processing, *Measurement*, Vol. 46, No. 7, 2065-2072, doi: [10.1016/j.measurement.2013.03.014](https://doi.org/10.1016/j.measurement.2013.03.014).
- [16] Morala-Argüello, P., Barreiro, J., Alegre, E. (2012). A evaluation of surface roughness classes by computer vision using wavelet transform in the frequency domain, *The International Journal of Advanced Manufacturing Technology*, Vol. 59, No. 1, 213-220, doi: [10.1007/s00170-011-3480-6](https://doi.org/10.1007/s00170-011-3480-6).
- [17] Palani, S., Natarajan, U. (2011). Prediction of surface roughness in CNC end milling by machine vision system using artificial neural network based on 2D Fourier transform, *The International Journal of Advanced Manufacturing Technology*, Vol. 54, No. 9, 1033-1042, doi: [10.1007/s00170-010-3018-3](https://doi.org/10.1007/s00170-010-3018-3).

- [18] Ho, S.Y., Lee, K.C., Chen, S.S., Ho, S.J. (2002). Accurate modeling and prediction of surface roughness by computer vision in turning operations using an adaptive neuro-fuzzy inference system, *International Journal of Machine Tools and Manufacture*, Vol. 42, No. 13, 1441-1446, doi: [10.1016/S0890-6955\(02\)00078-0](https://doi.org/10.1016/S0890-6955(02)00078-0).
- [19] Palani, S., Natarajan, U., Chellamalai, M. (2013). On-line prediction of micro-turning multi-response variables by machine vision system using adaptive neuro-fuzzy inference system (ANFIS), *Machine Vision and Applications*, Vol. 24, No. 1, 19-32, doi: [10.1007/s00138-011-0378-0](https://doi.org/10.1007/s00138-011-0378-0).
- [20] Natarajan, U., Palani, S., Anandampilai, B. (2012). Prediction of surface roughness in milling by machine vision using ANFIS, *Computer-Aided Design & Applications*, Vol. 9, No. 3, 269-288, doi: [10.3722/cadaps.2012.269-288](https://doi.org/10.3722/cadaps.2012.269-288).
- [21] Jeyapoovan, T., Murugan, M. (2013). Surface roughness classification using image processing, *Measurement*, Vol. 46, No. 7, 2065-2072, doi: [10.1016/j.measurement.2013.03.014](https://doi.org/10.1016/j.measurement.2013.03.014).
- [22] Zawada-Tomkiewicz, A. (2010). Estimation of surface roughness parameter based on machined surface image, *Metrology and Measurement Systems*, Vol. 17, No. 3, 493-504.
- [23] Priya, P., Ramamoorthy, B. (2007). The influence of component inclination on surface finish evaluation using digital image processing, *International Journal of Machine Tools and Manufacture*, Vol. 47, No. 3-4, 570-579, doi: [10.1016/j.ijmachtools.2006.05.005](https://doi.org/10.1016/j.ijmachtools.2006.05.005).
- [24] Lee, B.Y., Yu, S.F., Juan, H. (2004). The model of surface roughness inspection by vision system in turning, *Mechanics*, Vol. 14, No. 1, 129-141, doi: [10.1016/S0957-4158\(02\)00096-X](https://doi.org/10.1016/S0957-4158(02)00096-X).
- [25] Gadelmawla, E.S., Al-Mufadi, F.A., Al-Aboodi, A.S. (2014). Calculation of the machining time of cutting tools from captured images of machined parts using image texture features, *Proceedings of the Institution of Mechanical Engineers, Part B: Journal of Engineering Manufacture*, Vol. 228, No. 2, 203-214, doi: [10.1177/0954405413481291](https://doi.org/10.1177/0954405413481291).
- [26] Dutta, S., Datta, A., Das Chakladar, N., Pal, S.K., Mukhopadhyay, S., Sen, R. (2012). Detection of tool condition from the turned surface images using an accurate grey level co-occurrence technique, *Precision Engineering*, Vol. 36, No. 3, 458-466, doi: [10.1016/j.precisioneng.2012.02.004](https://doi.org/10.1016/j.precisioneng.2012.02.004).
- [27] Shahabi, H.H., Ratnam, M.M. (2009). In-cycle monitoring of tool nose wear and surface roughness of turned parts using machine vision, *The International Journal of Advanced Manufacturing Technology*, Vol. 40, No. 11, 1148-1157, doi: [10.1007/s00170-008-1430-8](https://doi.org/10.1007/s00170-008-1430-8).
- [28] Nathan, D., Thanigaiyarasu, G., Vani, K. (2014). Study on the relationship between surface roughness of AA6061 alloy end milling and image texture features of milled surface, *Procedia Engineering*, Vol. 97, 150-157, doi: [10.1016/j.proeng.2014.12.236](https://doi.org/10.1016/j.proeng.2014.12.236).
- [29] Kamguem, R., Tahan, S.A., Songmene, V. (2013). Evaluation of machined part surface roughness using image texture gradient factor, *International Journal of Precision Engineering and Manufacturing*, Vol. 14, No. 2, 183-190, doi: [10.1007/s12541-013-0026-x](https://doi.org/10.1007/s12541-013-0026-x).

# Visual measurement of layer thickness in multi-layered functionally graded metal materials

Zuperl, U.<sup>a,\*</sup>, Radic, A.<sup>a</sup>, Cus, F.<sup>a</sup>, Irgolic, T.<sup>a</sup>

<sup>a</sup>Faculty of Mechanical Engineering, University of Maribor, Maribor, Slovenia

## ABSTRACT

Multi-layered functionally gradient metal materials are formed by metal material depositing with Laser Engineered Net Shaping (LENS) technology. LENS is an additive manufacturing technique that employs a high-power laser as the power source to fuse powdered metals into fully dense three-dimensional structures layer by layer. Layer thickness is an important factor in machining and processing of such advanced materials, as well as in the production, as a feedback to LENS machine operator. Knowing the thickness of the manufactured layer of multi-layered metal material is fundamental for understanding the LENS process and optimizing the machining operations. In this paper, software for visual multi-layered functionally graded material layer thickness measurement is presented. The layer thickness is automatically determined by the software that is programmed in Matlab/Simulink, high-level programming language. The software is using cross-section metallographic images of clad layers for thickness measuring. Graphic User Interface (GUI) is also created and presented. The results of measurement are presented to demonstrate the efficiency of the developed measurement software.

© 2016 PEI, University of Maribor. All rights reserved.

## ARTICLE INFO

### Keywords:

Functionally graded material  
LENS  
Visual measuring  
Layer thickness  
Machining

### \*Corresponding author:

uros.zuperl@um.si  
(Zuperl, U.)

### Article history:

Received 21 January 2016  
Revised 19 May 2016  
Accepted 20 May 2016

## 1. Introduction

The beginning of LENS technology was in the 1960s, when the first functional laser was found by Maiman [1]. Industrial usage began in the 1980s. This technology is a non-conventional production technology [2]. LENS technology is based on selective continuous material deposition. Metal powder is melted by laser and deposited onto metal substrate. The process is planar. After finishing the first layer, laser head lifts up and deposition of second layer begins, as shown in Fig. 1. This production technology is used for rapid prototyping, product repair and coating [2].

LENS is still unexplored technology and optimal machine settings, such as Laser power and Cladding speed (speed of laser head) are difficult to determine. These two parameters have an impact on the hardness and thickness  $d$  of the manufactured layer in multi-layered functionally graded metal material. Furthermore, the undesirable effect of delayerization (shelling of clad layers) of the multi-layered material is tightly related with the thickness of deposited layers. The thicknesses of deposited layers have also a significant influence on cutting forces, generated in machining of these advanced materials. Nevertheless, Laser power and Cladding speed are usually determined based on technologist experience in order to produce the desired layer thickness. Therefore, there is a practical interest to investigate the impact of LENS process parameters on the thickness of the manufactured layer. The effective layer thickness measurement would help to determine the relation between the layer thickness and LENS process parameters [3].

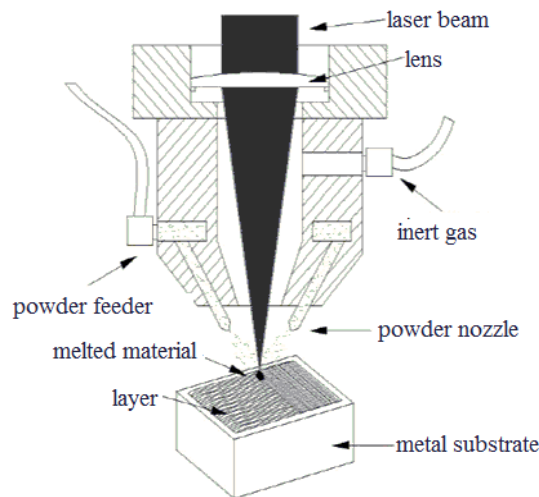


Fig. 1 Laser head [3]

The LENS machine operator could use the determined relation for the optimum selection of the LENS process parameters. The manufactured layer thickness is also an important parameter for optimizing of the machining of multi-layered metal materials. The detail knowledge about the produced layer thickness makes easier to find optimal cutting conditions for the milling processes. Especially in end-milling, the layer thickness is extremely important for optimum axial depth of cut determination.

In this paper, a visual layer thickness measurement algorithm is described. The detailed structure of the automated measurement algorithm is presented.

In the past, the layer thickness of the multi-layered functionally graded material was measured manually, from the prepared metallographic microscopic images. These images were suitable for the automated visual measurement. This procedure was time consuming, labour intensive and above all inaccurate.

The measurement software was developed for simplifying this procedure. Due to the very encouraging test results, the GUI has been also developed and embedded successfully into the measurement software.

There has been no published research on the inspecting of layer thickness of multi-layered gradient materials by using visual measurement systems.

In recent years, some optical measurement systems have been developed to inspect the surface roughness of the machined piece [4, 5]. One system employs a machine vision system to inspect the machined surface roughness [6]. Other uses fibre-optics to measure the diffuseness of the reflected light from the surface [7]. Coman in his research [8] outlines the application of distance measuring with Matlab/Simulink.

Advances in computer vision technology have led to the investigation of its application in tool wear measurement. Weis [9] have employed machine vision for measuring the condition of inserts on an end mill during the machining process. Dutta [10] and Shahabi [11] constructed a tool wear measuring system using a CCD camera in high speed machining. Jovanović [12] developed a measuring device for automated control of machined automobile parts. He developed measurement program and user interface in LabView for visual inspections of dimensions with commercial web camera. The use of all mentioned vision-based measuring systems is limited to the laboratory environment. These articles gave great encouragement for visual measuring method used in this article.

The rest of the paper is organized as follows. The developed layer thickness measurement algorithm is described in the second section. The third section is presenting the GUI development and the results. Conclusions and suggestions for further work and development are given in the final section.

## 2. Distance measurement software algorithm

The layer thickness is measured based on the metallographic microscopic images. The resolution of the images is  $1200 \times 720$  pixels. Fig. 2 shows a gradient material cross section of a metallographic microscopic image. This image is the input to the distance measurement software. The layer thickness  $d$  is a measured dimension.

The distance measurement software consists of a \*.m file which is an algorithm part and a \*.fig file which is a GUI (see Section 2) file. The output from the GUI is the layer thickness in micrometers and in pixels. The detail flowchart of the distance measurement algorithm is shown in Fig. 3.

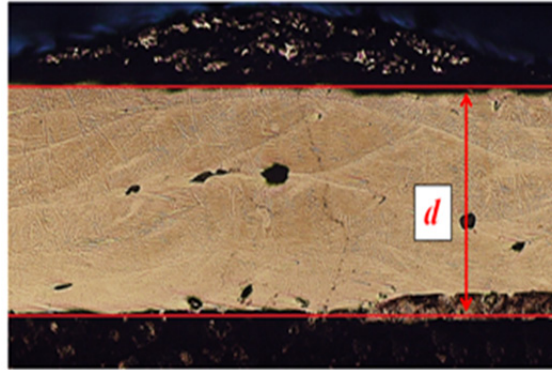


Fig. 2 Microscopic image with measurement distance marked.

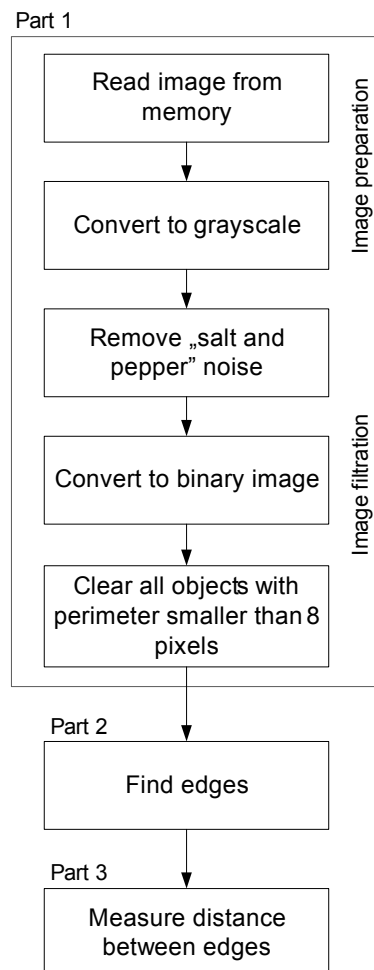


Fig. 3 Detailed flowchart for distance measurement



Measurement starts with image reading from the memory. The image must be saved in a jpg format and placed in the same folder as the m file (algorithm). Then the algorithm transfers the color image into a grayscale image with "rgb2gray" command.

This step is necessary for edge recognition. After the edge recognition, the distance  $d$  is measured (see, Fig 4).

The algorithm for measuring distance finds a top edge and a bottom edge of the multi-layered metal material layer. Image is saved as a matrix in Matlab software; white pixels have value "1", black pixels have "0" [13]. The algorithm finds the cells in the matrix with value "0". As the position of the top and bottom edge is known in the picture matrix (value "1"), it is possible to calculate the distance between two edges. Finally, the distance calculated in pixels is transformed into micrometers. The measurement result is shown in Fig. 4. The measured distance is marked with red lines on the image from memory (metallographic microscopic image). The grayscale image is visible in the middle. The image with the detected edges is shown at the bottom. Noise from edge detection is circled red, therefore edge detection is not successful, measured distance is not correct. The algorithm had found "edges" which are not layer edges. This problem was solved with image filtration. There are built-in functions in Matlab which are used for filtration [13].

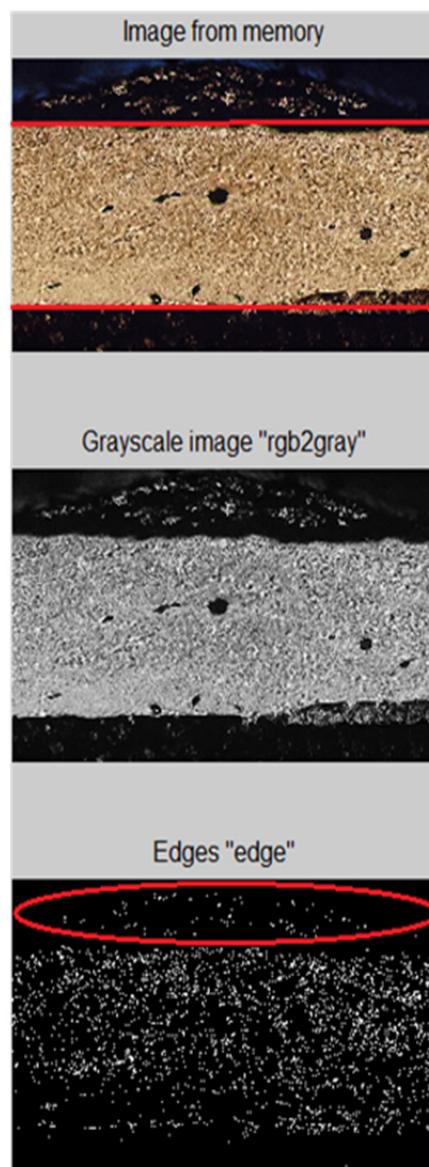


Fig. 4 Edge detection result



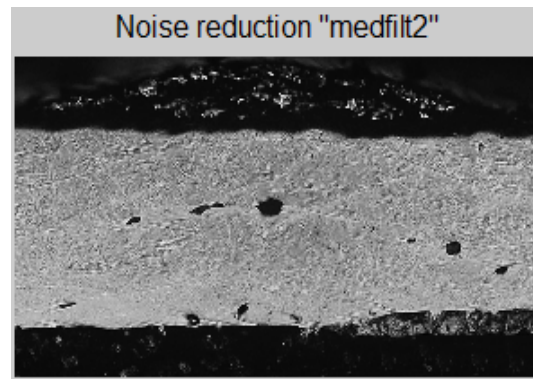


Fig. 5 “Salt and pepper” noise removed

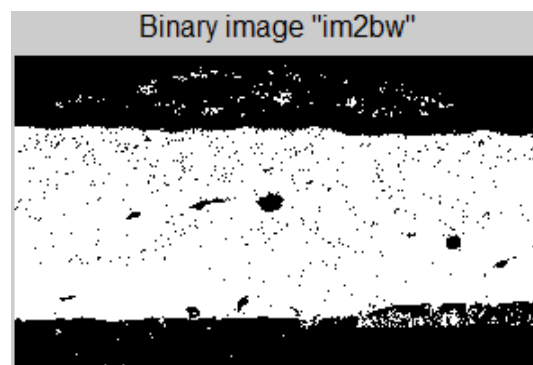


Fig. 6 Binary image

“Salt and pepper” noise is removed with median filtering, “medfilt2” command. Command “medfilt2” executes median filtering of the image in two dimensions.

Each output pixel contains the median value in a 3-by-3 neighbourhood around the corresponding pixel in the input image [13]. Image after noise reduction is shown in Fig. 5.

After noise reduction, image is transferred to a binary image. First step in this transformation is global threshold (level) computation. This is performed with “graythresh” command.

The “graythresh” computes a global threshold (level) that can be used to convert an intensity image to a binary image with command “im2bw”. The level is a normalized intensity value that lies in the range between “0” and “1” [13]. The second transformation step is conversion from the grayscale image to the binary image by using computed threshold from previous step. A command “im2bw” is used for this action.

Fig. 6 shows an image after the “im2bw” command. The command substitutes all pixels in the image with luminance greater than computed threshold with the value “1” (white) and substitutes the rest pixels with the value “0” (black) [13].

The objects forms with perimeter smaller than 8 pixels are cleaned in two steps. Circle shape with perimeter 8 pixels is chosen in the first step with a command “strel(‘disk’,8)”. In the second step, binary image is morphologically opened with a command “imopen”. The morphological open operation is an erosion followed by a dilation, using the same structuring element for both operations [13]. Final step in image filtration is extremes removing which is performed with a “imreconstruct” command. An image without extremes or objects with perimeter smaller than 8 pixels is shown in Fig. 7. Through the above mentioned steps, the image is prepared for edge detection. Command “edge” is used for this task. The prepared image for thickness measurement is shown in Fig. 8. The thickness is measured between two red lines. After edge detection, algorithm finds cells with value “1” in the image matrix. The top edge (cell) is found with command “max”. The bottom edge (cell) is found with command “min”. A difference between top and bottom edge is the layer thickness. This value is printed in “Command Window” of Matlab. Thickness from pixels to micrometers is calculated using Eq. 1.

$$d[\mu\text{m}] = \frac{d[\text{pixels}]}{k} \quad (1)$$

Transformation ratio  $k$  is determined from microscope measurement scale (circled red), as shown in Fig. 9.

To determine the transformation ratio, known distance, in this case 500  $\mu\text{m}$ , must be measured in pixels. Quotient between distance in pixels and distance in micrometres is transformation ratio  $k$  (Fig. 10).

In this paper, the algorithm was tested for two metallographic microscopic images. The first is shown above in Figs. 2 to 9 (measured thickness  $d = 889.5 \mu\text{m}$ ).

The second test is shown in Fig. 11.

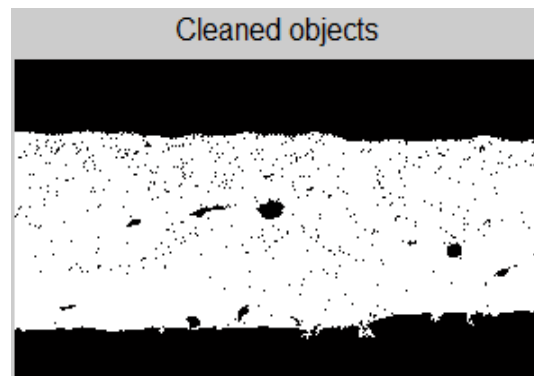


Fig. 7 Image without objects with perimeter smaller than 8 pixels

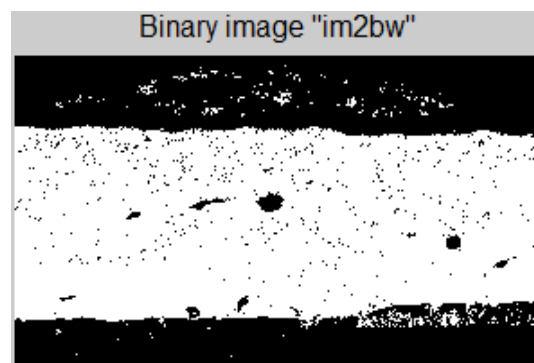
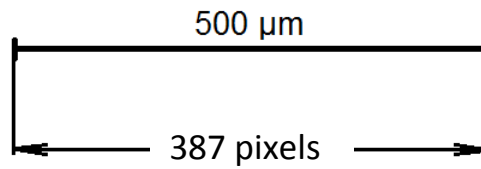


Fig. 8 Image prepared for thickness measurement



Fig. 9 Microscope measurement scale



**Fig. 10** Comparison between distance in pixels and distance in micrometers



**Fig. 11** Algorithm testing for second metallographic microscopic image,  $d = 920.4 \mu\text{m}$

### 3. Graphic user interface development, results and discussion

Graphic User Interface (GUI) was created after testing phase. Matlab “GUI Quick Start” was used for the GUI creation. The created GUI is saved as \*.fig file. Matlab automatically generates the \*.m file. The measuring algorithm is implemented in the generated \*.m file. The GUI is started with a “Run” command. An image for layer thickness measurement is chosen from a GUI drop-down menu.

The GUI (Fig. 12a) is consisted of three parts. The first part is located in the left side of the Fig. 12. It shows the image which is measured. The layer thickness which is measured is marked with two parallel red lines.

The second part of the GUI is located in the upper right side. This part shows the measured thickness, both in pixels and in micrometres. The third part of the GUI is a drop-down menu.

The developed GUI and the measurement results are shown in the Fig. 12(a) to 12(d).

The two-layered functionally graded metal material was used in these tests. The powder material is stainless steel 316L and substrate material is steel Ck 45. The materials are the same in all tests.

To minimize the porosity of multi-layered material, the laser head trajectories during cladding of two consecutive layers were programmed to be perpendicular and horizontal. The weld overlapping in all layers was set to 40 %. The diameter of laser ray was 0.8 mm. The influence of laser head trajectories during cladding on the properties of the manufactured layers was not investigated in this research. The scanning patterns could have an influence on the layer thickness.

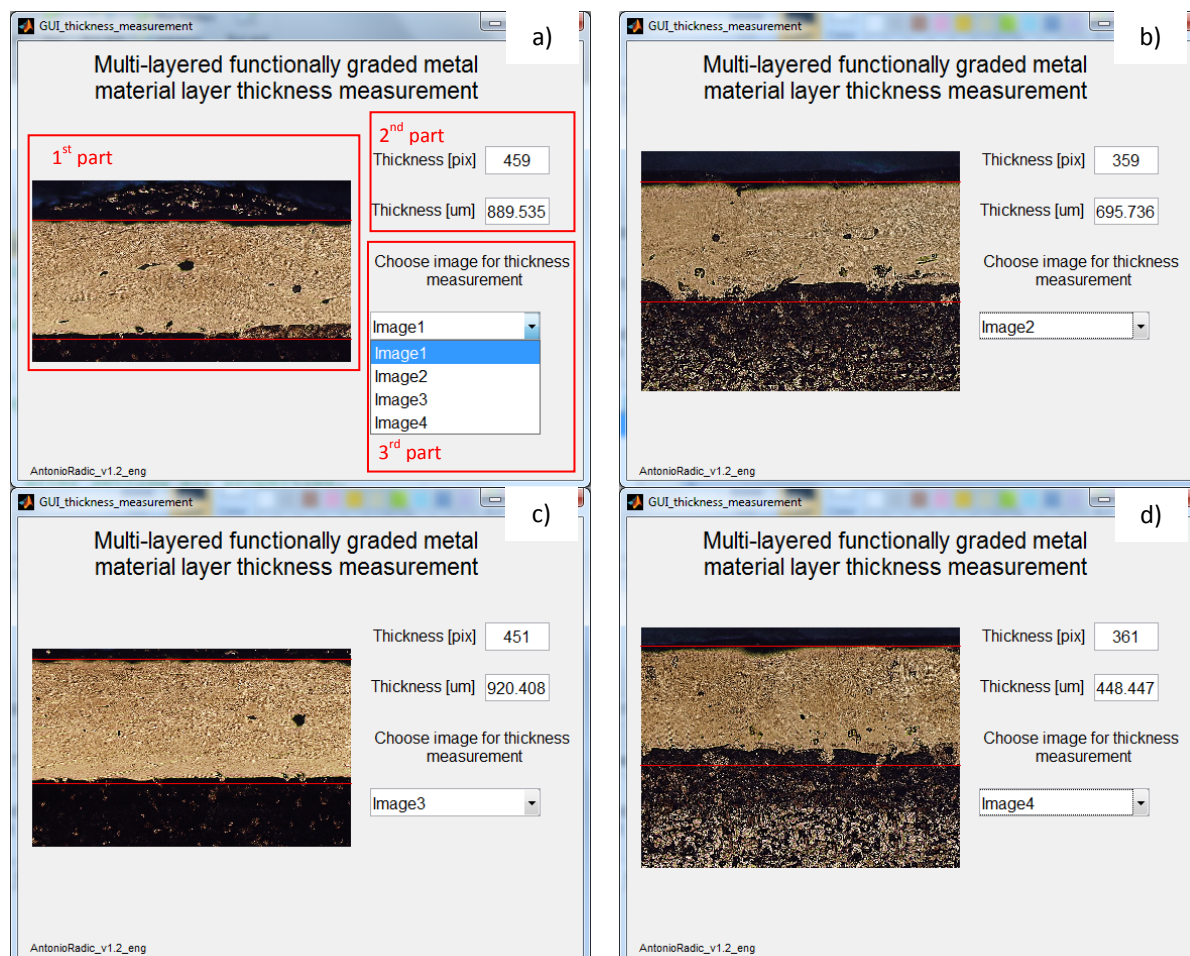


**Fig. 12** Measured multi-layered functionally graded metal material layer thickness for different LENS machine settings (cladding speed, laser power); a) 30 mm/s, 400 W; b) 48 mm/s, 380 W; c) 60 mm/s, 350 W; d) 90 mm/s, 320 W

A multi-layered functionally graded material with measured thickness of 889.5  $\mu\text{m}$  is shown in Fig. 12(a). The LENS machine settings for this test piece were: cladding speed 30 mm/s; laser power: 400 W. Real thickness of the analysed layer is 862.4  $\mu\text{m}$ . This gives an error of 3.14 %.

A multi-layered functionally graded material with measured thickness of 695.7  $\mu\text{m}$  is shown in Fig. 12(b). The LENS machine settings for this test piece were: cladding speed: 48 mm/s; laser power: 380 W. Real thickness of the analysed layer is 622.1  $\mu\text{m}$ . This gives an error of 11.8 %.

A test piece with measured thickness of 920.4  $\mu\text{m}$  is shown in Fig. 12(c). The LENS machine settings for this test piece were: 60 mm/s; laser power: 350 W. Real thickness of the analysed layer is 912.3  $\mu\text{m}$ . This gives an error of 0.9 %.

A test piece with measured thickness of 448.4  $\mu\text{m}$  is shown in Fig. 12(d). The LENS machine settings for this test piece were: cladding speed: 90 mm/s; laser power: 320 W. Real thickness of the analysed layer is 414.9  $\mu\text{m}$ . This gives an error of 8.1 %.

The distance measurement software needs approximately 1 second to complete the measurement of the thickness of one deposited layer. In this period seven steps of the measurement algorithm are executed automatically. The developed software is able to recognize multi-layers bounds and measure the thickness of a separate layer in the multi-layered workpiece where several layers of identical material are deposited on the substrate. The software requires two seconds to determine the distances between the four-layer bounds in four-layered material. The distances are displayed on the GUI in the order from the upper to the lower layer. Therefore, the measurement process is fast once the initial metallographic microscopic images are available in a JPEG file format.

#### 4. Conclusion

The scientific implication of this paper is to present a prototype for the visual measuring of layer thickness in multi-layered metal materials. The layer thickness is automatically determined by the software based on cross-section metallographic images in a few seconds. The developed algorithm can be used in industrial environment without special preparation and any knowledge of graphics and programming. This makes the proposed measuring algorithm practical and appropriate for industrial application.

The measurement algorithm consists of seven steps, which can be separated in 3 parts (Fig. 3). The first part is responsible for image preparation and noise filtration. The second part of the algorithm finds edges of the analyzed layer in the metallographic image. The third part measures distance between found edges. The developed GUI is intuitive, simple to use and easy to implement. The algorithm is not memory consuming.

Measurement error depends on the layer structure. For compact layer error is up to 3 %. For less compact layer error can be as high as 11 %. Therefore it can be used in controlled industrial environment.

Knowledge about multi-layered functionally graded metal materials layer thickness makes easier to find optimal cutting conditions for the milling process. Optimal cutting conditions are important for cutting tool durability. The critical parameter is an axial depth of cut. For technologist it is important to know whether the milling cutter is machining in the hard or soft layer of gradient material.

The LENS machine operator could use the measured layer thickness for the machine parameter setup. It would be useful to find correlation between LENS machine parameters and layer thickness. This will be the goal of future research.

The metallographic microscopic images shown in this paper are not taken with the same microscope zoom; therefore it would be beneficial to create an image base with identical zoom. Such base would make software easier to use. It is now necessary to adapt software for every measurement because of different transformation ratio  $k$ .

The future work focuses on the metallographic microscopic image base with identical microscope zoom. Additionally, automated measurement with camera is the ultimate goal for the developed measurement algorithm.

## References

- [1] Maiman, T.H. (1960). Optical and Microwave-Optical Experiments in Ruby, *Physical Review Letters*, Vol. 4, No. 11, 564-566, doi: [10.1103/physrevlett.4.564](https://doi.org/10.1103/physrevlett.4.564).
- [2] Taberero, I., Lamikiz, A., Martínez, S., Ukar, E., Figueras, J. (2011). Evaluation of the mechanical properties of Inconel 718 components built by laser cladding, *International Journal of Machine Tools and Manufacture*, Vol. 51, No. 6, 465-470, doi: [10.1016/j.ijmactools.2011.02.003](https://doi.org/10.1016/j.ijmactools.2011.02.003).
- [3] Articek, U., Milfelner, M., Anzel, I. (2013). Synthesis of functionally graded material H13/Cu by LENS technology, *Advances in Production Engineering & Management*, Vol. 8, No. 3, 169-176, doi: [10.14743/apem2013.3.164](https://doi.org/10.14743/apem2013.3.164).
- [4] Samtaş, G. (2014). Measurement and evaluation of surface roughness based on optic system using image processing and artificial neural network, *The International Journal of Advanced Manufacturing Technology*, Vol. 73, No. 1, 353-364, doi: [10.1007/s00170-014-5828-1](https://doi.org/10.1007/s00170-014-5828-1).
- [5] Klančnik, S., Ficko, M., Balic, J., Pahole, I. (2015). Computer vision-based approach to end mill tool monitoring. *International Journal of Simulation Modelling*, Vol. 14, No. 4, 571-583, doi: [10.2507/IJSIMM14\(4\)1.301](https://doi.org/10.2507/IJSIMM14(4)1.301).
- [6] Jurevicius, M., Skeivalas, J., Urbanavicius, R. (2014). Analysis of surface roughness parameters digital image identification, *Measurement*, Vol. 56, 81-87, doi: [10.1016/j.measurement.2014.06.005](https://doi.org/10.1016/j.measurement.2014.06.005).
- [7] Gupta, M., Raman, S. (2001). Machine vision assisted characterization of machined surfaces, *International Journal of Production Research*, Vol. 39, No. 4, 759-784, doi: [10.1080/00207540010011045](https://doi.org/10.1080/00207540010011045).
- [8] Coman, M., Stan, S.D., Manic, M., Balan, R. (2010). Application of distance measuring with Matlab/Simulink. HSI 10, In: *Proceedings of the 3rd International Conference on Human System Interaction*, 113-118, doi: [10.1109/hsi.2010.5514581](https://doi.org/10.1109/hsi.2010.5514581).
- [9] Shahabi, H.H., Ratnam, M.M. (2010). In-cycle detection of built-up edge (BUE) from 2-D images of cutting tools using machine vision, *The International Journal of Advanced Manufacturing Technology*, Vol. 46, No. 9, 1179-1189, doi: [10.1007/s00170-009-2180-y](https://doi.org/10.1007/s00170-009-2180-y).
- [10] Dutta, S., Pal, S.K., Mukhopadhyay, S., Sen, R. (2013). Application of digital image processing in tool condition monitoring: A review, *CIRP Journal of Manufacturing Science and Technology*, Vol. 6, No. 3, 212-232, doi: [10.1016/j.cirpj.2013.02.005](https://doi.org/10.1016/j.cirpj.2013.02.005).
- [11] Shahabi, H.H., Ratnam, M.M. (2009). Assessment of flank wear and nose radius wear from workpiece roughness profile in turning operation using machine vision, *The International Journal of Advanced Manufacturing Technology*, Vol. 43, No. 1, 11-21, doi: [10.1007/s00170-008-1688-x](https://doi.org/10.1007/s00170-008-1688-x).
- [12] Jovanovič, B. (2015). The device for automated control of bushes (Naprava za avtomatizirano kontrolo puš), In: *Proceedings of the 9th conference Automation in economy and industry*, Maribor, Slovenia, 1-7, from <http://www.aig.si/15/zbornik/clanki/jovanovic.pdf>, accessed February 8, 2016.
- [13] Blanchet, G., Charbit, M. (2015). Digital signal and image processing using MATLAB®, (2<sup>nd</sup> edition), John Wiley & Sons, Inc. doi: [10.1002/9781119054009](https://doi.org/10.1002/9781119054009).



# Modelling supply risks in interdependent manufacturing systems: A case study

Omega, R.S.<sup>a</sup>, Noel, V.M.<sup>a</sup>, Masbad, J.G.<sup>a</sup>, Ocampo, L.A.<sup>b,\*</sup>

<sup>a</sup>Department of Industrial Engineering, University of San Carlos, Cebu City, Philippines

<sup>b</sup>Department of Mechanical and Manufacturing Engineering, University of San Carlos, Cebu City, Philippines

## ABSTRACT

This paper proposes a supply-driven inoperability input-output model (SIIM) in analysing risks of manufacturing systems. The approach, derived from the Leontief's input-output model, was previously debated for its implausibility in analysing sectors in an economic system. This paper provides interesting insights in production risk analysis especially that the adoption of SIIM in micro-level systems particularly in manufacturing systems was not yet explored in the current literature. The resemblance of economic systems and manufacturing systems in terms of system components, input-output concept, and component-wise interdependencies makes the approach appealing and highly plausible. Thus, this work adopts SIIM in analysing the impact of supply perturbations in a manufacturing system brought about by natural and man-made disasters, economic shifts, and government policies. An actual case study was carried out in a manufacturing firm in the central Philippines and two scenarios were presented to illustrate the proposed approach. The proposed approach is highly significant for manufacturing and risk practitioners in formulating mitigation policies to achieve a resilient manufacturing system.

© 2016 PEI, University of Maribor. All rights reserved.

## ARTICLE INFO

### Keywords:

Manufacturing systems  
Supply chain  
Supply risk analysis  
Modelling  
Supply-driven inoperability  
Input-output model

### \*Corresponding author:

laocampo@usc.edu.ph  
(Ocampo, Lanndon A.)

### Article history:

Received 17 January 2016  
Revised 16 May 2016  
Accepted 23 May 2016

## 1. Introduction

Competition among manufacturing industries both at local and global contexts has been increasingly tighter today than in the previous decades. These industries have been implementing crucial strategic decisions in order to compete. Furthermore, to sustain competitiveness, managers must be critical in various manufacturing decision-making areas in the context of firms' benefits, opportunities, costs and risks. A significant input to any decision-making process in manufacturing systems is the analysis of risks brought about by disruptions of internal and external components where manufacturing firms are highly susceptible to. Organizations in general and manufacturing firms in particular must seek to understand the underlying effects of these disruptions; thus, making risk analysis and management an ongoing concern [1].

Various approaches on risk analysis of manufacturing at firm level have been proposed in domain literature but these methodologies are based on qualitative measures. The inoperability input-output model (IIM) developed by Santos and Haimés [2], an important extension of the award winning input-output model introduced by Wassily Leontief for risk analysis, assesses the inability of sectors to perform their intended functions known as 'inoperability' caused by external perturbations such as natural disasters, terrorism, epidemic diseases, among others [2]. On a macroeconomic scale, Santos and Haimés [2], Jiang and Haimés [3], Haimés et al. [4] and Santos [5] have successfully demonstrated the use of IIM for risk analysis of interdependent

systems. The strength of IIM lies in its capability of handling the cascading effects of a final demand perturbation with interdependent system components, e.g. sectors in an economy. In contrast, the supply-driven IIM (SIIM) addresses the risks of possible changes in supply, also known as 'value-added perturbation'. Nevertheless, both demand-driven and supply-driven IIM analyses the impact of perturbations brought about by internal or external, natural or man-made processes [6]. While IIM was applied generally for risk analysis in economic systems, it may also work for other similar interdependent systems such as manufacturing systems as shown in current literature.

The main argument adopted in this work is that the assessment of potential losses of manufacturing systems brought about by external or internal disruptions can be addressed by performing risk analysis and assessment from a systems perspective. This approach is a significant input to organizational decision-making in general and in the evaluation of production processes in particular. At the manufacturing firm level particularly in production systems, demand-side perturbation is less plausible as individual processes rarely have final demand. Thus, supply-side perturbation is more relevant as sources of raw materials are highly susceptible to disruptions caused by external shocks, e.g. climate change impacts, man-made disasters. This study attempts to explore the application of supply-driven IIM in manufacturing systems as supported by the notion that supply-side perturbations are more relevant than demand-side perturbations. This promotes the application of SIIM in manufacturing risk analysis. While former approaches provide insights on this problem domain, they fail to provide a quantitative analytical framework which is highly significant in manufacturing decision-making. The motivation of adopting such methodology is in its strength to holistically evaluate the processes and examine risks from a systems perspective. A case study in a mosquito coil manufacturing system is reported in this work. The contribution of this study is in presenting a new methodological framework that holistically addresses risk analysis in manufacturing systems.

## 2. Literature review

### 2.1 Risk management in organizational decision making

Risk management is the identification, assessment, and prioritization of potential losses brought about by disruptions [1]. Allocating scarce resources in the most effective manner in order to reduce the impact of disruptions is now becoming a challenge for decision-makers [7]. Zobel [8] presented a model that highlights perceived trade-offs in defining disaster resilience of an infrastructure, organization, or any system which has been made possible through an adjusted resilience function and optimization model. Wang et al. [9] adopted graph theory approach in analysing vulnerability for interdependent infrastructure systems while fuzzy set theory has been used in assessing the impact of flooding [10,11]. On the other hand, IIM, an extension of Leontief's input-output model, has also been adopted as a tool to aid practitioners and researchers in risk analysis and assessment – an important component of risk management [7]. Nevertheless, risk analysis has always been an integral part of decision-making processes of any organization. In manufacturing firms, such disruptions caused by unavailable workers, machine downtime, shortage of raw materials, natural disasters, among others yield potential inoperability of a production process. Understanding risks and how to mitigate these impacts from a systems approach advances current knowledge on manufacturing resilience research.

### 2.2 Risk analysis with input-output model

The Leontief input-output model (IOM) describes the behaviour and relation of different economic sectors and the interdependencies among them. IOM identifies the key sector in relation to its dependence with the other sectors [12]. Typically, once an economic sector is prioritized, there comes a need to provide risk mitigation policies on the impact of undesirable events and production disruptions. The inherent structure of IOM which is to address interdependencies of systems in general makes it attractive in risk analysis. Prioritization of the key sector entails



implementation of preventive measures, policies, and investments for development and improvement as well as reducing the impacts of risks [7].

In economic systems, an internal or external failure of one sector could make that sector unable to perform its intended functions. Furthermore, with the inherent interdependencies of economic sectors, the impact of this failure propagates to the entire system which may trigger system's dysfunction. Santos [5] coined the term "inoperability" for this phenomenon leading to a new perspective in systemic risk analysis. This leads to an emerging model developed by Santos and Haines [2] and Jiang and Haines [3] known as the inoperability input-output model (IIM) which is basically derived from the Leontief IOM. IIM is an extension of the widely-accepted input-output model which focuses on assessing the possible impacts of a sector disruption in an economic system.

### 2.3 Demand-driven inoperability input-output model

In 2004, Haines and Jiang [3] founded an extension of IOM which is the IIM – a simple tool used to quantify the possible losses and impacts of man-made or natural disasters to a disrupted sector and to the entire system as well. The works on IIM generally focus on the demand-side inoperability which is expressed as the percentage of economic loss due to a change in final demand. This definition was established by Santos and Haines [2]. The plausibility of the IIM has gained interests among domain scholars such that extensions have been developed capable of analysing the effects of certain disruptions [13]. Several extensions have been reported in analysing the cascading effects of disruptions which may eventually help decision-makers in developing and implementing risk mitigation policies.

IIM focuses on the demand-side perturbation caused by external factors such as man-made disasters and natural calamities on economic systems. Using the widely used notations of the IIM, it can be constructed as

$$q = A^*q + c^* \quad (1)$$

where  $c^*$  is demand-side perturbation vector,  $A^*$  is the interdependency matrix, and  $q$  is the inoperability vector.

The demand-side perturbation vector represents the degree of change in demand due to a disruption. This can be calculated as 'as-planned' final demand  $\hat{c}_i$  minus actual final demand  $\tilde{c}_i$  of the same sector, divided by the 'as-planned' its production level  $\hat{x}_i$  which can be written as

$$c^* = [diag(\hat{x})]^{-1}[\hat{c} - \tilde{c}] \quad (2)$$

The demand-side interdependency matrix, denoted by  $A^*$ , is associated with the Leontief technological matrix  $A$  and the 'as-planned' production vector  $\hat{x}$ . This can be obtained using

$$A^* = [diag(\hat{x})]^{-1}[A][diag(\hat{x})] \quad (3)$$

The demand-side inoperability vector  $q$  can be expressed as the percentage economic loss of a sector due to a reduced final demand. The economic loss can be described as the difference between the 'as-planned' production  $\hat{x}$  and the reduced level of production  $\tilde{x}$ . By normalizing economic loss in terms of the 'as-planned' production  $\hat{x}$ ,  $q$  can be expressed as follows

$$q = [diag(\hat{x})]^{-1}[\hat{x} - \tilde{x}] \quad (4)$$

With the general formulation of the IIM which is expressed in a matrix notation as  $q = A^*q + c^*$  the inoperability can then be assessed and analysed.

IIM describes the cascading effects of a perturbation of interconnected sectors using quantitative values. Tan et al. [1] suggested that organizations must seek to understand such disruptions and be able to quantify their impact on the focal sector and to the entire system as well in

order to formulate effective mitigation activities. IIM is able to assess the inoperabilities of interdependent sectors caused by disasters, terrorism, among others [2].

IIM has been widely used in different applications such as in evaluating the effect of terrorism attack [2], loss of natural resource inputs due to climate change [14], fuel issues [15], etc. Along with emerging applications of IIM, several hybrid approaches have been developed in current literature with IIM as its core. These include the application of IIM in economic sectors [16], application of IIM focusing on specific areas in a sector [17], developing different methodologies on measuring the maximum level of perturbation the sector or the system can tolerate [18], applications that highlight the analysis of impact propagation to the upstream and downstream sectors [19], using a different approach in translating qualitative information into quantitative data [20], risk-based applications of IIM and the development of other models to assess inoperability [7] as well as analysing the dynamic elements of the matrices used in IIM [21]. See Table 1 for a summary of the applications of IIM. Note that the list is not intended to be comprehensive.

**Table 1** Applications of Inoperability Input-output Model (IIM)

Classification of application	References	Descriptions
Application of IIM in different areas of the economy	[16]	Used a multi-regional IIM in transportation network
	[13]	Applied IIM to evaluate the impact of inoperability of international trade (IT-IIM)
Application of IIM in specific area in a sector	[17]	Focused on the role of inventory with respect to resilience and inoperability
	[22]	Used IIM to quantify the effect in supply chain network disruption
	[23]	Measured the efficacy of inventory due to perturbation
Used a different method to know the maximum level of initial perturbation the sector or system can withstand	[24]	Developed a risk index which is obtained in order to support the IIM in creating an action plan of a system
	[18]	Created a shock absorption index which measures the maximum level of initial perturbation the system is capable of absorbing so that the entire system will not be fully inoperable
	[25]	Developed functional dependency net analysis (FDNA) which determines the level of inoperability tolerable by the sector
	[26]	Sensitivity analysis through sensitivity index which can be carried out by computing fields of influence
Used another approach of IIM that further stipulate the interdependencies of sectors	[27]	Agent-based approach also is used to break down sectors into sub-sectors to further assess the inoperability of these interrelated sectors and the system as a whole
	[28]	Decomposition of preparedness problems done in order to calculate the trade-off between preparedness cost and resilience among regions
Focused on propagation analysis to the upstream and downstream sectors	[1]	Propagation analysis is used to know the impact of a certain perturbation to the downstream and upstream sectors
	[19]	Focused on the propagation of critical infrastructure interdependency
Translated qualitative information into quantitative data	[29]	Developed stockholder's influence expressed in terms of loss of a stakeholder functionality in a scenario
	[20]	Used fuzzy numbers that deals with imprecise values
Risk management application of IIM	[7]	Applied IIM and provided risk management measures to potential disruption
	[3]	Risk-based framework of IIM to have for a more effective risk management
Development a dynamic technical coefficient	[21]	Focuses on the temporary or permanent values of the technical coefficient
Dynamic inoperability input-output model	[30]	Focuses on the inoperability of sectors with respect to time

The application of IIM in assessing the impact of disruptions in economic sectors provides guidance to decision-makers and policy-makers in implementing policies, preventive measures, and other investments to reduce the impacts of risks. However, the framework of IIM is not only limited to macro-economic analysis. Being a systems approach, it is also applicable to other areas that can be represented as systems, e.g. in production systems with processes as subsystems. Production processes are the series of steps required in transforming raw materials into finished goods which can be analogously treated as sectors of an economic system. These processes generate outputs that become inputs to other processes in converting work-in-process inventories into finished goods. Consequently, production processes establish interconnections with other processes making the entire system an interdependent one. The strength of IIM lies in its

capability in handling the cascading effects of a final demand perturbation to interdependent system components, e.g. sectors. In contrast, the supply-driven IIM (SIIM), which is an analogous methodology of IIM, investigates the risks of possible changes in supply or the so-called 'value-added perturbations'.

## 2.4 Supply-driven inoperability input-output model

The supply-driven static IIM (SIIM) was derived by Leung et al. [6]. SIIM is capable of quantifying the loss brought about by a value-added disruption or a supply perturbation of a certain component in a system and its effect to the other components. However, the implausibility of SIIM has become an emerging issue in current literature. However, in this study, its relevance in evaluating manufacturing process systems is presented. The SIIM is represented as

$$p = (I - A_s^*)^{-1} z^* \quad (5)$$

where  $p$  is the vector of the cost change in output due to value-added perturbation,  $A_s^*$  is the supply-based interdependency matrix, and  $z^*$  is the initial value-added or supply perturbation vector. Suppose that  $(I - A_s^*)^{-1} = (b_{ij})_{n \times n}$ , and

$$z^* = \text{diag}(\hat{x})^{-1}(\tilde{z} - \hat{z}) \quad (6)$$

$$p = \text{diag}(\hat{x})^{-1}(\tilde{x} - \hat{x}) \quad (7)$$

$$A_s^* = \text{diag}(\hat{x})^{-1} A_s \text{diag}(\hat{x}) \quad (8)$$

The vector  $\hat{z}$  is the value of nominal value-added and  $\tilde{z}$  is the value of degraded value-added after perturbation. The computations necessary in carrying out the SIIM are analogous to those of the IIM.

SIIM has been adopted for uncertainty and sensitivity analysis of interdependent infrastructure sectors [31]. While IIM works for risk analysis in economic systems, it also works for other similar interdependent systems such as manufacturing systems. The relevance of SIIM is on analysing the interdependent components in a system, e.g. processes in a manufacturing system, where supply is more considered relevant than demand. SIIM is more suitable in analysing the risks in a manufacturing system because of the presence of value-added inputs such as the raw materials, labour, and machineries that are highly susceptible to disruptions. Consequently, SIIM is likewise more relevant than the IIM as supply disruptions are more prevalent in the context of manufacturing due to the limited final demand requirements of each individual processes. For instance, most manufacturing systems have final demand in their end-of-line processes rather than on individual processes. Thus, a final demand perturbation is considered trivial in this context. With this, value-added input disruptions characterize most manufacturing systems which are caused by man-made or natural disasters forcing input prices to rise.

## 3. Case Study

### 3.1 Background of the Case Firm

Firm X is a mosquito coil manufacturing firm situated in central Philippines. It is one of the most competitive firm in its industry and has been a distributor for more than five decades. These mosquito coils vary in sizes, scents and effectiveness. Although these coils vary greatly in terms of composition and characteristics, their processes do not differ significantly. There are ten processes that these products generally undergo: vertical mixing, weighing, blending, kneading, stamping, air drying, tunnel drying, coil harvesting, spraying, and packing. Two scenarios are presented in this study to illustrate the application of IIM in the context of manufacturing systems and to quantify the impact of supply disruption of a process to the entire system. See Appendix A for the flow of processes of Firm X.

### 3.2 First scenario: *Coffee skin shortage due to tropical typhoons*

Coffee is known to be a natural insect repellent which makes coffee skin an essential material for the production of mosquito coils. The Philippines is one of the few countries that are capable of cultivating and growing four varieties of commercially-viable coffee namely Arabica, Liberia (Barako), Excelsa and Robusta. The agriculture and cultivation of crops in various types including coffee beans have been at risk over the last decade due to the fact that the Philippines has been struck by numerous disasters. Not only are the local farmers affected with this current issue, but also to the industries that need coffee products in its production [32]. In recent news, at least 116 hectares of coffee beans in 10 towns in Antique, located also in central Philippines were destroyed by Typhoon Haiyan, with local name Yolanda [33].

SIIM is used to analyse the effect of this disruption to the manufacturing system of Firm X which primarily acquires coffee skin from different parts of the country for its production. Given the possibility of a typhoon to strike the source of coffee beans, SIIM is used to quantify the loss in terms of cost-price change due to this possible value-added or supply disruption. A supposed 20 % price increase of coffee skin due to scarcity of supply which directly perturbs the blending process. Applying SIIM in the scenario makes it possible to see the effects of this perturbation to each of the individual production processes.

Having a 20 % value-added perturbation in blending process, caused by coffee skin shortage, results to relative cost-price changes to the other processes with final perturbation values shown in Table 2. The initial perturbation vector  $z^*$  is obtained by placing 0.20 in the blending process where the system is initially perturbed and 0 values for the rest of the entries which means that there are no initial perturbation in these respective processes. Final perturbation vector  $p$  was obtained using Eq. 5. The blending process obtained the largest  $p$  value because its value-added is directly and initially perturbed. Due to the initial perturbation in the blending process, the other processes in the system are also affected which can be observed by their final perturbation due to the indirect and direct interrelationships that they have with the blending process. Except for the vertical mixing process because it is a preceding process of the perturbed blending process. It has a zero value thus, a value-added change in the blending process does not result to a cost-price change in the inputs of vertical mixing. Since vertical mixing is the first process in the system, it does not require inputs from other processes, e.g. blending process. It can be also realized that the processes with direct relationship with the initially perturbed blending process have larger  $p$  values compared to the other processes.

**Table 2** Value-added perturbation caused by coffee skin shortage

Processes	$z^*$ (initial perturbation)	$p$ (final perturbation)
Vertical Mixing	0	0.0000
Weighing	0	0.1981
Blending	0.2	0.3769
Kneading	0	0.1182
Stamping	0	0.0841
Air Drying	0	0.0828
Tunnel Drying	0	0.0251
Coil Harvesting	0	0.0247
Spraying	0	0.0232
Packing	0	0.0218

### 3.3 Second scenario: *Coal price increase due to mine collapse*

Mosquito coils need to be hard to serve its purpose well and be an effective repellent. Thus, the drying process play a crucial role in manufacturing these products. These coils go through the tunnel drying process with the use of a steam boiler which primarily consumes up to 3,240 kg of coal for every 912 pairs of coil. With the daily demand of coils, coal is considered one of the high-volume raw materials used in production.

Coals are obtained through mining. Mining however, is considered one of the most dangerous industrial activities globally as several disasters have occurred in mining industries which are

very unpredictable in nature. At an open-pit mine of the largest coal producer in the Philippines, the western wall of the mine collapsed due to heavy rains and 13 miners were buried under the soil. This occurrence led to a four-month suspension of work in the firm as mandated by the Department of Energy of the Republic of the Philippines. Almost 94 % of the country's coal requirements is supplied by the firm and the suspension of the mining operation is believed to have a large impact on the market [34]. This resulted to a disrupted supply of coal to manufacturing firms in their operations which eventually increased the price of coal.

With the risk of recurrence, the scenario aims to look into the effect of the coal price increase to the mosquito coil firm's processes. A value-added perturbation of 36 % in the tunnel drying process is assumed which is caused by the increase in price of coal due to mining operation suspension. Results are shown in Table 3. It can be seen in Table 3 that the tunnel drying has the same percentage of perturbation in the initial and final perturbation, unlike the previous scenario, mainly because of the interrelationships it has with the other processes.

As seen in Appendix A the process flow of Firm X is generally straightforward thus the affected processes are those succeeding the perturbed process. These affected processes namely coil harvesting, spraying, and packing is not capable of contributing a perturbation to the tunnel drying process as this process does not require inputs from these processes. Hence, it is not dependent on these processes. Coil harvesting has a final perturbation value more or less similar with tunnel drying mainly because it directly receives the outputs of the tunnel drying process. Mindful of the concept of linear process flow or straightforward interrelationship of processes, processes preceding tunnel drying have no cost-price change values  $p$  since these processes (vertical mixing down to air drying) do not receive inputs from tunnel drying.

**Table 3** Value-added perturbation caused coal price increase

Processes	$z^*$ (initial perturbation)	$p$ (final perturbation)
Vertical mixing	0	0.0000
Weighing	0	0.0000
Blending	0	0.0000
Kneading	0	0.0000
Stamping	0	0.0000
Air drying	0	0.0000
Tunnel drying	0.36	0.3600
Coil harvesting	0	0.3545
Spraying	0	0.3333
Packing	0	0.3128

### 3.4 Discussion

In SIIM, two different scenarios of value-added perturbations were presented in the case study. For Firm X, scenario 1 shows coffee skin shortage brought about by tropical typhoons while scenario 2 illustrates coal price increase due to a disaster in mining operations. Results of the scenarios have quantified the final perturbation or cost-price changes of the value of outputs of the individual processes. It can be observed that Firm X has several processes with zero final perturbation values due its straightforward flow of processes. The final perturbation value of a particular process other than the perturbed process depends on its relationship and dependence with the initially perturbed process and the other processes. If that particular process precedes the perturbed process with no feedback loop, the impact of the initial perturbation is zero; that is  $p$  is zero, since it does not receive inputs from the perturbed process. In contrary, succeeding processes of the perturbed process are affected and the impact decreases as the distance, in terms of sequence, of a process with the perturbed one increases.

In this case study, SIIM has been successfully implemented in analysing and quantifying the impact of supply or value-added perturbations to the directly affected process and its cascading effects on the other processes due to the interdependencies among processes. In this study, two scenarios are presented to further explore the applicability of SIIM in micro-level application, i.e. in manufacturing firms. For both scenarios, it has been shown that when a certain process is disrupted through a supply or value-added perturbation, it will inflict cascading effects to pro-

cesses it has interrelationships with. The perturbation directly affects other processes the perturbed process has strong relationships with i.e. the proceeding process which needs the perturbed process' outputs and in contrary, yield small effects to processes that are weakly interrelated with the perturbed one. Therefore, the changes in the value of required output as manifested by the  $p$  values, which show the cascading effects of the initial perturbation, depend on the process being perturbed and its interrelationships among other processes.

#### 4. Conclusion and future work

The supply-driven inoperability input-output model adopted in this work addresses risk analysis in an interdependent system which is an inherent characteristic of most manufacturing systems. Contrary to current literature and practice where risks are assessed on individual component of the manufacturing system, the proposed approach identifies risks taken from the perspective of analysing the system as an integrated structure of components. SIIM quantifies the risks of cost-price increase of manufacturing process outputs brought about by the increase in prices of process value-added inputs which may be caused by natural or man-made disasters. It simultaneously considers production processes as a system rather than isolating each process for analysis. From the study reported in this work, it can be inferred that SIIM effectively quantifies the actual impact on each process after a value-added perturbation has occurred. Results of this risk assessment process help manufacturing managers and practitioners in establishing policies and infrastructures that would eventually minimize the systemic risks. SIIM aids the firm's management and other manufacturing practitioners in risk analysis and in decision-making collectively. No approach in manufacturing systems research has been reported that has the capability SIIM framework has to offer and this is considered as the main contribution of this work in the literature of risk analysis and manufacturing research. The proposed methodology is considered to be most suitable for manufacturing firms rather than the demand-driven approach mainly because each process in a manufacturing system generally does not have any final exogenous demand unlike economic sectors where final demand of each sector is naturally present.

A number of future works can be implemented with the proposed framework. First, the impreciseness of the data used in the input-output tables is crucial in enhancing the quality of the results. To address this, fuzzy set theory may be applied where data values become fuzzy numbers with membership functions. Future work can be done on this area and then compare the results with the results reported in this study in order to assess the robustness of the proposed approach. Secondly, SIIM framework can be extended to a dynamic SIIM in order to assess the behaviour of process perturbations with time. The dynamic SIIM may have the capability in determining the time when the manufacturing system achieves a status quo after the occurrence of a disruption. Third, the proposed approach can be applied in understanding supply-side risks of a supply chain brought about by supply-demand uncertainty [35]. When supply chain risks are assessed, the proposed method may be able to quantify the risks associated with the individual members of the supply chain. An interesting future work might be the integration of the proposed approach with the current directions of a sustainable supply chain [36]. The assessment may be incorporated with supply chain analysis frameworks that address the trade-off of maximising customer service level and minimising work-in-process inventory as proposed, for instance, by Smew et al. [37]. Finally, the emerging concerns on cyber-risks generated from hackers, employees, competitors and malicious software [38] can be also addressed using the proposed approach.

#### Acknowledgment

We sincerely thank the reviewers of this journal for their insightful comments which helped us improve the quality of this paper. We are grateful for the support provided by the management of the case firm. We also acknowledge the support from the University of San Carlos in terms of resource use.

## References

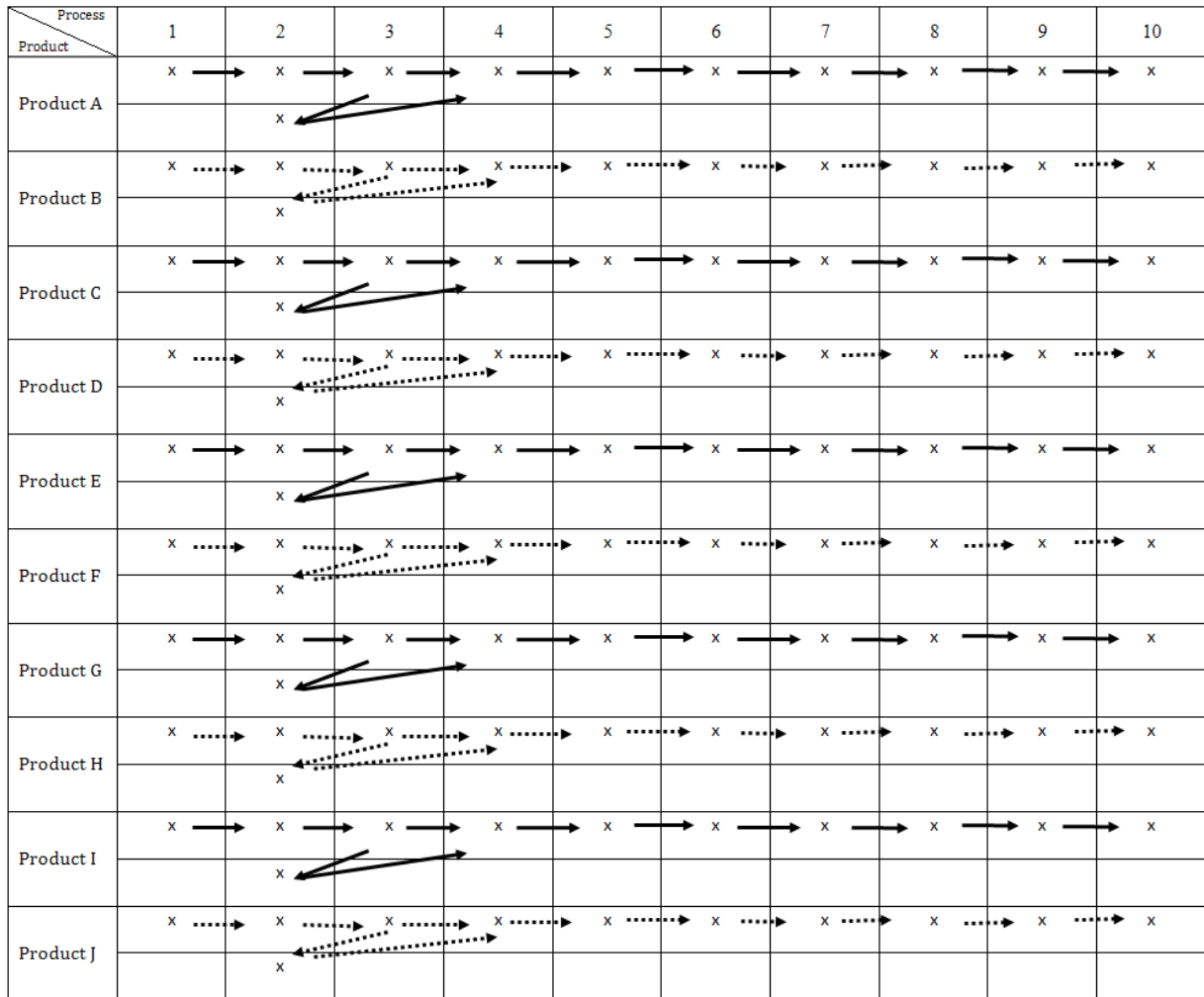
- [1] Tan, C.S., Tan, P.S., Lee, S.S.G., Pham, M.T. (2013). An inoperability input-output model (IIM) for disruption propagation analysis, *Proceedings of the 2013 IEEE International Conference on Industrial Engineering and Engineering Management (IEEM)*, 186-190, doi: [10.1109/IEEM.2013.6962400](https://doi.org/10.1109/IEEM.2013.6962400).
- [2] Santos, J.R., Haimes, Y.Y. (2004). Modeling the demand reduction input-output (I-O) inoperability due to terrorism of interconnected infrastructures, *Risk Analysis*, Vol. 24, No. 6, 1437-1451, doi: [10.1111/j.0272-4332.2004.00540.x](https://doi.org/10.1111/j.0272-4332.2004.00540.x).
- [3] Jiang P., Haimes, Y.Y. (2004). Risk management for Leontief-based interdependent systems, *Risk Analysis*, Vol. 24, No. 5, 1215-1229, doi: [10.1111/j.0272-4332.2004.00520.x](https://doi.org/10.1111/j.0272-4332.2004.00520.x).
- [4] Haimes, Y.Y., Horowitz, B.M., Lambert, J.H., Santos, J.R., Lian, C., Crowther, K.G. (2005). Inoperability input-output model for interdependent infrastructure sectors: Theory and methodology, *Journal of Infrastructure Systems*, Vol. 11, No. 2, 67-79, doi: [10.1061/\(ASCE\)1076-0342\(2005\)11:2\(67\)](https://doi.org/10.1061/(ASCE)1076-0342(2005)11:2(67)).
- [5] Santos, J.R. (2006). Inoperability input-output modeling of disruptions to interdependent economic systems, *Systems Engineering*, Vol. 9, No. 1, 20-34, doi: [10.1002/sys.20040](https://doi.org/10.1002/sys.20040).
- [6] Leung, M., Haimes, Y.Y., Santos, J.R. (2007). Supply-and output-side extensions to the inoperability input-output model for interdependent infrastructures, *Journal of Infrastructure Systems*, Vol. 13, No. 4, 299-310, doi: [10.1061/\(ASCE\)1076-0342\(2007\)13:4\(299\)](https://doi.org/10.1061/(ASCE)1076-0342(2007)13:4(299)).
- [7] Anderson, C.W., Santos, J.R., Haimes, Y.Y. (2007). A risk-based input-output methodology for measuring the effects of the August 2003 Northeast blackout, *Economic Systems Research*, Vol. 19, No. 2, 183-204, doi: [10.1080/09535310701330233](https://doi.org/10.1080/09535310701330233).
- [8] Zobel, C.W. (2011). Representing perceived tradeoffs in defining disaster resilience, *Decision Support Systems*, Vol. 50, No. 2, 394-403, doi: [10.1016/j.dss.2010.10.001](https://doi.org/10.1016/j.dss.2010.10.001).
- [9] Wang, S., Hong, L., Chen, X. (2012). Vulnerability analysis of interdependent infrastructure systems: A methodological framework, *Physica A: Statistical Mechanics and its Applications*, Vol. 391, No. 11, 3323-3335, doi: [10.1016/j.physa.2011.12.043](https://doi.org/10.1016/j.physa.2011.12.043).
- [10] Lei, T., Liangyu, W., Rijia, D., Lijia, L. (2011). Study on the dynamic input-output model with coal mine safety, *Procedia Engineering*, Vol. 26, 1997-2002, doi: [10.1016/j.proeng.2011.11.2396](https://doi.org/10.1016/j.proeng.2011.11.2396).
- [11] Jiang, W., Deng, L., Chen, L., Wu, J., Li, J. (2009). Risk assessment and validation of flood disaster based on fuzzy mathematics, *Progress in Natural Science*, Vol. 19, No. 10, 1419-1425, doi: [10.1016/j.pnsc.2008.12.010](https://doi.org/10.1016/j.pnsc.2008.12.010).
- [12] Miller, R.E., Blair, P.D. (2009). *Input-output analysis: Foundations and extensions*, (2<sup>nd</sup> edition), Cambridge University Press, New York, USA, doi: [10.1017/CBO9780511626982](https://doi.org/10.1017/CBO9780511626982).
- [13] Jung, J., Santos, J.R., Haimes, Y.Y. (2009). International trade inoperability input-output model (IT-IIM): Theory and application, *Risk Analysis*, Vol. 29, No. 1, 137-154, doi: [10.1111/j.1539-6924.2008.01126.x](https://doi.org/10.1111/j.1539-6924.2008.01126.x).
- [14] Tan, R.R., Aviso, K.B., Promentilla, M.A.B., Yu, K.D.S., Santos, J.R. (2015). Development of a fuzzy linear programming model for allocation of inoperability in economic sectors due to loss of natural resource inputs, *DLSU Business & Economics Review*, Vol. 24, No. 2, 1-12.
- [15] Tan, R.R., Aviso, K.B., Promentilla, M.A.B., Yu, K.D.S., Santos, J.R. (2014). Fuzzy inoperability input-output analysis of mandatory biodiesel blending programs: The Philippine case, *Energy Procedia*, Vol. 61, 45-48, doi: [10.1016/j.egypro.2014.11.902](https://doi.org/10.1016/j.egypro.2014.11.902).
- [16] Pant, R., Barker, K., Grant, F.H., Landers, T.L. (2011). Interdependent impacts of inoperability at multi-modal transportation container terminals, *Transportation Research Part E: Logistics and Transportation Review*, Vol. 47, No. 5, 722-737, doi: [10.1016/j.tre.2011.02.009](https://doi.org/10.1016/j.tre.2011.02.009).
- [17] Resurreccion, J.Z., Santos, J.R. (2012). Stochastic modeling of manufacturing-based interdependent inventory for formulating sector prioritization strategies in reinforcing disaster preparedness, In: *Proceedings of the 2012 IEEE Systems and Information Design Symposium (SIEDS)*, 134-139, doi: [10.1109/SIEDS.2012.6215127](https://doi.org/10.1109/SIEDS.2012.6215127).
- [18] Tan, R.R., Aviso, K.B., Promentilla, M.A.B., Solis, F.D.B., Yu, K.D.S., Santos, J.R. (2015). A shock absorption index for inoperability input-output models, *Economic Systems Research*, Vol. 27, No. 1, 43-59, doi: [10.1080/09535314.2014.922462](https://doi.org/10.1080/09535314.2014.922462).
- [19] Owusu, A., Mohamed, S., Anissimov, Y. (2010). Input-output impact risk propagation in critical infrastructure interdependency, In: *Proceedings of the 13<sup>th</sup> International Conference on Computing in Civil and Building Engineering*, Nottingham, UK.
- [20] Setola, R., De Porcellinis, S., Sforza, M. (2009). Critical infrastructure dependency assessment using the input-output inoperability model, *International Journal of Critical Infrastructure Protection*, Vol. 2, No. 4, 170-178, doi: [10.1016/j.ijcip.2009.09.002](https://doi.org/10.1016/j.ijcip.2009.09.002).
- [21] Percoco, M. (2006). A note on the inoperability input-output model, *Risk Analysis*, Vol. 26, No. 3, 589-594, doi: [10.1111/j.1539-6924.2006.00765.x](https://doi.org/10.1111/j.1539-6924.2006.00765.x).
- [22] Wei, H., Dong, M., Sun, S. (2010). Inoperability input-output modeling (IIM) of disruptions to supply chain networks, *Systems Engineering*, Vol. 13, No. 4, 324-339, doi: [10.1002/sys.20153](https://doi.org/10.1002/sys.20153).
- [23] Barker, K., Santos, J.R. (2010). Measuring the efficacy of inventory with a dynamic input-output model, *International Journal of Production Economics*, Vol. 126, No. 1, 130-143, doi: [10.1016/j.ijpe.2009.08.011](https://doi.org/10.1016/j.ijpe.2009.08.011).
- [24] Benjamin, M.F.D., Tan, R.R., Razon, L.F. (2015). Probabilistic multi-disruption risk analysis in bioenergy parks via physical input-output modeling and analytic hierarchy process, *Sustainable Production and Consumption*, Vol. 1, 22-33, doi: [10.1016/j.spc.2015.05.001](https://doi.org/10.1016/j.spc.2015.05.001).

- [25] Garvey, P.R., Pinto, C.A., Santos, J.R. (2014). Modelling and measuring the operability of interdependent systems and systems of systems: advances in methods and applications, *International Journal of System of Systems Engineering*, Vol. 5, No. 1, 1-24, doi: [10.1504/IJSSE.2014.060880](https://doi.org/10.1504/IJSSE.2014.060880).
- [26] Percoco, M. (2011). On the local sensitivity analysis of the inoperability input-output model, *Risk Analysis*, Vol. 31, No. 7, 1038-1042, doi: [10.1111/j.1539-6924.2010.01574.x](https://doi.org/10.1111/j.1539-6924.2010.01574.x).
- [27] Oliva, G., Panzieri, S., Setola, R. (2010). Agent-based input-output interdependency model, *International Journal of Critical Infrastructure Protection*, Vol. 3, No. 2, 76-82, doi: [10.1016/j.ijcip.2010.05.001](https://doi.org/10.1016/j.ijcip.2010.05.001).
- [28] Crowther, K.G. (2008). Decentralized risk management for strategic preparedness of critical infrastructure through decomposition of the inoperability input-output model, *International Journal of Critical Infrastructure Protection*, Vol. 1, 53-67, doi: [10.1016/j.ijcip.2008.08.009](https://doi.org/10.1016/j.ijcip.2008.08.009).
- [29] Hester, P.T., Adams, K.MacG. (2013). Determining stakeholder influence using input-output modeling, *Procedia Computer Science*, Vol. 20, 337-341, doi: [10.1016/j.procs.2013.09.282](https://doi.org/10.1016/j.procs.2013.09.282).
- [30] Lian, C., Santos, J.R., Haimes, Y.Y. (2007). Extreme risk analysis of interdependent economic and infrastructure sectors, *Risk Analysis*, Vol. 27, No. 4, 1053-1064, doi: [10.1111/j.1539-6924.2007.00943.x](https://doi.org/10.1111/j.1539-6924.2007.00943.x).
- [31] Xu, W., Wang, Z. (2015). The uncertainty and sensitivity analysis of the interdependent infrastructure sectors based on the supply-driven inoperability input-output model, *International Journal of Innovative Computing, Information and Control*, Vol. 11, No. 2, 615-625.
- [32] Whiteman, H. (2014). Philippines gets more than its share of disasters, from <http://edition.cnn.com/2013/11/08/world/asia/philippines-typhoon-destruction/>, accessed January 4, 2016.
- [33] Mondragon, A. (2013). Antique's agriculture still reeling from Yolanda, from <http://www.rappler.com/move-ph/46911-antique-agriculture-yolanda>, accessed January 6, 2016.
- [34] Olchondra, R.T., Abadilla, D.D. (2015). 5 dead, 4 missing in coal mine collapse. Inquirer News, from <http://newsinfo.inquirer.net/705980/5-dead-4-missing-in-coal-mine-collapse>, accessed January 6, 2016.
- [35] Li, M., Wu, G.-D., Lai, X.D. (2014). Capacity coordination mechanism for supply chain under supply-demand uncertainty, *International Journal of Simulation Modelling*, Vol. 13, No. 3, 364-376, doi: [10.2507/IJSIMM13\(3\)CO14](https://doi.org/10.2507/IJSIMM13(3)CO14).
- [36] Seuring, S. (2013). A review of modeling approaches for sustainable supply chain management, *Decision Support Systems*, Vol. 54, No. 4, 1513-1520, doi: [10.1016/j.dss.2012.05.053](https://doi.org/10.1016/j.dss.2012.05.053).
- [37] Smew, W., Young, P., Geraghty, J. (2013). Supply chain analysis using simulation, Gaussian process modelling and optimisation, *International Journal of Simulation Modelling*, Vol. 12, No. 3, 178-189, doi: [10.2507/IJSIMM12\(3\)4.239](https://doi.org/10.2507/IJSIMM12(3)4.239).
- [38] Očevčić, H., Nenadić, K., Šolić, K. (2014). Decision support based on the risk assessment of information systems and Bayesian learning, *Tehnički vjesnik – Technical Gazette*, Vol. 21, No. 3, 539-544.



## Appendix A

### Process flow of Products of Firm X



# Analysis for prevalence of carpal tunnel syndrome in shocker manufacturing workers

Kumar, S.<sup>a</sup>, Muralidhar, M.<sup>a,\*</sup>

<sup>a</sup>Department of Mechanical Engineering, North Eastern Regional Institute of Science and Technology, Itanagar, Arunachal Pradesh, India

## ABSTRACT

Carpal tunnel syndrome (CTS) is the most commonly reported work-related musculoskeletal disorder of the upper extremity. In this communication, a comparison of CTS and associated risk factors amongst traditional and semi-ergonomic shocker manufacturing assembly line workers in the actual industrial environment has been studied through questionnaire and physical tests. Fisher's exact test and Surface electromyography (sEMG) signal values have been used for statistical data analysis. Symptoms present are numbness (in 80 % of traditional and in 16.66 % of semi-ergonomic), tingling (in 50 % of traditional and in 8.33 % of semi-ergonomic), and difficulty in grasping (in 80 % of traditional and 20 % of semi-ergonomic). Tinel's and Phalen's sign also show an almost similar trend. The results reflect that the traditional shocker manufacturing workers have more CTS symptoms occurrence than the semi-ergonomic shocker manufacturing workers. The sEMG signal analysis result reveals that the lesser muscle activity values (EMG-RMS values) indicate the contribution of CTS symptom in shocker assembly line workers. It is found that there is a significant difference in EMG-RMS values of CTS symptoms and control subjects in traditional and semi-ergonomic shocker manufacturing industries. It is observed that if a subject is affected with CTS symptoms, then the sEMG signal value is 0.01223 mV in case of traditional and 0.02625 mV in case of semi-ergonomic shocker assembly, and for control subjects sEMG signal value is 0.15614 mV in traditional and 0.17563 mV in case of semi-ergonomic shocker assembly.

© 2016 PEI, University of Maribor. All rights reserved.

## ARTICLE INFO

### Keywords:

Manufacturing workers  
Musculoskeletal disorders  
Carpal tunnel syndrome  
Fisher's exact test  
Surface electromyography

### \*Corresponding author:

mm@nerist.ac.in  
(Muralidhar, M.)

### Article history:

Received 3 August 2015  
Revised 24 January 2016  
Accepted 8 March 2016

## 1. Introduction

Occupational health problems, injuries and disorders are primarily due to the work characteristics and environment in industries worldwide [1, 2]. Research survey on Repetitive Strain Injuries (RSI) has been observed as the most common form of work related illness of physical and psychological affecting various organizations [3-6]. RSI directly affect the quality and production rate of work, health of workers, work satisfaction, and absenteeism [7-10]. One of the common RSI Carpal Tunnel Syndrome (CTS) and associated risk factors among assembly line workers engaged in traditional and semi-ergonomic shocker manufacturing industries are due to work-related musculoskeletal disorders (WMSDs). Assembly line workstations and their operations are executed repeatedly and hence result WMSDs [11, 12]. Musculoskeletal disorders (MSDs) means conditions associated with the upper extremities (arm and hand) affecting the muscles, nerves or other soft tissues, tendons, ligaments, and joints. MSDs are common occupational diseases among assembly line workers due to repetitive movements or heavy workloads [13, 14].

The assembly line workers of automotive industry are one of several industries that have high incidence of MSDs [15, 16]. The common risk factor may possibly be the repetitive awkward posture of the worker relative to the work while trying to access different tasks in automotive assembly line. Previous studies for automotive industry workforce have shown that awkward postures increase the risk of MSDs [17-19]. Published literature indicate that reducing workplace exposure to known risk factors including awkward posture results in reduced MSD risk [20-22]. The Ovako Working Posture Analysis System (OWAS) method using 3D simulation to identify and evaluate harmful working posture was carried out [23]. CTS is one of the type of MSDs affects 1 % of general population and 5 % of working population undergoing repetitive movements of wrists and hands in daily living. CTS is a narrow tunnel in the wrist formed by ligament and bone. The common symptoms of hand pain, wrist pain, numbness, tingling, and pain within the median nerve were analysed [24, 25]. Investigation on carpal tunnel and osteofibrotic tunnel surrounded by carpal bones and the strong transverse carpal ligament was done. Nine tendons run through the tunnel, as well as the median nerve, which is the closest to the surface, and the associated blood vessels. CTS occurs when the ligaments running through the carpal tunnel get inflamed due to relatively small yet lasting or repeated pressure or vibration, which causes swelling of tendon sheaths resulting in elevated pressure in the carpal tunnel and hence entrapment of the median nerve against the transverse carpal ligament [26]. Studies on CTS by over-worked, over-strained muscles of arms and hands, possibly leading to muscle strength problems were carried out [27].

A review on long exposure to repetitive flexion and extension of the wrist studies were analysed and the diagnostic procedure were highlighted [28]. The detection, amplification and recording of changes in skin voltage produced by underlying skeletal muscle contraction are termed as electromyography and recording obtained is called Electromyogram. The Abductor Pollicis Brevis (APB) and its affect by muscle entropy associated with CTS were discussed [29-31]. Many clinical and biomechanical studies on CTS, the electrophysiological properties of the APB muscle were investigated [32-35]. EMG signal is a biomedical signal that measures electrical currents generated in muscles during its contraction and expansion representing neuromuscular activities. The nervous system always controls the muscular activity. The analysis of EMG signal and physiological properties of muscles was carried out [36]. Study on EMG to detect muscular disorder along with muscular abnormalities caused by other system disease such as nerve dysfunction was done [37]. Investigation on surface EMG and its use by personnel other than medical doctors was carried out [38]. Studies on anthropometric characteristics of the hand, muscle tensile strength related to hand grip movement was carried out [39]. Several studies confirmed persons with high BMI to be a group at high risk for developing CTS. High BMI is also associated with decreased sensory conductivity of the median nerve [40-43].

In the present study an attempt has been made to monitor the impact of CTS and associated risk factors in traditional and semi-ergonomic shocker manufacturing industries through Fisher's exact test and sEMG signal analysis.

## 2. Materials and methods

This work was carried out at two shocker industries in Haryana State, India. 140 workers of two shocker manufacturing industries, one is based on traditional and other on semi-ergonomic standards, were included in the study. In traditional shocker assembly all parts are assembled manually and some operation by machines (like cylinder bottom pressing, cylinder valve tightening with the help of riveting machine) are performed on an assembly line. Semi-ergonomic shocker assembly is a system of using machines considering human machine interface and ergonomical aspects for assembly of shock absorber. There are 70 workforce in traditional, with a mean age of  $39.29 \pm 7.76$  years, range 25-56, and 70 in semi-ergonomic, with a mean age of  $29.23 \pm 3.54$  years, range 23-40. The number of workers at the studied line was 91 in traditional and 85 in semi-ergonomic. In the present study we excluded those who did not work at the line, those who were off work due to sick-leave, pregnancy, education, chronic illness or due to other

reasons. The study included those 140 that were present at their workstation on the day of examination of those specific workstations. The full questionnaire is shown in the Appendix A.

## 2.1 Shock absorber operations and assembly systems

The ergonomics study has been conducted on total 140 workers of two shocker manufacturing industries. One is based on traditional and other on semi-ergonomic standards having manual operations such as case tube cleaning, cylinder cleaning, component cleaning, guide disk assembly, piston valve tightening/riveting, cylinder bottom valve assembly/tightening, oil filling in cylinder, cylinder bottom pressing, piston rod circlipping, oil seal assembly, oil seal pressing and beading and Sealing. A brief description of each operation is given below.

### *Case tube cleaning*

In this operation the outer tube is cleaned extensively so that the shocker can work properly. It is made up of mild steel and having weighs around 2 kg. The operation is performed in a cleaning chamber with a suitable brush in both the industries.

### *Cylinder cleaning*

To remove foreign particles properly from outer surface of cylinder the phosphate solution is used. In semi-ergonomic industry both case tube cleaning and cylinder cleaning operations are performed at same work station as shown in Fig. 1.



**Fig. 1** A typical photograph of case tube and cylinder cleaning event at traditional and semi-ergonomic shocker assembly line

### *Component cleaning*

Small components like bush, washer and oil seal are cleaned in a tray by the air pressure to wipe out the dust and foreign particles properly. The number of operators engaged in traditional shocker assembly unit are five whereas in semi-ergonomic industry are four. In both the industries the operation was performed in cleaning chamber as shown in Fig. 2.



**Fig. 2** A typical photograph of component cleaning event at traditional and semi-ergonomic shocker assembly line

*Guide disk assembly*

In this operation guide disk is used for piston and main spring support. The assembly is done by spanner and air nut runner. The four numbers of operators are engaged in traditional and semi-ergonomic industries. In traditional manufacturing unit, the operation is performed by a conventional spanner at guide disk assembly station whereas in semi-ergonomic industry, it is performed on a moving conveyor by air nut runner as shown in Fig. 3.

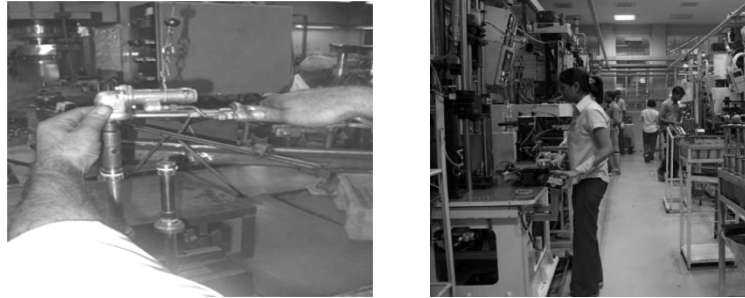


**Fig. 3** A typical photograph of guide disk assembly event at traditional and semi-ergonomic shocker assembly line

*Piston valve tightening/riveting*

In both the industries, the operation is performed by a riveting press at piston valve tightening station. The operation is performed on moving conveyor and piston valve is tightened by riveting machine. The number of operators engaged is five in both the industries as shown in Fig. 4.

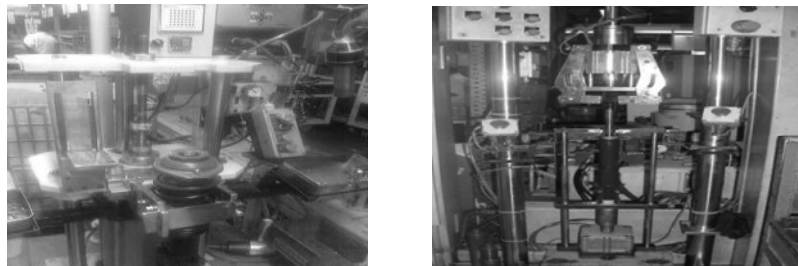


**Fig. 4** A typical photograph of piston valve tightening event at traditional and semi-ergonomic shocker assembly line

*Cylinder bottom valve assembly/tightening*

In both the industries, the operation is performed at cylinder bottom valve assembly station and cylinder bottom valve is tightened by riveting press. The operation is performed on a moving conveyor and piston valve is tightened by air nut runner. The number of operators engaged in traditional and semi-ergonomic industries is four and five respectively as shown in Fig. 5.

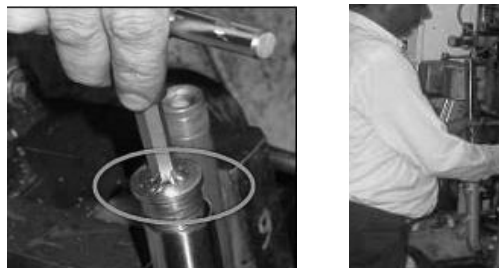


**Fig. 5** A typical photograph of cylinder bottom valve assembly event at traditional and semi-ergonomic shocker assembly line

### *Oil filling in cylinder*

For friction control the lubricant oil is poured manually in the cylinder in traditional manufacturing unit whereas in semi-ergonomic industry, it is done by oil filling machine. Number of operators engaged in traditional and semi-ergonomic industry is five and three respectively as shown in Fig. 6.

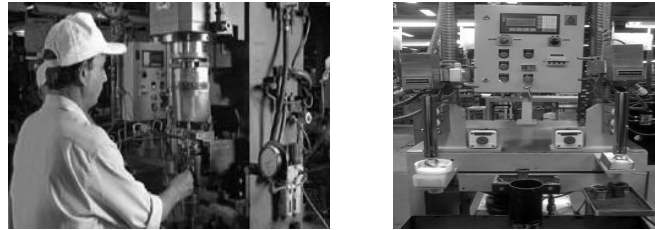


**Fig. 6** A typical photograph of oil filling event at traditional and semi-ergonomic shocker assembly line

### *Cylinder bottom pressing*

In this operation, after tightening the cylinder bottom valve, cylinder bottom is pressed by five tonnage presses. In traditional industry four operators are engaged whereas in semi-ergonomic industry three operators are engaged as shown in Fig. 7.

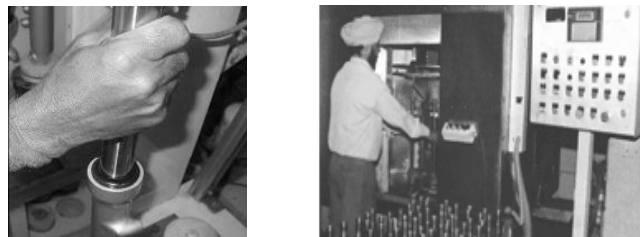


**Fig. 7** A typical photograph of cylinder bottom pressing event at traditional and semi-ergonomic shocker assembly line

### *Piston rod circlipping*

In traditional industry the operation is performed with the help of conventional spanner whereas in semi-ergonomic industry the operation is performed by air nut runner. The operator engaged in this operation is four in both the industries as shown in Fig. 8.



**Fig. 8** A typical photograph of piston rod circlipping event at traditional and semi-ergonomic shocker assembly line

### *Oil seal assembly*

Oil seal prevents the oil leakage from cylinder during movement of piston in cylinder. In this operation oil seal is assembled to the top of cylinder. It contains rubber seal, valve inlet and a nut which is assembled manually with the help of spanner in both industries. The operators engaged in this operation are five in both the industries as shown in Fig. 9.



**Fig. 9** A typical photograph of oil seal assembly event at traditional and semi-ergonomic shocker assembly line

*Oil seal pressing*

In this operation, oil seal assembly is pushed with the help of a riveting machine in both the industries. The number of operators engaged in the operation is five in both the industries as shown in Fig. 10.



**Fig. 10** A typical photograph of oil seal pressing event at traditional and semi-ergonomic shocker assembly line

*Beading and sealing*

In beading operation, the casing chamber of shocker is closed with special purpose machine called beading machine. In traditional manufacturing unit, five operators are engaged. The sealing operation is similar to beading operation but it is performed on a similar kind of special purpose machine, for the enforcement of beading joint to ensure the leakage of hydraulic oil and air in the casing tube chamber. In semi-ergonomic industry, the beading and sealing operation is performed on the same machine and total eleven operators are engaged in this combined task as shown in Fig. 11 and Fig. 12.

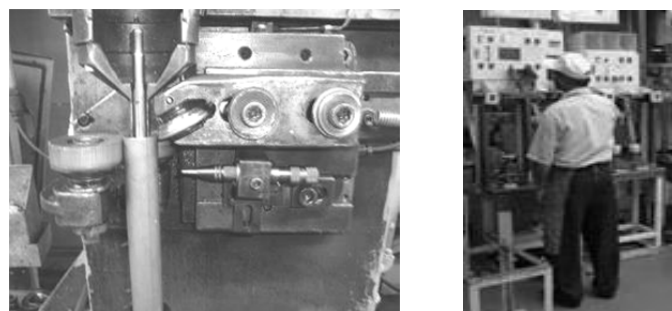


**Fig. 11** A typical photograph of beading event at traditional and semi-ergonomic shocker assembly line



**Fig. 12** A typical photograph of sealing event at traditional and semi-ergonomic shocker assembly line

## 2.2. Methods

The study was conducted at two shocker manufacturing plants. The companies provided a list of all jobs in the facility. The present study was conducted in traditional and semi- ergonomic assembly profile section. The workers were interviewed and examined at the work-site. The health questionnaire was designed and statistical measurements were taken. Verbal consent of the workers was being taken and physical tests have been conducted. The health questionnaire included statistical description, investigation through physical examination, CTS symptom severity scale and on-job observation. Physical examination included height, weight, BMI, and grip strength measurement in assembly line as shown in Table 1. All physical examinations were being conducted through analog instruments. Readings were noted and tabulated. The descriptive statistics of the parameters with mean and standard deviation were computed and shown in the Table 1.

Hand grip strengths were taken so as to find out there relationships with potential CTS symptoms. CTS symptom severity scale is divided into four levels, namely 0, 1, 2 and 3. The level 0 for no, 1 for mild, 2 for moderate, and 3 is for severe CTS symptoms condition. No means zero pain, one means pain in Abductor Pollicis Brevis (APB) muscle. Mild means pain in APB and Flexor Pollicis Brevis (FPB) muscle, moderate means pain in fingers, thenar muscles and hands occasionally, severe means intolerable pain in fingers, thenar muscles, hands, elbow up to shoulder. CTS symptom severity scale has been applied upon potential CTS symptoms namely wrist pain, hand pain, numbness, tingling, difficulty in grasping and weakness to investigate the impact of CTS symptoms. Repetitiveness in the job has been categorized into two levels namely high and low based on cycle time. The physical examination included 4 items namely shoulders, hands, wrist and fingers. The work exposure evaluation was done in two ways; the workers own opinion in the questionnaire and an evaluation by the investigators including an ergonomic study. The whole examination took place in the supervisor's office, nearby the actual workstation.

The results from these sources were compared for each of the operations investigated. Workers at the same workstation did the same job, and there was job rotation every two hours. The standard values of weight of the job and magnitude of the force applied during operations by the workers was provided by the company.

## 2.3 Statistical description

The collected data from questionnaire and physical tests is summarized based on age, weight, height, BMI, hand grip strength, and job duration in assembly line as shown in Table 1. The descriptive statistics of the parameters with mean and standard deviation have been mentioned in the Table 1.

**Table 1** Statistics of two shocker manufacturing assembly line workers

Factor of concern	Traditional shocker manufacturing workers (Mean $\pm$ S.D.)	Semi-ergonomic shocker manufacturing workers (Mean $\pm$ S.D.)
Number	70	70
Age (years)	39.29 $\pm$ 7.76	29.23 $\pm$ 3.54
Weight (kg)	67.54 $\pm$ 7.91	64.33 $\pm$ 5.60
Height (m)	1.667 $\pm$ 0.072	1.664 $\pm$ 0.067
BMI (kg/m <sup>2</sup> )	23.29 $\pm$ 0.65	23.18 $\pm$ 0.59
Grip strength (kg)	42.06 $\pm$ 16.57	50.67 $\pm$ 18.83
Employment time at present site (years)	12.57 $\pm$ 7.40	4.57 $\pm$ 3.08

## 2.4 Experimental set up of sEMG

Myoelectric signal represents the electrical activity of muscles and its signal value is represented in millivolts obtained by surface electromyography (sEMG) technique. sEMG signals have been taken by BIOPAC MP-45 data acquisition unit as shown in Fig. 13. The MP-45 unit is an electrically isolated data acquisition unit, designed for biophysical measurements. The MP-45 receives power from the computer (USB port). The MP Unit has an internal microprocessor to control



data acquisition and communication with the computer. The MP-45 Unit takes incoming signals and converts them into digital signals that can be processed with the computer. There are analog input channels (two on MP-45), one of which can be used as a trigger input. In the present study 140 workers have been examined by the BIOPAC MP-45 instrument. To take readings from the muscles of a subject three electrodes are used. The negative electrode (white) is placed on APB muscle and positive electrode (red) is placed 6 to 10 cm away from negative electrode. The third electrode (black) is grounded. An EMG reading of APB muscle of dominant hand is recorded for 180 s for a series of clenching fists as hard as possible, and then followed by slow release. Low voltage stimulator, electrodes and electrode lead set are shown in Figs. 14, 15, and 16.



Fig. 13 EMG Experimentation set-up



Fig. 14 Low voltage stimulator

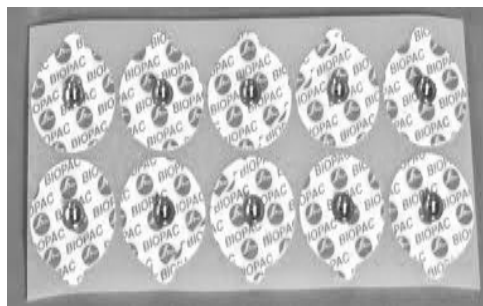


Fig. 15 Electrodes



Fig. 16 Electrode Lead Set

**2.5. Statistical tool for CTS analysis**

Following statistical tool has been used for CTS analysis.

*Fisher's exact test*

Fisher's exact test is used to check statistical significance of 2x2 contingency Tables. In present study Fisher's exact test has been used to check all the symptoms of CTS in collected data of traditional and semi-ergonomic industries workers for comparison on the basis of response of workers for all the symptoms in yes or no. Notations *a*, *b*, *c* and *d* are assigned to cells for fisher's exact test and the grand total is assigned the notation *n* and are presented in Table 2.

**Table 2** A 2 x 2 contingency table set-up for Fisher's exact test

Description	Traditional shocker manufacturing worker	Semi-ergonomic shocker manufacturing worker	Total
Symptom present (Test positive)	<i>a</i>	<i>b</i>	<i>a + b</i>
Symptom not present (Test negative)	<i>c</i>	<i>d</i>	<i>c + d</i>
Total	<i>a + c</i>	<i>b + d</i>	<i>n</i>

The probability value  $p$  is computed by the hyper geometric distribution and expressed as

$$p = \frac{\left(\frac{a+b}{a}\right)! \left(\frac{c+d}{c}\right)!}{\left(\frac{n}{a+c}\right)!} = \frac{(a+b)! (c+d)! (a+c)! (b+d)!}{a! b! c! d! n!} \quad (1)$$

where the number of observations obtained for analysis is small (sample size  $\leq 30$ ) [44].

### 3. Results and discussions

#### 3.1 CTS symptoms based analysis by Fisher's exact test

The CTS symptoms like hand pain (pain is felt in the part of upper extremity distal to wrist joint), wrist pain (pain is felt in between distal portion of forearm and proximal portion of hand), numbness (loss of sensation), tingling (sensation of having sharp object pressure on affected area), difficulty in grasping (inability of holding any object in palmer aspect of hand properly), weakness (lack of strength to do a particular job), Tinel's sign, and Phenal's sign in traditional and semi-ergonomic shocker manufacturing workers with their percentage of presence are computed from the collected data and Eq. 1. The p-value so obtained is used to check the significance of the symptoms as shown in Table 3.

**Table 3** Test of difference between traditional and semi-ergonomic shocker manufacturing workers considering CTS related symptoms, and by applying Fisher's exact test

Symptoms	Traditional shocker manufacturing worker			Semi-ergonomic shocker manufacturing worker			p-value	Significance
	No. of workers	CTS symptoms sufferer	%	No. of workers	CTS symptoms sufferer	%		
Hand pain	10	2	20	5	1	20	0.4945	Not significant
Wrist pain	12	1	8.33	3	1	33.33	0.3428	Not significant
Numbness	5	4	80	12	2	16.66	0.0266	Significant (P < 0.05)
Tingling	10	5	50	12	1	8.33	0.0405	Significant (P < 0.05)
Difficulty in grasping	5	4	80	10	2	20	0.0449	Significant (P < 0.05)
Weakness	7	1	14.28	3	1	33.33	0.4660	Not significant
Tinel's sign	12	8	66.67	11	2	18.18	0.0237	Significant (P < 0.05)
Phenal's sign	9	5	55.55	14	2	14.28	0.0467	Significant (P < 0.05)

From the Table 3 it is observed that due to difficulty in grasping problems 80 % of traditional and 20 % of semi-ergonomic shocker manufacturing workers ( $p < 0.05$ ), have been unable to perform the usual activities. The data analyzed from questionnaire also show that traditional shocker manufacturing workers have more percentage of CTS symptoms like numbness, tingling, Tinel's and Phalen's sign. Tinel's sign occurred in 66.67 % of the traditional and 18.18 % of the Semi-ergonomic shocker manufacturing workers ( $p < 0.05$ ). Phalen's sign also show almost similar trend. Hand pain, wrist pain and feeling of weakness cannot correlate to CTS in the present study, as these are recognized as insignificant by Fisher's exact test. The results reflect that the traditional shocker manufacturing workers had more CTS symptoms occurrence than the Semi-ergonomic shocker manufacturing workers.

#### 3.2 Analysis of sEMG signal

The mean RMS value of sEMG signals has been taken from 10-40 s for each worker. All the signal values of sEMG are in millivolts (mV). The sEMG signal graph of a worker for time interval 20-24 s in traditional and semi-ergonomic shocker assembly line is shown in Fig. 17 and Fig. 18. The wave form of a subject is shown in Fig. 19. Mean EMG-RMS value (mV) of 140 workers was obtained using BIOPAC MP-45 aqua-knowledge software. From the sEMG data the values of Raw-

EMG, Integrated-EMG and Root-mean square EMG are obtained. The Raw-EMG is the unprocessed signal of amplitude between 0-6 mV measured from peak to peak and represents the amount of muscle energy measured. Raw-EMG signal helps mostly in qualitative analysis. Integrated-EMG is the calculation of area under the rectified signal. Values are summed over the specified time then divided by the total number of values. Values will increase continuously over time. It quantifies the muscle activity. Root-mean square EMG (EMG-RMS) values are calculated by squaring each data point, summing the squares, dividing the sum of squares by number of observations, and taking the square root and it represent the quantification of muscle activity.

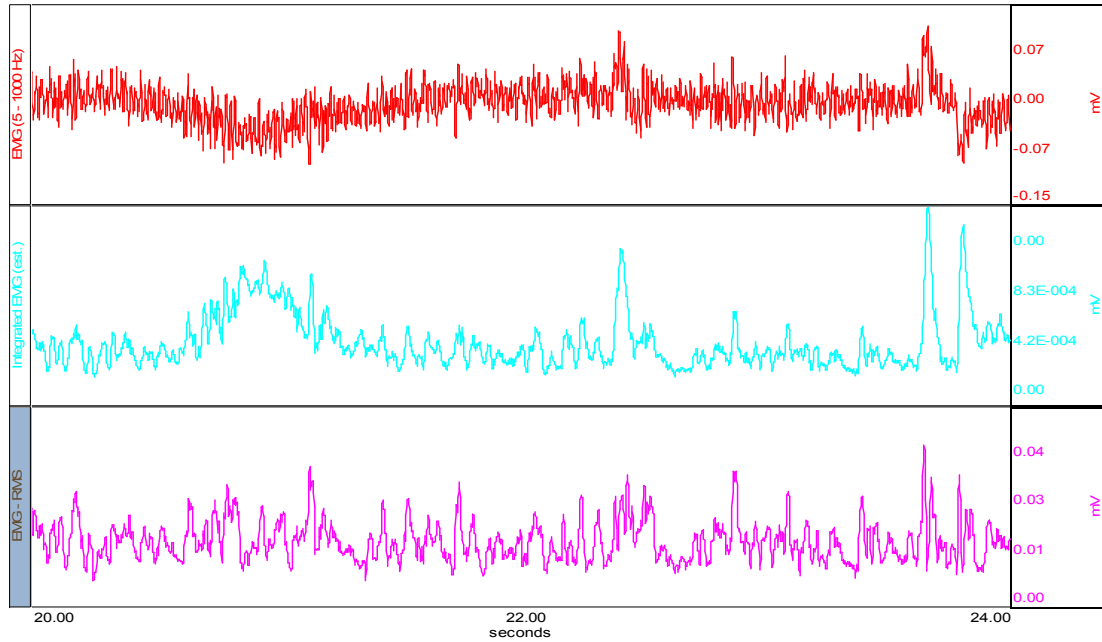


Fig. 17 sEMG signal graph of a worker for time interval 20-24 s in traditional shocker assembly line

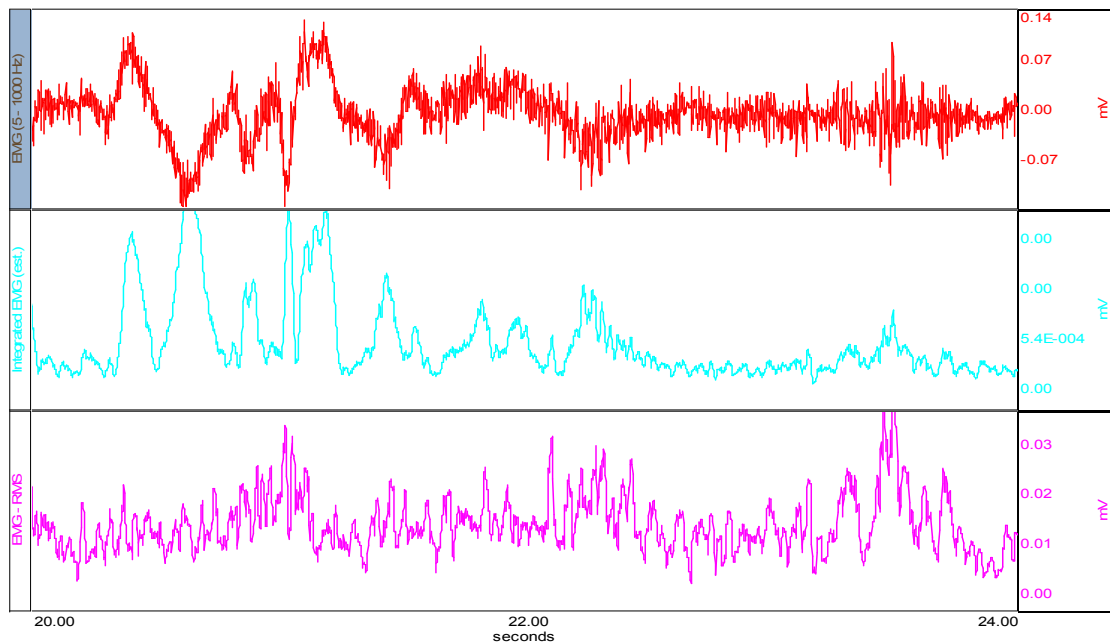


Fig. 18 sEMG signal graph of a worker for time interval 20-24 s in semi-ergonomic shocker assembly line

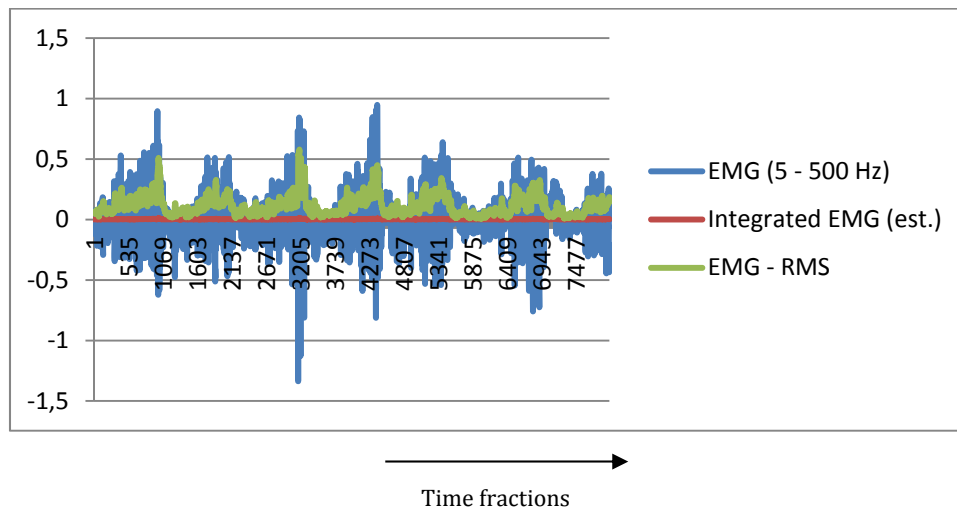


Fig. 19 Wave data graph of shocker manufacturing worker for time interval 20-24 s

Mean EMG-RMS value were calculated on the basis of CTS symptoms occurrence in traditional and semi-ergonomic shocker manufacturing assembly line workers as shown in Table 4. Average of mean EMG-RMS values of workers having CTS symptoms was found to be lower than the value of control subjects. Hence, lower muscle activity amongst workers having potential CTS symptoms confirms the presence of CTS symptoms.

Table 4 Mean EMG-RMS value of shocker assembly line workers

Workers	CTS symptoms subjects	Control subjects
Traditional shocker assembly	0.01223	0.15614
Semi-ergonomic shocker assembly	0.02625	0.17563

#### 4. Conclusions

The results elicit that CTS symptoms are present among the workers engaged in shocker assembly line doing the repetitive job. It has been observed that traditional shocker manufacturing workers are more at risk of CTS symptoms occurrence than the semi-ergonomic shocker manufacturing workers. Positive Tinel's sign occurred in 66.67 % of the traditional and 18.18 % of the semi-ergonomic shocker manufacturing workers. Positive Phalen's sign occurred in 55.55 % of the traditional and 14.28 % of the semi-ergonomic shocker manufacturing workers. Difficulty in grasping occurred in 80 % of the traditional and in 20 % of the semi-ergonomic shocker manufacturing workers. The study also shows 50 % of cases of tingling in traditional shocker manufacturing workers as compared to 8.33 % of semi-ergonomic shocker manufacturing workers. This may be due to more involvement of manual repetition, awkward posture and stressful exertion in traditional manufacturing industry as compared to semi-ergonomic industry. The sEMG signal analysis result reveals that the lesser muscle activity values (EMG-RMS values) indicate the contribution of CTS symptom in shocker assembly line workers. It is observed that if a subject is affected with CTS symptoms then sEMG signal value is 0.01223 mV in case of traditional and 0.02625 mV in case of semi-ergonomic shocker assembly and for control subjects sEMG signal value is 0.15614 mV in traditional and 0.17563 mV in case of semi-ergonomic shocker assembly. The lesser EMG-RMS value of CTS symptoms subjects may be due to the muscular disorder and abnormalities caused by nerve dysfunction.

#### Acknowledgment

Authors gratefully acknowledge North Eastern Regional Institute of Science and Technology (NERIST), Itanagar and Shocker Manufacturing Industries, Haryana for the necessary help rendered in the present work.

## References

- [1] Sprigg, C.A., Stride, C.B., Wall, T.D., Holman, D.J., Smith, P.R. (2007). Work characteristics, musculoskeletal disorders, and the mediating role of psychological strain: A study of call center employees, *Journal of Applied Psychology*, Vol. 92, No. 5, 1456-1466, doi: [10.1037/0021-9010.92.5.1456](https://doi.org/10.1037/0021-9010.92.5.1456).
- [2] Schultz, G., Mostert, K., Rothmann, I. (2012). Repetitive strain injury among South African employees: The relationship with burnout and work engagement, *International Journal of Industrial Ergonomics*, Vol. 42, No. 5, 449-456, doi: [10.1016/j.ergon.2012.06.003](https://doi.org/10.1016/j.ergon.2012.06.003).
- [3] Robertson, V., Stewart, T. (2004). *Risk perception in relation to musculoskeletal disorders (Research report)*, Health & Safety Executive, London, UK.
- [4] Harcombe, H., McBride, D., Derrett, S., Gray, A. (2009). Prevalence and impact of musculoskeletal disorders in New Zealand nurses, postal workers and office workers, *Australian and New Zealand Journal of Public Health*, Vol. 33, No. 5, 437-441, doi: [10.1111/j.1753-6405.2009.00425.x](https://doi.org/10.1111/j.1753-6405.2009.00425.x).
- [5] Health and Safety Executive (2009). *Self-reported work-related illness and workplace injuries in 2008/2009: Results from the labour force survey*, from <http://www.hse.gov.uk/statistics/overall/hssh0809.pdf>, accessed June 19, 2010.
- [6] Dunning, K.K., Davis, K.G., Cook, C., Kotowski, S.E., Hamrick, C., Jewell, G., Lockey, J. (2010). Costs by industry and diagnosis among musculoskeletal claims in a state workers compensation system: 1999-2004, *American Journal of Industrial Medicine*, Vol. 53, No. 3, 276-284, doi: [10.1002/ajim.20774](https://doi.org/10.1002/ajim.20774).
- [7] Silverstein, B.A., Hughes, R.E. (1996). Upper extremity musculoskeletal disorders at a pulp and paper mill, *Applied Ergonomics*, Vol. 27, No. 3, 189-194, doi: [10.1016/0003-6870\(95\)00076-3](https://doi.org/10.1016/0003-6870(95)00076-3).
- [8] Gorsche, R.G., Wiley, J.P., Renger, R.F., Brant, R.F., Gerner, T.Y., Sasyniuk, T.M. (1999). Prevalence and incidence of carpal tunnel syndrome in a meat packing plant, *Occupational & Environmental Medicine*, Vol. 56, No. 6, 417-422, doi: [10.1136/oem.56.6.417](https://doi.org/10.1136/oem.56.6.417).
- [9] Fagarasanu, M., Kumar, S. (2003). Carpal tunnel syndrome due to keyboarding and mouse tasks: a review, *International Journal of Industrial Ergonomics*, Vol. 31, No. 2, 119-136, doi: [10.1016/S0169-8141\(02\)00180-4](https://doi.org/10.1016/S0169-8141(02)00180-4).
- [10] Babski-Reeves, K.L., Crumpton-Young, L.L. (2002). Comparisons of measures for quantifying repetition in predicting carpal tunnel syndrome, *International Journal of Industrial Ergonomics*, Vol. 30, No. 1, 1-6, doi: [10.1016/S0169-8141\(02\)00072-0](https://doi.org/10.1016/S0169-8141(02)00072-0).
- [11] Carnahan, B.J., Norman, B.A., Redfern, M.S. (2001). Incorporating physical demand criteria into assembly line balancing, *IIE Transactions*, Vol. 33, No. 10, 875-887, doi: [10.1080/07408170108936880](https://doi.org/10.1080/07408170108936880).
- [12] Xu, Z., Ko, J., Cochran, D.J., Jung, M.-C. (2012). Design of assembly lines with the concurrent consideration of productivity and upper extremity musculoskeletal disorders using linear models, *Computers & Industrial Engineering*, Vol. 62, No. 2, 431-441, doi: [10.1016/j.cie.2011.10.008](https://doi.org/10.1016/j.cie.2011.10.008).
- [13] Carayon, P., Smith, M.J., Haims, M.C. (1999). Work organization, job stress, and work-related musculoskeletal disorders, *Human Factors*, Vol. 41, No. 4, 644-663, doi: [10.1518/001872099779656743](https://doi.org/10.1518/001872099779656743).
- [14] Kumar, S., Muralidhar, M. (2016). Ergonomical study of hand-arm vibrational exposure in a gear manufacturing plant in India, In: *18<sup>th</sup> International Conference on Applied Human Factors and Ergonomics*, Kuala Lumpur, Malaysia, 1-4.
- [15] Ulin, S.S., Keyserling, W.M. (2004). Case studies of ergonomic interventions in automotive parts distribution operations, *Journal of Occupational Rehabilitation*, Vol. 14, No. 4, 307-326, doi: [10.1023/B:JOOR.0000047432.07837.64](https://doi.org/10.1023/B:JOOR.0000047432.07837.64).
- [16] Ferguson, S.A., Marras, W.S., Allread, W.G., Knapik, G.G., Vandlen, K.A., Splittstoesser, R.E., Yang, G. (2011). Musculoskeletal disorder risk as a function of vehicle rotation angle during assembly tasks, *Applied Ergonomics*, Vol. 42, No. 5, 699-709, doi: [10.1016/j.apergo.2010.11.004](https://doi.org/10.1016/j.apergo.2010.11.004).
- [17] Silverstein, B.A., Stetson, D.S., Keyserling, W.M., Fine, L.J. (1997). Work-related musculoskeletal disorders: Comparison of data sources for surveillance, *American Journal of Industrial Medicine*, Vol. 31, No. 5, 600-608, doi: [10.1002/\(SICI\)1097-0274\(199705\)31:5<600::AID-AJIM15>3.0.CO;2-2](https://doi.org/10.1002/(SICI)1097-0274(199705)31:5<600::AID-AJIM15>3.0.CO;2-2).
- [18] Punnett, L., Gold, J., Katz, J.N., Gore, R., Wegman, D.H. (2004). Ergonomic stressors and upper extremity musculoskeletal disorders in automobile manufacturing: a one year follow up study, *Occupational & Environmental Medicine*, Vol. 61, No. 8, 668-674, doi: [10.1136/oem.2003.008979](https://doi.org/10.1136/oem.2003.008979).
- [19] Keyserling, W.M., Sudarsan, S.P., Martin, B.J., Haig, A.J., Armstrong, T.J. (2005). Effects of low back disability status on lower back discomfort during sustained and cyclical trunk flexion, *Ergonomics*, Vol. 48, No. 3, 219-233, doi: [10.1080/0014013042000327689](https://doi.org/10.1080/0014013042000327689).
- [20] Bernard, B.P. (1997). *Musculoskeletal disorders and workplace factors: A critical review of epidemiologic evidence for work-related musculoskeletal disorders of the neck, upper extremity, and low back*, US Department of Health and Human Services, DHHS (NIOSH) Publication No. 97B141, Cincinnati, Ohio, USA.
- [21] National Research Council and Institute of Medicine (2001). *Musculoskeletal disorders and the workplace: Low back and upper extremities*, The National Academies Press, Washington D.C., USA, doi: [10.17226/10032](https://doi.org/10.17226/10032).
- [22] Punnett, L., Wegman, D.H. (2004). Work-related musculoskeletal disorders: The epidemiologic evidence and the debate, *Journal of Electromyography and Kinesiology*, Vol. 14, No. 1, 13-23, doi: [10.1016/j.jelekin.2003.09.015](https://doi.org/10.1016/j.jelekin.2003.09.015).
- [23] Vujica Herzog, N., Vujica Beharic, R., Beharic, A., Buchmeister, B. (2014). Ergonomic analysis of ophthalmic nurse workplace using 3D simulation, *International Journal of Simulation Modelling*, Vol. 13, No. 4, 409-418, doi: [10.2507/IJSIMM13\(4\)2.265](https://doi.org/10.2507/IJSIMM13(4)2.265).
- [24] Bland, J.D.P. (2007). Carpal tunnel syndrome, *BMJ*, Vol. 335, 343-346, doi: [10.1136/bmj.39282.623553.AD](https://doi.org/10.1136/bmj.39282.623553.AD).

- [25] Visser, L.H., Ngo, Q., Groeneweg, S.J.M., Brekelmans, G. (2012). Long term effect of local corticosteroid injection for carpal tunnel syndrome: A relation with electrodiagnostic severity, *Clinical Neurophysiology*, Vol. 123, No. 4, 838-841, doi: [10.1016/j.clinph.2011.08.022](https://doi.org/10.1016/j.clinph.2011.08.022).
- [26] Hlebs, S., Majhenic, K., Vidmar, G. (2014). Body mass index and anthropometric characteristics of the hand as risk factors for carpal tunnel syndrome, *Collegium Antropologicum*, Vol. 38, No. 1, 219-226.
- [27] Kate, M. (1995). A nonsurgical approach to carpal tunnel syndrome, In: *Proceedings of the International Forum on New Science*, Fort Collins, Colorado, USA, 13-17.
- [28] Jagga, V., Lehri, A., Verma, S.K. (2011). Occupation and its association with carpal tunnel syndrome – A review, *Journal of Exercise Science and Physiotherapy*, Vol. 7, No. 2, 68-78.
- [29] Kulick, M.I., Gordillo, G., Javidi, T., Kilgore, E.S. Jr., Newmeyer III, W.L. (1986). Long-term analysis of patients having surgical treatment for carpal tunnel syndrome, *The Journal of Hand Surgery*, Vol. 11, No. 1, 59-66, doi: [10.1016/S0363-5023\(86\)80104-6](https://doi.org/10.1016/S0363-5023(86)80104-6).
- [30] MacDermid, J.C., Wessel, J. (2004). Clinical diagnosis of carpal tunnel syndrome: a systematic review, *Journal of Hand Therapy*, Vol. 17, No. 2, 309-319, doi: [10.1197/j.jht.2004.02.015](https://doi.org/10.1197/j.jht.2004.02.015).
- [31] Barandun, M., von Tscharnner, V., Meuli-Simmen, C., Bowen, V., Valderrabano, V. (2009). Frequency and conduction velocity analysis of the abductor pollicis brevis muscle during early fatigue, *Journal of Electromyography and Kinesiology*, Vol. 19, No. 1, 65-74, doi: [10.1016/j.jelekin.2007.07.003](https://doi.org/10.1016/j.jelekin.2007.07.003).
- [32] Bland, J.D.P. (2000). A neurophysiological grading scale for carpal tunnel syndrome, *Muscle & Nerve*, Vol. 23, No. 8, 1280-1283, doi: [10.1002/1097-4598\(200008\)23:8<1280::AID-MUS20>3.0.CO;2-Y](https://doi.org/10.1002/1097-4598(200008)23:8<1280::AID-MUS20>3.0.CO;2-Y).
- [33] Liu, F., Carlson, L., Watson, H.K. (2000). Quantitative abductor pollicis brevis strength testing: reliability and normative values, *Journal of Hand Surgery*, Vol. 25, No. 4, 752-759, doi: [10.1053/jhsu.2000.6462](https://doi.org/10.1053/jhsu.2000.6462).
- [34] Nobuta, S., Sato, K., Komatsu, T., Miyasaka, Y., Hatori, M. (2005). Clinical results in severe carpal tunnel syndrome and motor nerve conduction studies, *Journal of Orthopaedic Science*, Vol. 10, No. 1, 22-26, doi: [10.1007/s00776-004-0852-x](https://doi.org/10.1007/s00776-004-0852-x).
- [35] Olmo, G., Laterza, F., Presti, L.L. (2000). Matched wavelet approach in stretching analysis of electrically evoked surface EMG signal, *Signal Processing*, Vol. 80, No. 4, 671-684, doi: [10.1016/S0165-1684\(99\)00160-7](https://doi.org/10.1016/S0165-1684(99)00160-7).
- [36] Reaz, M.B.I., Hussain, M.S., Mohd-Yasin, F. (2006). Techniques of EMG signal analysis: Detection, processing, classification and applications, *Biological Procedures Online*, Vol. 8, No. 1, 11-35, doi: [10.1251/bpo115](https://doi.org/10.1251/bpo115).
- [37] Imteyaz, A., Ansari, F., Dey, U.K. (2012). A review of EMG recording technique, *International Journal of Engineering Science and Technology*, Vol. 4, No. 2, 530-539.
- [38] Day, S. (2002). *Important factors in surface EMG measurement*, Bortec Biomedical Ltd., Calgary, Canada, 1-16.
- [39] Delgrosso, I., Boillat, M.-A. (1991). Carpal tunnel syndrome: Role of occupation, *International Archives of Occupational and Environmental Health*, Vol. 63, No. 4, 267-270, doi: [10.1007/BF00386376](https://doi.org/10.1007/BF00386376).
- [40] Boz, C., Ozmenoglu, M., Altunayoglu, V., Velioglu, S., Alioglu, Z. (2004). Individual risk factors for carpal tunnel syndrome: An evaluation of body mass index, wrist index and hand anthropometric measurements, *Clinical Neurology & Neurosurgery*, Vol. 106, No. 4, 294-299, doi: [10.1016/j.clineuro.2004.01.002](https://doi.org/10.1016/j.clineuro.2004.01.002).
- [41] Kouyoumdjian, J.A., Zanetta, D.M.T., Morita, M.P.A. (2002). Evaluation of age, body mass index, and wrist index as risk factors for carpal tunnel syndrome severity, *Muscle & Nerve*, Vol. 25, No. 1, 93-97, doi: [10.1002/mus.10007](https://doi.org/10.1002/mus.10007).
- [42] Moghtaderi, A., Izadi, S., Sharafadinzadeh, N. (2005). An evaluation of gender, body mass index, wrist circumference and wrist ratio as independent risk factors for carpal tunnel syndrome, *Acta Neurologica Scandinavica*, Vol. 112, No. 6, 375-379, doi: [10.1111/j.1600-0404.2005.00528.x](https://doi.org/10.1111/j.1600-0404.2005.00528.x).
- [43] Kouyoumdjian, J.A., Morita, M.P.A., Rocha, P.R.F., Miranda, R.C., Gouveia, G.M. (2000). Body mass index and carpal tunnel syndrome, *Arquivos de Neuro-Psiquiatria*, Vol. 58, No. 2A, 252-256, doi: [10.1590/S0004-282X2000000200008](https://doi.org/10.1590/S0004-282X2000000200008).
- [44] Douglas, C.M. (2005). *Design and analysis of experiments*, (6<sup>th</sup> edition), J. Wiley & Sons, New York, USA.

## Appendix A

### North Eastern Regional Institute of Science and Technology

(Deemed University, Nirjuli, Arunachal Pradesh, Established by Government of India)

To study Carpal Tunnel Syndrome (CTS) among personnel in shocker manufacturing plants

#### GENERAL INFORMATION

Name:	Date:
Age:	Email Id:
Gender:	Contact No.:
Employers Name/Company:	Occupation:
Main functional areas of job, Major tools, equipment machinery used in performing job Previous diagnosis of a musculoskeletal disorder	Level of education Previous wrist Fracture

Repetitive task in job	Cycle time	Weight	R/L/Both	h/Day	Bending	Breaks	Partially/whole body vibration

Hand grip strength (kg)	LH	Shoulder strength (kg) (push + pull)	RH
Weight:		Push:	
Height:		Pull:	
Do you fell the job is of repetitive nature :      Yes ( )      No ( )			
(if Yes specify the rating)			
_____/s			
_____/min			
_____/h			

### WORK SYMPTOM SEVERITY SCALE

INSTRUCTIONS: The following questions refer to your symptoms during the past two weeks (circle one answer to each question)

	Wrist pain	Hand pain	Numbness	Tingling	Difficulty in grasping	Weakness	Tinel's sign	Phalen's sign
Case tube cleaning	0 1 2 3 4	0 1 2 3 4	0 1 2 3 4	0 1 2 3 4	0 1 2 3 4	0 1 2 3 4	0 1 2 3 4	0 1 2 3 4
Cylinder cleaning	0 1 2 3 4	0 1 2 3 4	0 1 2 3 4	0 1 2 3 4	0 1 2 3 4	0 1 2 3 4	0 1 2 3 4	0 1 2 3 4
Component cleaning	0 1 2 3 4	0 1 2 3 4	0 1 2 3 4	0 1 2 3 4	0 1 2 3 4	0 1 2 3 4	0 1 2 3 4	0 1 2 3 4
Guide disk assembly	0 1 2 3 4	0 1 2 3 4	0 1 2 3 4	0 1 2 3 4	0 1 2 3 4	0 1 2 3 4	0 1 2 3 4	0 1 2 3 4
Cylinder bottom pressing	0 1 2 3 4	0 1 2 3 4	0 1 2 3 4	0 1 2 3 4	0 1 2 3 4	0 1 2 3 4	0 1 2 3 4	0 1 2 3 4
Oil filling in cylinder	0 1 2 3 4	0 1 2 3 4	0 1 2 3 4	0 1 2 3 4	0 1 2 3 4	0 1 2 3 4	0 1 2 3 4	0 1 2 3 4
Cylinder bottom valve assembly	0 1 2 3 4	0 1 2 3 4	0 1 2 3 4	0 1 2 3 4	0 1 2 3 4	0 1 2 3 4	0 1 2 3 4	0 1 2 3 4
Piston valve/Tightening/Riveting	0 1 2 3 4	0 1 2 3 4	0 1 2 3 4	0 1 2 3 4	0 1 2 3 4	0 1 2 3 4	0 1 2 3 4	0 1 2 3 4
Piston rod circlipping	0 1 2 3 4	0 1 2 3 4	0 1 2 3 4	0 1 2 3 4	0 1 2 3 4	0 1 2 3 4	0 1 2 3 4	0 1 2 3 4
Oil seal assembly	0 1 2 3 4	0 1 2 3 4	0 1 2 3 4	0 1 2 3 4	0 1 2 3 4	0 1 2 3 4	0 1 2 3 4	0 1 2 3 4
Oil seal pressing	0 1 2 3 4	0 1 2 3 4	0 1 2 3 4	0 1 2 3 4	0 1 2 3 4	0 1 2 3 4	0 1 2 3 4	0 1 2 3 4
Beading and sealing	0 1 2 3 4	0 1 2 3 4	0 1 2 3 4	0 1 2 3 4	0 1 2 3 4	0 1 2 3 4	0 1 2 3 4	0 1 2 3 4

How long have you been in the present job?

Describe some difficulties in performing the job like – lack of concentration, focusing problem, depression due to CTS prone job etc.

# 0 = No, 1 = Mild, 2 = Moderate, 3 = High, 4 = Severe

Personal Risk Factors (Yes/No)	Occupational Risk Factor (Yes/No)
1) Diabetes/BP/Heart problem/asthma	1) Manual material handling
2) Hand preference	2) Frequent bending and twisting
3) Obesity and lack of sport	3) Heavy physical load
4) Grasp with force	4) Static work posture
5) Turn and screw	5) Whole body vibration
6) Arm above the shoulder	6) Force applied
7) Use of vibrating tools	7) Localized mechanical compression
	8) Awkward posture
	9) Working in cold environments
	10) Working with cold hands



# Simultaneous determination of production and shipment decisions for a multi-product inventory system with a rework process

Chiu, Y.P.<sup>a</sup>, Chiang, K.-W.<sup>a</sup>, Chiu, S.W.<sup>b,\*</sup>, Song, M.-S.<sup>a</sup>

<sup>a</sup>Department of Industrial Engineering and Management, Chaoyang University of Technology, Wufong, Taichung, Taiwan, R.O.C.

<sup>b</sup>Department of Business Administration, Chaoyang University of Technology, Wufong, Taichung, Taiwan, R.O.C.

## ABSTRACT

In a turbulent and highly competitive business environment, management always pursues options to reduce overall operating costs. The vendor-buyer integrated system has recently drawn attention from managers, because it can benefit both parties of the supply chain and it is suitable to be applied to a so-called intra-supply chain system within the present-day globalized enterprise. This study attempts to simultaneously determine production and shipment decisions for a multi-product vendor-buyer integrated inventory system with a rework process, wherein multiple products are fabricated in sequence by a single machine under a rotation cycle time policy. All defective items produced in regular production are assumed repairable, and are reworked right after the regular production ends. Finished goods of each product are transported to sales offices/customers after rework. A multi-delivery policy is applied, wherein a fixed quantity of  $n$  instalments of the finished batch is delivered at fixed intervals during the delivery timeframe. Mathematical modelling and optimization techniques are used to help simultaneously determine the optimal production and shipment decisions that minimize the expected overall system costs. A numerical example is used to show the applicability of our research results.

© 2016 PEI, University of Maribor. All rights reserved.

## ARTICLE INFO

### Keywords:

Multi-product inventory system  
Vendor-buyer integrated system  
Intra-supply chain  
Common production cycle time  
Rework

### \*Corresponding author:

[swang@cyut.edu.tw](mailto:swang@cyut.edu.tw)  
(Chiu, S.W.)

### Article history:

Received 31 January 2016  
Revised 20 May 2016  
Accepted 22 May 2016

## 1. Introduction

This study attempts to simultaneously determine production and shipment decisions for a multi-product vendor-buyer integrated inventory system with a rework process. Higher machine utilization and minimum total production-inventory-delivery costs are two important operating goals, among others, for present-day producers in supply-chain environments. In order to achieve higher machine utilization, the management of manufacturing firms often proposes making multiple products in sequence on a single machine [1-3]. Gaalman [4] proposed a multi-item production smoothing model using an aggregation technique that uses structural properties of the inventory-production model. Leachman and Gascon [5] studied a multi-product single-machine manufacturing system where demand is stochastic and time-varying. Heuristic scheduling policy is proposed and it can integrate feedback control according to inventory levels of economic production cycles. The policy can be applied to decision making involving the type and quantity of items to be produced during the next time period. Zipkin [6] studied the perfor-

mance of a multi-item production-inventory system. Two alternative policies representing different modes of collecting and utilizing information are considered and compared. He derived a closed-form measure of performance for one of them, namely the first-come-first-served (FCFS) policy, and proposed a comparable approximation for the other, namely the longest-queue policy. These results were illustrated and tested via simulations, and used to address several basic managerial issues. Muramatsu et al. [7] studied a multi-product, multi-process dynamic lot-size scheduling problem with setup time, lot sizing, lot sequencing, and dispatching features. A near-optimal solution method along with computational procedure was presented for the proposed problem. They also solved sub problems with known values of Lagrange multiplier. Jodlbauer and Reitner [8] explored a stochastic multi-product, make-to-order fabrication system under common cycle policy. The effects of demand, cycle time, safety stock, processing time and setup time on service levels, and total system cost were determined. Algorithms for calculating the cycle time that leads to maximum service levels at constant safety stocks was introduced. Additional studies [9-15] are related to different aspects of the multi-item production management and optimization issues.

Unlike conventional economic production quantity (EPQ) model [16] that assumes a continuous inventory issuing policy, multiple or periodic product delivery policies are often used in real vendor-buyer integrated production-delivery systems. Hahm and Yano [17] derived optimal frequency of production and delivery for a single-product vendor-buyer integrated inventory model, with the objective of minimizing the long-run average cost per unit time. Production setup costs and inventory holding costs for both vendor and buyer, and transportation costs are considered. They proved that in an optimal solution, the ratio between production interval and delivery interval must be an integer. Eben-Chaime [18] studied the effect of discreteness in vendor-buyer relationships. An analytical methodology was developed to characterize the effect of the cycle ratio on inventory levels. Sarmah et al. [19] explored a coordination problem in a situation where there is a single producer and multiple heterogeneous customers. Two cases were studied: (i) an ex-site distribution case that considered vendor dominance, where a vendor transports end product to a group of customers at a common replenishment time and (ii) an ex-factory distribution case considering customer dominance and a common replenishment time for distribution. They developed a coordination mechanism to improve supply chain performance and focused on the ways of negotiations to obtain a due share of extra savings for business parties. Other studies that addressed various aspects of periodic or multi-delivery issues in vendor-buyer integrated systems can also be found in [20-27].

Product quality assurance is another critical success factor for most present-day manufacturing firms. In real-world production environments, the generation of random nonconforming products is almost inevitable. Reworking these defective items can be an alternative to not only assuring product quality but also lowering the quality costs in production [28]. Consequently, it helps to minimize production-inventory costs. For example, the production of plastic goods in the plastic injection process, printed circuit board assemblies (PCBAs) in PCBA manufacturing, and so on. Zargar [29] explored the effects of two different reworking policies on the cycle time. One is that the "mother" lot is held back, while the "child" sub-lots are reworked, after rework is completed both members are reunited for the next process; the other is that the mother lot is permitted to proceed to the next process, while the child is held back. Queuing models for these policies were developed and a simulation of a wafer production model is used to demonstrate the effectiveness and impacts of the proposed policies. Inderfurth et al. [30] examined a production system with a rework process using the same facility. They assumed that the defective items deteriorate while waiting for rework. There is a given deterioration time limit and deterioration increases in time. A polynomial dynamic programming algorithm was proposed for resolving the problem and the objective was to derive lot sizes and aspects of items to be reworked that minimizes overall costs. Chiu et al. [31] explored the optimal common cycle time for multiple products finite production rate (FPR) system with rework and multiple shipments policies. Their study focused on derivation of an optimal cycle time for the *producer* to minimize producer's overall production-inventory costs. Chiu et al. [32] studied a *single-product* intra-supply chain system with multiple sales offices and quality assurance. They considered that a *single product* is

fabricated by the production unit of a firm, and upon completion of the quality assurance tasks, the entire lot is transported to multiple sales locations of the firm. Their objective is to decide the optimal production-shipment policy that minimizes total costs for the intra-supply chain of the firm. Additional studies [33-40] address different aspects of imperfection issues in production systems.

Since the vendor-buyer integrated type of system can benefit both parties of the supply chain, and it is suitable to be applied to an intra-supply chain system within the present-day globalized enterprise to assist managers in achieving the goal of lowering overall operating costs. Motivated by this concept [32], the present study extends the multi-product FPR problem [31] to a so-called *multi-product intra-supply chain problem*, and attempts to simultaneously determine production and shipment decisions for such a practical multi-product vendor-buyer integrated inventory system with a rework process. As little attention has been paid to this specific research area, the present study is intended to fill the gap.

## 2. The proposed model and formulation

This study attempts to simultaneously determine the production and shipment decisions for a multi-item vendor-buyer integrated inventory system with a rework process. Fabricating multiple products on a single machine with the aim of maximizing machine utilization is an operating goal of most manufacturing firms. In the proposed multi-product intra-supply chain system, the production rate is  $P_{1i}$  per year and the annual demand rate is  $\lambda_i$ , where  $i = 1, 2, \dots, L$ . All products made are checked for their quality, and the unit screening cost is included in the unit production cost  $C_i$ . It is also assumed that the production process can randomly produce  $x_i$  portion of non-conforming items at a rate  $d_i$ , where  $d_i$  can be expressed as  $d_i = x_i P_{1i}$ , and  $(P_{1i} - d_i - \lambda_i) > 0$  must be satisfied in order to sustain regular operations (i.e., avoid the occurrence of shortage). All defective items produced are reworked and fully repaired at the rate of  $P_{2i}$  at the end of each production cycle, with additional rework cost  $C_{Ri}$  per item. After the rework process, the entire quality assured lot of each product  $i$  are transported to sales offices/customers under a multi-delivery policy, in which  $n$  fixed quantity instalments of the lot are shipped at fixed intervals of time in  $t_{3i}$  (see Figs. 1 and 2 [31]).

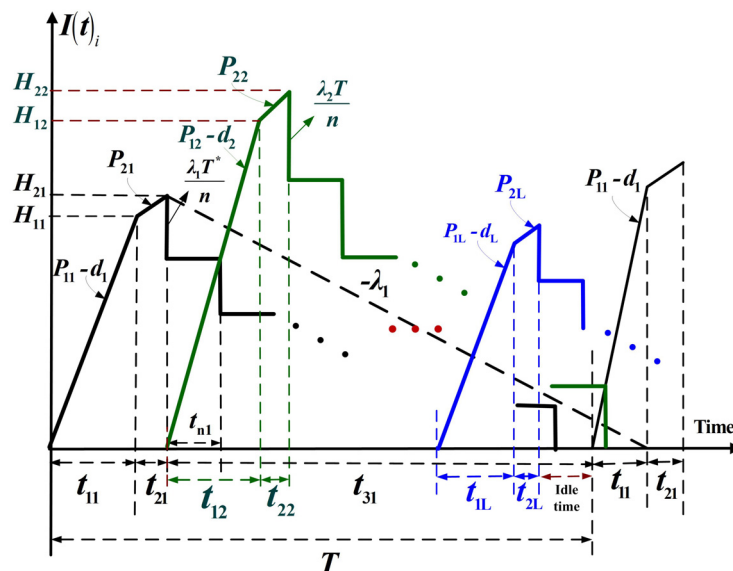


Fig. 1 On-hand inventory level of perfect quality product  $i$  at time  $t$  in the proposed system [31]

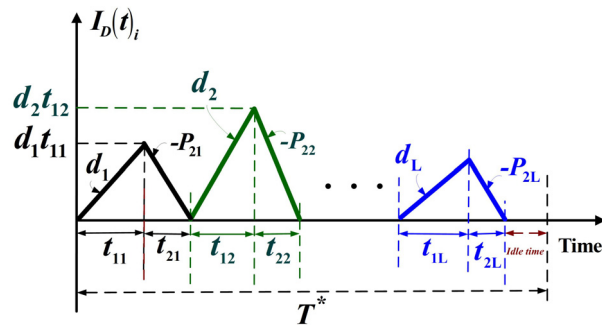


Fig. 2 On-hand inventory level of defective product  $i$  at time  $t$  in the proposed system [31]

The on-hand inventory of product  $i$  stored at the sales offices/customers' side is illustrated in Fig. 3. Accordingly, the sales offices' holding cost along with delivery cost for all  $L$  products are included in the proposed cost analysis. Moreover, in order to ensure the production equipment has sufficient capacity in regular and rework processes so as to meet demands for all  $L$  products, the following formula must hold:  $\sum_{i=1}^L ((\lambda_i/P_{1i}) + (x_i\lambda_i/P_{2i})) < 1$ .

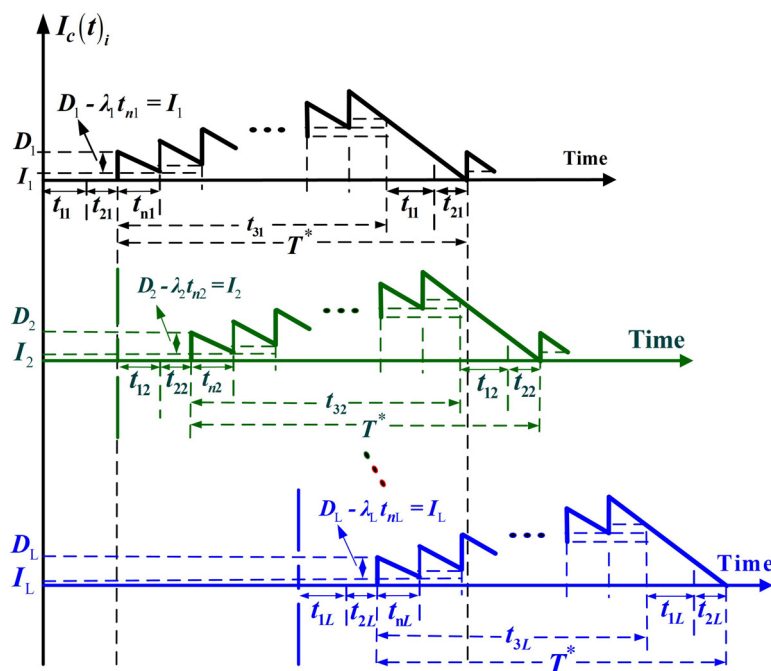


Fig. 3 On-hand inventory level of product  $i$  stored at the sales offices at time  $t$  in the proposed system

In the proposed mathematical analysis, for each product  $i$  the following cost-correlated parameters are used: producer's production setup cost  $K_i$ , unit inventory holding cost  $h_i$ , holding cost  $h_{1i}$  per item undergoing rework, sales offices' unit holding cost  $h_{2i}$ , fixed transportation cost  $K_{1i}$  per shipment, and unit delivery cost  $C_{Ti}$ . Other notations used are listed below:

- $H_{1i}$  – maximum on-hand inventory in units of product  $i$  when regular production finishes
- $H_{2i}$  – maximum on-hand inventory in units of product  $i$  when rework process terminates
- $t_{1i}$  – production uptime of product  $i$  in the proposed system
- $t_{2i}$  – rework time of product  $i$  in the proposed system
- $t_{3i}$  – delivery time of product  $i$  in the proposed system
- $t_{ni}$  – fixed interval of time between each delivery of product  $i$  in  $t_{3i}$
- $n$  – number of shipments transported to sales offices per cycle (a decision variable)
- $T$  – the common production cycle time (the other decision variable)
- $Q_i$  – production batch size per cycle for product  $i$

- $I(t)_i$  – level of on-hand inventory of perfect quality product  $i$  at time  $t$
- $I_D(t)_i$  – level of on-hand inventory of defective product  $i$  at time  $t$
- $I_c(t)_i$  – level of on-hand inventory of product  $i$  stored at the sales offices at time  $t$
- $D_i$  – fixed quantity of finished items of product  $i$  transported to sales offices/customers per shipment
- $I_i$  – left over items of product  $i$  per shipment at the end  $t_{ni}$
- $TC(Q_i, n)$  – overall production-inventory-transportation costs per cycle for product  $i$
- $E[TCU(Q_i, n)]$  – overall expected production-inventory-transportation costs per year for producing  $L$  products in the proposed system
- $E[TCU(T, n)]$  – overall expected production-inventory-transportation costs per year for producing  $L$  products in the proposed system using the common cycle time rather than lot size as decision variable.

By observing Figs. 1 and 2, the following formulas can be obtained:

$$H_{1i} = (P_{1i} - d_i)t_{1i} \tag{1}$$

$$H_{2i} = H_{1i} + P_{2i}t_{2i} \tag{2}$$

$$t_{1i} = \frac{Q_i}{P_{1i}} = \frac{H_{1i}}{P_{1i} - d_i} \tag{3}$$

$$t_{2i} = \frac{x_i Q_i}{P_{2i}} \tag{4}$$

$$t_{3i} = nt_{ni} = T - (t_{1i} + t_{2i}) \tag{5}$$

$$T = t_{1i} + t_{2i} + t_{3i} \tag{6}$$

$$d_i t_{1i} = x_i Q_i \tag{7}$$

Total delivery costs of  $n$  shipments of product  $i$  at  $t_{3i}$  is

$$nK_{1i} + C_{Ti}Q_i \tag{8}$$

From Fig. 1, the holding cost of the finished items of product  $i$  at  $t_3$  is

$$h_i \left( \frac{n-1}{2n} \right) H_{2i} t_{3i} \tag{9}$$

According to the proposed multi-delivery policy, when  $n$  fixed quantity (i.e.,  $D$ ) instalments of finished lot of product  $i$  are transported to sales offices at a fixed time interval  $t_{ni}$ , the following formulas are obtained:

$$t_{ni} = \frac{t_{3i}}{n} \tag{10}$$

$$D_i = \frac{H_{2i}}{n} \tag{11}$$

$$I_i = D_i - \lambda_i t_{ni} \tag{12}$$

The sales offices' stock holding cost of product  $i$  is [36]

$$h_{2i} \left[ n \frac{(D_i - I_i)}{2} t_{ni} + \frac{nI_i}{2} (t_{1i} + t_{2i}) + \frac{n(n+1)}{2} I_i t_{ni} \right] \tag{13}$$

Therefore,  $TC(Q_i, n)$  for  $i = 1, 2, \dots, L$ , comprises the variable fabrication cost, setup cost, variable reworking cost, production units' inventory holding cost during the periods  $t_{1i}$ ,  $t_{2i}$ , and  $t_{3i}$  (including holding cost of nonconforming items in  $t_{1i}$ ), inventory holding cost of reworked items

in  $t_{2i}$ , fixed and variable transportation costs, and the stock holding cost from the sales offices/customers, is

$$\sum_{i=1}^L TC(Q_i, n) = \sum_{i=1}^L \left\{ C_i Q_i + K_i + C_{Ri}(x_i Q_i) + h_i \left[ \frac{H_{1i} + d_{1i} t_{1i}}{2} (t_{1i}) + \frac{H_{1i} + H_{2i}}{2} (t_{2i}) + \frac{(n-1)}{2n} (H_{2i} t_{3i}) \right] + h_{1i} \frac{d_{1i} t_{1i}}{2} (t_{2i}) + n K_{1i} + C_{Ti} Q_i + h_{2i} \left[ n \frac{(D_i - I_i)}{2} (t_{ni}) + \frac{n I_i}{2} (t_{1i} + t_{2i}) + \frac{n(n+1)}{2} I_i t_{ni} \right] \right\} \tag{14}$$

Substituting relevant parameters from Eqs. 1 to 13 in Eq. 14, using the expected values of  $x$  to take randomness of defective rate into account, and applying the renewal reward theorem,  $E[TCU(Q_i, n)]$  is obtained as follows:

$$E[TCU(Q_i, n)] = \sum_{i=1}^L \left\{ \left[ C_i \lambda_i + \frac{K_i \lambda_i}{Q_i} + C_{Ri} \lambda_i E[x_i] \right] + \frac{h_i Q_i \lambda_i}{2} \left[ -\frac{1}{\lambda_i n} + \frac{1}{n P_{1i}} + \frac{E[x_i]}{n P_{2i}} + \frac{1}{\lambda_i} + \frac{E[x_i]}{P_{2i}} + \frac{E[x_i]^2}{P_{2i}} \right] + \frac{h_{1i} Q_i \lambda_i E[x_i]^2}{2 P_{2i}} + \left[ C_{Ti} \lambda_i + \frac{n K_{1i} \lambda_i}{Q_i} \right] + \frac{h_{2i} Q_i \lambda_i}{2} \left[ \frac{1}{\lambda_i n} - \frac{1}{n P_{1i}} - \frac{E[x_i]}{n P_{2i}} + \frac{1}{P_{1i}} + \frac{E[x_i]}{P_{2i}} \right] \right\} \tag{15}$$

Since  $Q_i = T \lambda_i$ , Eq. 15 becomes

$$E[TCU(T, n)] = \sum_{i=1}^L \left\{ C_i \lambda_i + \frac{K_i}{T} + C_{Ri} \lambda_i E[x_i] + \frac{h_i \lambda_i^2 T}{2} \left[ \frac{1}{\lambda_i} + \frac{E[x_i]}{P_{2i}} - \frac{E[x_i]^2}{P_{2i}} \right] + \frac{h_{1i} \lambda_i^2 E[x_i]^2 T}{2 P_{2i}} + C_{Ti} \lambda_i + \frac{n K_{1i}}{T} + \frac{h_{2i} \lambda_i^2 T}{2} \left[ \frac{1}{P_{1i}} + \frac{E[x_i]}{P_{2i}} \right] + \frac{\lambda_i^2 T}{2n} \left[ \frac{1}{\lambda_i} - \frac{1}{P_{1i}} - \frac{E[x_i]}{P_{2i}} \right] (h_{2i} - h_i) \right\} \tag{16}$$

**2.1 Deriving optimal production-shipment policy**

In this section, Hessian matrix equations (Rardin [41]) are used to help determine the optimal operating policy of the common production cycle time  $T^*$  and the number of deliveries  $n^*$ . In order to prove that the expected system cost function is convex, we must first verify that Eq. 17 holds:

$$[T \quad n] \cdot \begin{bmatrix} \frac{\partial^2 E[TCU(T, n)]}{\partial T^2} & \frac{\partial^2 E[TCU(T, n)]}{\partial T \partial n} \\ \frac{\partial^2 E[TCU(T, n)]}{\partial T \partial n} & \frac{\partial^2 E[TCU(T, n)]}{\partial n^2} \end{bmatrix} \cdot \begin{bmatrix} T \\ n \end{bmatrix} > 0 \tag{17}$$

The following equations can be obtained from Eq. 16:

$$\frac{\partial E[TCU(T, n)]}{\partial n} = \sum_{i=1}^L \left\{ \frac{K_{1i}}{T} - \frac{\lambda_i^2 T}{2n^2} \left[ \frac{1}{\lambda_i} - \frac{1}{P_{1i}} - \frac{E[x_i]}{P_{2i}} \right] (h_{2i} - h_i) \right\} \tag{18}$$

$$\frac{\partial^2 E[TCU(T, n)]}{\partial n^2} = \sum_{i=1}^L \left\{ \frac{\lambda_i^2 T}{n^3} \left[ \frac{1}{\lambda_i} - \frac{1}{P_{1i}} - \frac{E[x_i]}{P_{2i}} \right] (h_{2i} - h_i) \right\} \tag{19}$$

$$\frac{\partial E[TCU(T, n)]}{\partial T} = \sum_{i=1}^L \left\{ -\frac{K_i}{T^2} - \frac{nK_{1i}}{T^2} + \frac{h_i \lambda_i^2}{2} \left[ \frac{1}{\lambda_i} + \frac{E[x_i]}{P_{2i}} - \frac{E[x_i]^2}{P_{2i}} \right] + \frac{h_{1i} \lambda_i^2 E[x_i]^2}{2P_{2i}} \right. \\ \left. + \frac{h_{2i} \lambda_i^2}{2} \left[ \frac{1}{P_{1i}} + \frac{E[x_i]}{P_{2i}} \right] + \frac{\lambda_i^2}{2n} \left[ \frac{1}{\lambda_i} - \frac{1}{P_{1i}} - \frac{E[x_i]}{P_{2i}} \right] (h_{2i} - h_i) \right\} \quad (20)$$

$$\frac{\partial^2 E[TCU(T, n)]}{\partial T^2} = \sum_{i=1}^L \left\{ \frac{2(K_i + nK_{1i})}{T^3} \right\} \quad (21)$$

$$\frac{\partial^2 E[TCU(T, n)]}{\partial T \partial n} = \sum_{i=1}^L \left\{ -\frac{K_{1i}}{T^2} - \frac{\lambda_i^2}{2n^2} \left[ \frac{1}{\lambda_i} - \frac{1}{P_{1i}} - \frac{E[x_i]}{P_{2i}} \right] (h_{2i} - h_i) \right\} \quad (22)$$

Substituting Eqs. 19, 21, and 22 in Eq. 17, the following equation is obtained:

$$[T \quad n] \cdot \begin{bmatrix} \frac{\partial^2 E[TCU(T, n)]}{\partial T^2} & \frac{\partial^2 E[TCU(T, n)]}{\partial T \partial n} \\ \frac{\partial^2 E[TCU(T, n)]}{\partial T \partial n} & \frac{\partial^2 E[TCU(T, n)]}{\partial n^2} \end{bmatrix} \cdot \begin{bmatrix} T \\ n \end{bmatrix} = \sum_{i=1}^L \frac{2K_i}{T} > 0 \quad (23)$$

Since  $K_i$  and  $T$  are all positive, Eq. 23 is positive. Therefore,  $E[TCU(T, n)]$  is strictly convex for all  $T$  and  $n$  not equal to zero, and  $E[TCU(T, n)]$  has a minimum value. In order to determine the optimal operating production-shipment policy (i.e.,  $T^*$  and  $n^*$ ), we set the first derivatives of  $E[TCU(T, n)]$  with respect to  $T$  and with respect to  $n$  equal to zeros, and solve the linear system (i.e., Eqs. 18 and 20). With further derivations, the following equation is obtained:

$$T^* = \sqrt{\frac{2 \sum_{i=1}^L (K_i + nK_{1i})}{\sum_{i=1}^L \left\{ h_i \lambda_i^2 \left[ \frac{1}{\lambda_i} + \frac{E[x_i]}{P_{2i}} - \frac{E[x_i]^2}{P_{2i}} \right] + h_{2i} \lambda_i^2 \left[ \frac{1}{P_{1i}} + \frac{E[x_i]}{P_{2i}} \right] + \frac{h_{1i} \lambda_i^2 E[x_i]^2}{P_{2i}} + \frac{\lambda_i^2}{n} \left[ \frac{1}{\lambda_i} - \frac{1}{P_{1i}} - \frac{E[x_i]}{P_{2i}} \right] (h_{2i} - h_i) \right\}} \quad (24)$$

and

$$n^* = \sqrt{\frac{\sum_{i=1}^L K_i \cdot \sum_{i=1}^L \left[ \lambda_i^2 (h_{2i} - h_i) \left( \frac{1}{\lambda_i} - \frac{1}{P_{1i}} - \frac{E[x_i]}{P_{2i}} \right) \right]}{(\sum_{i=1}^L K_{1i}) \cdot \sum_{i=1}^L \left[ h_i \lambda_i^2 \left( \frac{1}{\lambda_i} + \frac{E[x_i]}{P_{2i}} - \frac{E[x_i]^2}{P_{2i}} \right) + \frac{h_{1i} \lambda_i^2 E[x_i]^2}{P_{2i}} + h_{2i} \lambda_i^2 \left( \frac{1}{P_{1i}} + \frac{E[x_i]}{P_{2i}} \right) \right]} \quad (25)$$

Eq. 25 results in a real number, but in reality the number of deliveries should be represented as an integer. Two adjacent integers to  $n$  are examined, respectively, to determine the integer value of  $n^*$  that minimizes  $E[TCU(T, n)]$ . Let  $n^-$  denote the largest integer less than or equal to  $n$  and  $n^+$  denote the smallest integer greater than or equal to  $n$  (as derived from Eq. 25). First, we apply  $n^-$  and  $n^+$  in Eq. 24 to obtain their corresponding  $T$  values, respectively. Next, we plug each pair in  $E[TCU(T, n)]$  and choose the production-shipment policy that has the minimal system costs [13].

### 3. Numerical example

Consider five products being manufactured in sequence on a machine under the common cycle time policy in a multi-product inventory system with a rework process. Their annual production rates  $P_{1i}$  are 58,000, 59,000, 60,000, 61,000, and 62,000, respectively, and their annual demand rates  $\lambda_i$  are 3,000, 3,200, 3,400, 3,600, and 3,800, respectively. For each product, the production units has experienced the random nonconforming rates that follow the uniform distribution over intervals of [0, 0.05], [0, 0.10], [0, 0.15], [0, 0.20], and [0, 0.25], respectively. All nonconforming products are assumed to be repairable and are reworked at the end of the regular production, at annual rates  $P_{2i}$  of 46,400, 47,200, 48,000, 48,800, and 49,600, respectively. Addition-

al costs for rework are \$50, \$55, \$60, \$65, and \$70 per nonconforming product, respectively. Other values of system variables used in this example are listed below:

- $K_i$  – production setup costs are \$17,000, \$17,500, \$18,000, \$18,500, and \$19,000, respectively.
- $C_i$  – fabrication cost per item are \$80, \$90, \$100, \$110, and \$120, respectively.
- $h_i$  – inventory holding cost per item are \$10, \$15, \$20, \$25, and \$30, respectively.
- $h_{1i}$  – unit holding costs during rework are \$30, \$35, \$40, \$45, and \$50, respectively.
- $K_{1i}$  – fixed cost per delivery are \$1,800, \$1,900, \$2,000, \$2,100, and \$2,200, respectively.
- $h_{2i}$  – stock holding cost per item at sales offices are \$70, \$75, \$80, \$85, and \$90, respectively.
- $C_{Ti}$  – transporting cost per item are \$0.1, \$0.2, \$0.3, \$0.4, and \$0.5, respectively.

First, in order to determine the number of deliveries, one can apply Eq. 25 and obtain  $n^* = 4.4278$ . As stated in section 2.1, practically,  $n^*$  should be an integer number only, and to find the integer value of  $n^*$  one can plug  $n^+ = 5$  and  $n^- = 4$  in Eq. 24 and obtain ( $T = 0.6666, n^+ = 5$ ) and ( $T = 0.6193, n^- = 4$ ), respectively. Next, apply Eq. 16 with these two different policies to obtain  $E[TCU(0.6666, 5)] = \$2,229,865$  and  $E[TCU(0.6193, 4)] = \$2,229,658$ , respectively. By choosing a policy with minimum cost, the optimal production-shipment policy for the proposed system is determined as  $n^* = 4, T^* = 0.6193$ , and  $E[TCU(T^*, n^*)] = \$2,229,658$ . The effect of the variation in the rotation cycle time  $T$  and the number of shipments  $n$  on  $E[TCU(T, n)]$  is illustrated in Fig. 4.

Further analysis indicates that for the same system without considering rework process (i.e., treating all nonconforming items as scrap),  $E[TCU(T, n)] = \$2,352,622$ . This cost is \$122,964 higher than our proposed model, or 25.91 % of other related costs (i.e., total system costs exclude the variable manufacturing costs) when considering the rework of nonconforming items.

Another interesting finding from our numerical analysis is the rate of the rework process. The effect of the variation in the ratio of rework and regular production rates (i.e.,  $P_{2i}/P_{1i}$ ) on the optimal rotation cycle time  $T^*$  and on the expected system cost  $E[TCU(T^*, n^*)]$ , is illustrated in Figs. 5 and 6, respectively. It can be noted that as the  $P_{2i}/P_{1i}$  ratio decreases,  $T^*$  decreases slightly, and when the  $P_{2i}/P_{1i}$  ratio drops below 0.5,  $T^*$  starts to decrease significantly (i.e., when the time required to rework a nonconforming item is twice or more than twice as much as the regular time needed to produce an item).

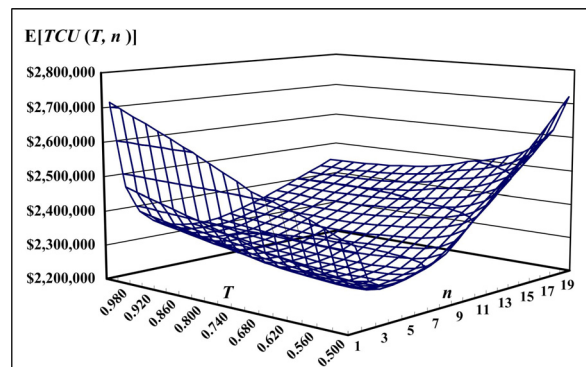


Fig. 4 Effects of the variations in common production cycle time  $T$  and number of deliveries  $n$  on  $E[TCU(T, n)]$

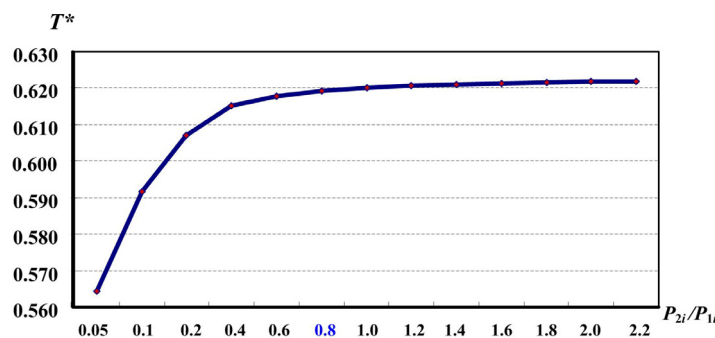


Fig. 5 Effects of the variation in the  $P_{2i}/P_{1i}$  ratio on optimal common production cycle time  $T^*$



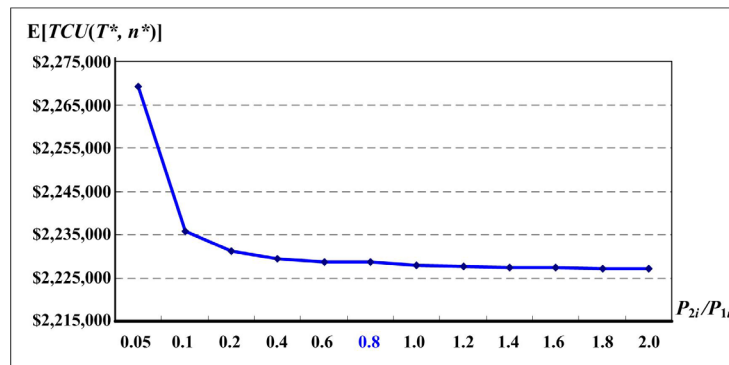


Fig. 6 Effects of the variation in the  $P_{2i}/P_{1i}$  ratio on the expected system cost  $E[TCU(T^*, n^*)]$

From Fig. 6, it may be noted that as the  $P_{2i}/P_{1i}$  ratio decreases, the expected system cost  $E[TCU(T^*, n^*)]$  increases slightly, and when  $P_{2i}/P_{1i}$  drops below 0.5,  $E[TCU(T^*, n^*)]$  starts to increase significantly.

#### 4. Conclusion

The vendor-buyer integrated system has recently drawn attention from managers, because it can benefit both parties of the supply chain and it is suitable to be applied to a so-called intra-supply chain system within the present-day globalized enterprise. Optimization of such an intra-supply chain system assists managers in achieving the goal of lowering overall operating costs. Motivated by this concept, the present study developed an exact mathematical model to simultaneously determine the production and shipment decisions for a multi-product vendor-buyer integrated inventory system with a rework process. The research results not only can assist management of such a realistic system in making a best operational decision, but also enable the practitioners in the fields to better understand and control over the effects of variations in different system parameters on the optimal production-shipment policy and on the expected system costs (see Figs. 5 and 6).

One interesting topic for future study will be to consider the effect of stochastic demand on the optimal production-shipment decision. To cope with the non-deterministic nature in demand, the following extra features may be considered: (1) identification of the probability distribution of the actual demand; (2) safety stock, lost sales, or backordering (when demand exceeds supply); and (3) optional discount sales (when supply exceeds demand), etc.

#### Acknowledgement

Authors sincerely appreciate National Science Council (NSC) of Taiwan for supporting this study under grant number: NSC 102-2410-H-324-015-MY2.

#### References

- [1] Tersine, R.J. (1994). *Principles of inventory and materials management*, PTR Prentice-Hall, New Jersey, USA.
- [2] Zipkin, P.H. (2000). *Foundations of inventory management*, McGraw-Hill, New York, USA.
- [3] Nahmias, S. (2009). *Production and operations analysis*, (6<sup>th</sup> edition), McGraw-Hill, New York, USA.
- [4] Gaalman, G.J. (1978). Optimal aggregation of multi-item production smoothing models, *Management Science*, Vol. 24, No. 16, 1733-1739, doi: [10.1287/mnsc.24.16.1733](https://doi.org/10.1287/mnsc.24.16.1733).
- [5] Leachman, R.C., Gascon, A. (1988). A heuristic scheduling policy for multi-item, single-machine production systems with time-varying, stochastic demands, *Management Science*, Vol. 34, No. 3, 377-390, doi: [10.1287/mnsc.34.3.377](https://doi.org/10.1287/mnsc.34.3.377).
- [6] Zipkin, P.H. (1995). Performance analysis of a multi-item production-inventory system under alternative policies, *Management Science*, Vol. 41, No. 4, 690-703, doi: [10.1287/mnsc.41.4.690](https://doi.org/10.1287/mnsc.41.4.690).
- [7] Muramatsu, K., Warman, A., Kobayashi, M. (2003). A near-optimal solution method of multi-item multi-process dynamic lot size scheduling problem, *JSME International Journal, Series C: Mechanical Systems, Machine Elements and Manufacturing*, Vol. 46, No. 1, 46-53, doi: [10.1299/jsmec.46.46](https://doi.org/10.1299/jsmec.46.46).

- [8] Jodlbauer, H., Reitner, S. (2012). Optimizing service-level and relevant cost for a stochastic multi-item cyclic production system, *International Journal of Production Economics*, Vol. 136, No. 2, 306-317, doi: [10.1016/j.ijpe.2011.12.015](https://doi.org/10.1016/j.ijpe.2011.12.015).
- [9] Gordon, G.R., Surkis, J. (1975). A control policy for multi-item inventories with fluctuating demand using simulation, *Computers & Operations Research*, Vol. 2, No. 2, 91-100, doi: [10.1016/0305-0548\(75\)90012-X](https://doi.org/10.1016/0305-0548(75)90012-X).
- [10] Aggarwal, V. (1984). Grouping multi-item inventory using common cycle periods, *European Journal of Operational Research*, Vol. 17, No. 3, 369-372, doi: [10.1016/0377-2217\(84\)90132-2](https://doi.org/10.1016/0377-2217(84)90132-2).
- [11] Federgruen, A., Katalan, Z. (1998). Determining production schedules under base-stock policies in single facility multi-item production systems, *Operations Research*, Vol. 46, No. 6, 883-898, doi: [10.1287/opre.46.6.883](https://doi.org/10.1287/opre.46.6.883).
- [12] Guchhait, P., Maiti, M.K., Maiti, M. (2010). Multi-item inventory model of breakable items with stock-dependent demand under stock and time dependent breakability rate, *Computers & Industrial Engineering*, Vol. 59, No. 4, 911-920, doi: [10.1016/j.cie.2010.09.001](https://doi.org/10.1016/j.cie.2010.09.001).
- [13] Chiu, Y.-S.P., Huang, C.-C., Wu, M.-F., Chang, H.-H. (2013). Joint determination of rotation cycle time and number of shipments for a multi-item EPQ model with random defective rate, *Economic Modelling*, Vol. 35, 112-117, doi: [10.1016/j.econmod.2013.06.024](https://doi.org/10.1016/j.econmod.2013.06.024).
- [14] Wu, M.-F., Chiu, Y.-S.P., Sung, P.-C. (2014). Optimization of a multi-product EPQ model with scrap and an improved multi-delivery policy, *Journal of Engineering Research*, Vol. 2, No. 4, 103-118, doi: [10.7603/s40632-014-0027-7](https://doi.org/10.7603/s40632-014-0027-7).
- [15] Chiu, Y.-S.P., Sung, P.-C., Chiu, S.W., Chou, C.-L. (2015). Mathematical modeling of a multi-product EMQ model with an enhanced end items issuing policy and failures in rework, *SpringerPlus*, Vol. 4:679, No. 1, 1-11, doi: [10.1186/s40064-015-1487-4](https://doi.org/10.1186/s40064-015-1487-4).
- [16] Taft, E.W. (1918). The most economical production lot, *Iron Age*, Vol. 101, 1410-1412.
- [17] Hahm, J., Yano, C.A. (1992). The economic lot and delivery scheduling problem: The single item case, *International Journal of Production Economics*, Vol. 28, No. 2, 235-252, doi: [10.1016/0925-5273\(92\)90036-7](https://doi.org/10.1016/0925-5273(92)90036-7).
- [18] Eben-Chaime, M. (2004). The effect of discreteness in vendor-buyer relationships, *IIE Transactions*, Vol. 36, No. 6, 583-589, doi: [10.1080/07408170490438717](https://doi.org/10.1080/07408170490438717).
- [19] Sarmah, S.P., Acharya, D., Goyal, S.K. (2008). Coordination of a single-manufacturer/multi-buyer supply chain with credit option, *International Journal of Production Economics*, Vol. 111, No. 2, 676-685, doi: [10.1016/j.ijpe.2007.04.003](https://doi.org/10.1016/j.ijpe.2007.04.003).
- [20] Schwarz, L.B., Deuermeyer, B.L., Badinelli, R.D. (1985). Fill-rate optimization in a one-warehouse N-identical retailer distribution system, *Management Science*, Vol. 31, No. 4, 488-498, doi: [10.1287/mnsc.31.4.488](https://doi.org/10.1287/mnsc.31.4.488).
- [21] Hall, R.W. (1996). On the integration of production and distribution: economic order and production quantity implications, *Transportation Research Part B: Methodological*, Vol. 30, No. 5, 387-403, doi: [10.1016/0191-2615\(96\)00002-1](https://doi.org/10.1016/0191-2615(96)00002-1).
- [22] Sarker, R.A., Khan, L.R. (1999). An optimal batch size for a production system operating under periodic delivery policy, *Computers & Industrial Engineering*, Vol. 37, No. 4, 711-730, doi: [10.1016/S0360-8352\(00\)00006-1](https://doi.org/10.1016/S0360-8352(00)00006-1).
- [23] Çömez, N., Stecke, K.E., Çakanyıldırım, M. (2012). Multiple in-cycle transshipments with positive delivery times, *Production and Operations Management*, Vol. 21, No. 2, 378-395, doi: [10.1111/j.1937-5956.2011.01244.x](https://doi.org/10.1111/j.1937-5956.2011.01244.x).
- [24] Chiu, S.W., Sung, P.-C., Tseng, C.-T., Chiu, Y.-S.P. (2015). Multi-product FPR model with rework and multi-shipment policy resolved by algebraic approach, *Journal of Scientific and Industrial Research*, Vol. 74, No. 10, 555-559.
- [25] Safaei, M. (2014). An integrated multi-objective model for allocating the limited sources in a multiple multi-stage lean supply chain, *Economic Modelling*, Vol. 37, 224-237, doi: [10.1016/j.econmod.2013.10.018](https://doi.org/10.1016/j.econmod.2013.10.018).
- [26] Ocampo, L.A. (2015). A hierarchical framework for index computation in sustainable manufacturing, *Advances in Production Engineering & Management*, Vol. 10, No. 1, 40-50, doi: [10.14743/apem2015.1.191](https://doi.org/10.14743/apem2015.1.191).
- [27] Chiu, S.W., Huang, C.-C., Chiang, K.-W., Wu, M.-F. (2015). On intra-supply chain system with an improved distribution plan, multiple sales locations and quality assurance, *SpringerPlus*, Vol. 4:687, No. 1, 1-11, doi: [10.1186/s40064-015-1498-1](https://doi.org/10.1186/s40064-015-1498-1).
- [28] Silver, E.A., Pyke, D.F., Peterson, R. (1998). *Inventory management and production planning and scheduling*, (3<sup>rd</sup> edition), John Wiley & Sons, New York, USA.
- [29] Zargar, A.M. (1995). Effect of rework strategies on cycle time, *Computers & Industrial Engineering*, Vol. 29, No. 1-4, 239-243, doi: [10.1016/0360-8352\(95\)00078-F](https://doi.org/10.1016/0360-8352(95)00078-F).
- [30] Inderfurth, K., Janiak, A., Kovalyov, M.Y., Werner, F. (2006). Batching work and rework processes with limited deterioration of reworkables, *Computers & Operations Research*, Vol. 33, No. 6, 1595-1605, doi: [10.1016/j.cor.2004.11.009](https://doi.org/10.1016/j.cor.2004.11.009).
- [31] Chiu, Y.-S.P., Pan, N., Chiu, S.W., Chiang, K.-W. (2012). Optimal production cycle time for multi-item FPR model with rework and multi-shipment policy, *International Journal for Engineering Modelling*, Vol. 25, No. 1-4, 51-57.
- [32] Chiu, S.W., Lee, C.-H., Chiu, Y.-S.P., Cheng, F.-T. (2013). Intra-supply chain system with multiple sales locations and quality assurance, *Expert Systems with Applications*, Vol. 40, No. 7, 2669-2676, doi: [10.1016/j.eswa.2012.11.008](https://doi.org/10.1016/j.eswa.2012.11.008).
- [33] Yu, K.-Y.C., Bricker, D.L. (1993). Analysis of a Markov chain model of a multistage manufacturing system with inspection, rejection, and rework, *IIE Transactions*, Vol. 25, No. 1, 109-112, doi: [10.1080/07408179308964271](https://doi.org/10.1080/07408179308964271).
- [34] Biswas, P., Sarker, B.R. (2008). Optimal batch quantity models for a lean production system with in-cycle rework and scrap, *International Journal of Production Research*, Vol. 46, No. 23, 6585-6610, doi: [10.1080/00207540802230330](https://doi.org/10.1080/00207540802230330).
- [35] Widyadana, G.A., Wee, H.M. (2011). Optimal deteriorating items production inventory models with random machine breakdown and stochastic repair time, *Applied Mathematical Modelling*, Vol. 35, No. 7, 3495-3508, doi: [10.1016/j.apm.2011.01.006](https://doi.org/10.1016/j.apm.2011.01.006).

- [36] Chiu, Y.-S.P., Chen, Y.-C., Lin, H.-D., Chang, H.-H. (2014). Combining an improved multi-delivery policy into a single-producer multi-retailer integrated inventory system with scrap in production, *Economic Modelling*, Vol. 39, 163-167, doi: [10.1016/j.econmod.2014.02.031](https://doi.org/10.1016/j.econmod.2014.02.031).
- [37] Tseng, C.-T., Wu, M.-F., Lin, H.-D., Chiu, Y.-S.P. (2014). Solving a vendor-buyer integrated problem with rework and a specific multi-delivery policy by a two-phase algebraic approach, *Economic Modelling*, Vol. 36, 30-36, doi: [10.1016/j.econmod.2013.09.013](https://doi.org/10.1016/j.econmod.2013.09.013).
- [38] Lin, G.C., Gong, D.-C., Chang, C.-C. (2014). On an economic production quantity model with two unreliable key components subject to random failures, *Journal of Scientific and Industrial Research*, Vol. 73, 149-152.
- [39] Chiu, Y.-S.P., Chang, H.-H. (2014). Optimal run time for EPQ model with scrap, rework and stochastic breakdowns: A note, *Economic Modelling*, Vol. 37, 143-148, doi: [10.1016/j.econmod.2013.11.006](https://doi.org/10.1016/j.econmod.2013.11.006).
- [40] Haider, A., Mirza, J. (2015). An implementation of lean scheduling in a job shop environment, *Advances in Production Engineering & Management*, Vol. 10, No. 1, 5-17, doi: [10.14743/apem2015.1.188](https://doi.org/10.14743/apem2015.1.188).
- [41] Rardin, R.L. (1998). *Optimization in operations research*, Prentice-Hall, New Jersey, USA.

## Calendar of events

- 14th Annual Industrial Simulation Conference, Bucharest, Romania, June 6-8, 2016.
- 3rd CIRP Conference on Surface Integrity, Charlotte, NC, USA, June 8-10, 2016.
- International Symposium on Green Manufacturing and Applications, Bali, Indonesia, June 21-25, 2016.
- 8th IFAC Conference on Manufacturing Modelling, Management and Control, Troyes, France, June 28-30, 2016.
- 28th European Conference on Operational Research, Poznan, Poland, July 3-6, 2016.
- 10th CIRP Conference on Intelligent Computation in Manufacturing Engineering, Gulf of Naples, Italy, July 20-22, 2016.
- International Conference on Design and Production Engineering, Berlin, Germany, July 25-26, 2016.
- 21st IEEE International Conference on Emerging Technologies and Factory Automation, Berlin, Germany, September 6-9, 2016.
- 20th International Research/Expert Conference – Trends in the Development of Machinery and Associated Technology, Mediterranean Sea Cruising, 24 September to 1st October, 2016.
- 5th CIRP Global Web Conference – Research and Innovation for Future Production, Patras, Greece, October 4-6, 2016.
- 27th DAAAM International Symposium, Mostar, Bosnia and Herzegovina, October 26-29, 2016.
- 3rd International Conference on Mechatronics, Automation and Manufacturing, Tokyo, Japan, October 29-31, 2016.
- 10th International Conference on Industrial Tools and Advances Processing Technologies, Ljubljana, Slovenia, April 24-26, 2017.
- 19th International Conference on Production Engineering and Management, Boston, USA, April 24-25, 2017.

## Notes for contributors

### General

Articles submitted to the *APEM journal* should be original and unpublished contributions and should not be under consideration for any other publication at the same time. Manuscript should be written in English. Responsibility for the contents of the paper rests upon the authors and not upon the editors or the publisher. Authors of submitted papers automatically accept a copyright transfer to *Production Engineering Institute, University of Maribor*. For most up-to-date information on publishing procedure please see the *APEM journal* homepage [apem-journal.org](http://apem-journal.org).

### Submission of papers

A submission must include the corresponding author's complete name, affiliation, address, phone and fax numbers, and e-mail address. All papers for consideration by *Advances in Production Engineering & Management* should be submitted by e-mail to the journal Editor-in-Chief:

---

**Miran Brezocnik**, Editor-in-Chief  
UNIVERSITY OF MARIBOR  
Faculty of Mechanical Engineering  
Production Engineering Institute  
Smetanova ulica 17, SI – 2000 Maribor  
Slovenia, European Union  
E-mail: [editor@apem-journal.org](mailto:editor@apem-journal.org)

---

### Manuscript preparation

Manuscript should be prepared in *Microsoft Word 2007* (or higher version) word processor. *Word .docx* format is required. Papers on A4 format, single-spaced, typed in one column, using body text font size of 11 pt, should not exceed 12 pages, including abstract, keywords, body text, figures, tables, acknowledgements (if any), references, and appendices (if any). The title of the paper, authors' names, affiliations and headings of the body text should be in *Calibri* font. Body text, figures and tables captions have to be written in *Cambria* font. Mathematical equations and expressions must be set in *Microsoft Word Equation Editor* and written in *Cambria Math* font. For detail instructions on manuscript preparation please see instruction for authors in the *APEM journal* homepage [apem-journal.org](http://apem-journal.org).

### The review process

Every manuscript submitted for possible publication in the *APEM journal* is first briefly reviewed by the editor for general suitability for the journal. Notification of successful submission is sent. After initial screening, and checking by a special plagiarism detection tool, the manuscript is passed on to at least two referees. A double-blind peer review process ensures the content's validity and relevance. Optionally, authors are invited to suggest up to three well-respected experts in the field discussed in the article who might act as reviewers. The review process can take up to eight weeks. Based on the comments of the referees, the editor will take a decision about the paper. The following decisions can be made: accepting the paper, reconsidering the paper after changes, or rejecting the paper. Accepted papers may not be offered elsewhere for publication. The editor may, in some circumstances, vary this process at his discretion.

### Proofs

Proofs will be sent to the corresponding author and should be returned within 3 days of receipt. Corrections should be restricted to typesetting errors and minor changes.

### Offprints

An e-offprint, i.e., a PDF version of the published article, will be sent by e-mail to the corresponding author. Additionally, one complete copy of the journal will be sent free of charge to the corresponding author of the published article.

# APEM

*journal*

## Advances in Production Engineering & Management

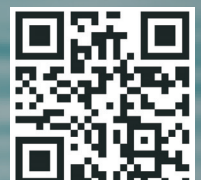
Production Engineering Institute (PEI)  
University of Maribor  
APEM homepage: [apem-journal.org](http://apem-journal.org)

Volume 11 | Number 2 | June 2016 | pp 73-154

### Contents

<b>Scope and topics</b>	76
<b>A simulation approach to the process planning problem using a modified particle swarm optimization</b> Wang, J.F.; Kang, W.L.; Zhao, J.L.; Chu, K.Y.	77
<b>Surface roughness assessing based on digital image features</b> Simunovic, G.; Svalina, I.; Simunovic, K.; Saric, T.; Havrlisan, S.; Vukelic, D.	93
<b>Visual measurement of layer thickness in multi-layered functionally graded metal materials</b> Zuperl, U.; Radic, A.; Cus, F.; Irgolic, T.	105
<b>Modelling supply risks in interdependent manufacturing systems: A case study</b> Omega, R.S.; Noel, V.M.; Masbad, J.G.; Ocampo, L.A.	115
<b>Analysis for prevalence of carpal tunnel syndrome in shocker manufacturing workers</b> Kumar, S.; Muralidhar, M.	126
<b>Simultaneous determination of production and shipment decisions for a multi-product inventory system with a rework process</b> Chiu, Y.P.; Chiang, K.-W.; Chiu, S.W.; Song, M.-S.	141
<b>Calendar of events</b>	152
<b>Notes for contributors</b>	153

Copyright © 2016 PEI. All rights reserved.



[apem-journal.org](http://apem-journal.org)